JAERI-Research
2000-016

ANALYTICAL EVALUATION ON LOSS OF OFF-SITE ELECTRIC POWER SIMULATION OF THE HIGH TEMPERATURE ENGINEERING TEST REACTOR

March 2000

Takeshi TAKEDA, Shigeaki NAKAGAWA, Yukio TACHIBANA,
Eiji TAKADA and Kazuhiko KUNITOMI

日本原子力研究所
Japan Atomic Energy Research Institute

本レポートは，日本原子力研究所が不定期に公刊している研究報告書です。
入手の問合わせは，日本原子力研究所研究情報部研究情報課（〒319-1195　茨城県那珂郡東海村）あて，お申し越しください。なお，このほかに財団法人原子力弘済会資料センター（〒319-1195　茨城県那珂郡東海村日本原子力研究所内）で複写による実費頒布をおこなっております。

This report is issued irregularly.
Inquiries about availability of the reports should be addressed to Research Information Division, Department of Intellectual Resources, Japan Atomic Energy Research Institute, Tokai-mura, Naka-gun, Ibaraki-ken, 319-1195, Japan.

編集兼発行　　日本原子力研究所

JAERI-Research 2000-016

Analytical Evaluation on Loss of Off-site Electric Power Simulation of the High Temperature Engineering Test Reactor

Takeshi TAKEDA, Shigeaki NAKAGAWA, Yukio TACHIBANA, Eiji TAKADA and Kazuhiko KUNITOMI

Department of HTTR Project
Oarai Research Establishment
Japan Atomic Energy Research Institute
Oarai-machi, Higashiibaraki-gun, Ibaraki-ken

(Received February 3, 2000)

A rise-to-power test of the high temperature engineering test reactor (HTTR) started on September 28 in 1999 for establishing and upgrading the technological basis for the high temperature gas-cooled reactor (HTGR). A loss of off-site electric power test of the HTTR from the normal operation under 15 and 30MW thermal power will be carried out in the rise-to-power test. Analytical evaluations on transient behaviors of the reactor and plant during the loss of off-site electric power were conducted. These estimations are proposed as benchmark problems for the IAEA coordinated research program on "Evaluation of HTGR Performance". This report describes an event scenario of transient during the loss of off-site electric power, the outline of major components and system, detailed thermal and nuclear data set for these problems and pre-estimation results of the benchmark problems by an analytical code 'ACCORD' for incore and plant dynamics of the HTGR.

Keywords: HTGR, HTTR, Rise-to-power Test, Off-site Electric Power, Evaluation, Analysis, Benchmark Problem, Validation, Analytical Code, Plant Dynamics

高温工学試験研究炉の商用電源喪失シミュレーションの解析評価

日本原子力研究所大洗研究所高温工学試験研究炉開発部
竹田 武司・中川 繁昭・橘　幸男・高田 英治・國富 一彦

(2000年2月3日受理)

高温工学試験研究炉（ＨＴＴＲ）の出力上昇試験は，高温ガス炉（ＨＴＧＲ）技術基盤の確立と高度化のため1999年9月28日に開始した。出力上昇試験の中で，通常運転（原子炉出力15，30MW）からの商用電源喪失試験が計画されている。そこで，ＨＴＴＲの商用電源喪失時の原子炉およびプラント過渡挙動の解析評価を行った。なお，本解析評価は，ＨＴＧＲの性能評価に関するＩＡＥＡ協力研究計画用ベンチマーク問題として提案されている。本報は，商用電源喪失事象のシナリオ，ＨＴＴＲの主なコンポーネントおよびシステムの概要，詳細な熱および核データセット，ＨＴＧＲ用プラント動特性解析コード'ACCORD'を用いたベンチマーク問題の事前評価結果を報告するものである。

大洗研究所：〒311-1394　茨城県東茨城郡大洗町成田町新堀3607

Contents

目　次

List of Tables

List of Figures

This is a blank page.

1. Introduction

The high temperature gas-cooled reactor (HTGR) is expected to be one of alternative energy sources in the future because it can supply high temperature heat and have high thermal efficiency together with inherent safety features. Japan Atomic Energy Research Institute (JAERI) built a graphite-moderated and helium-gas-cooled reactor, the high temperature engineering test reactor (HTTR) [1.1]. Figure 1.1 shows a bird's-eye view of the reactor pressure vessel and core of the HTTR. Table 1.1 shows the major specifications of the HTTR. Evaluations of the first criticality, insertion depth of control rods and excess reactivity of annular cores during startup core physics tests of the HTTR were proposed as previous benchmark problems for the IAEA coordinated research program [1.2]. Participants in the research coordination meeting presented results of the benchmark calculations in August 1998 [1.3] and in October 1999. The HTTR attained its first criticality on November 10 in 1998, and then the startup core physics tests were successfully finished in January 1999. A rise-to-power test of the HTTR started on September 28 in 1999 under higher temperature and pressure conditions for establishing and upgrading the HTGR technological basis [1.4].

Simulation, testing and evaluation of an anticipated operational occurrence are essential to check functional features and thermal performance of the HTTR system. Since the reactor core of the HTTR has a large heat capacity, its temperature changes slowly in the anticipated operational occurrence. Figure 1.2 shows a schematic diagram of the reactor cooling system of the HTTR. The reactor cooling system consists of the main cooling system, auxiliary cooling system and vessel cooling system. The auxiliary cooling system automatically starts up when the reactor is scrammed in an accident. In the rise-to-power test, a loss of off-site electric power test from the normal operation under 15 and 30MW thermal power will be conducted for investigating the coolability of the auxiliary cooling system. They are simulated by a manual shutdown of off-site electric power of the HTTR. The loss of electric power supply causes stop of all the primary and secondary helium circulators as well as a water pump for the pressurized water cooling system of the HTTR. After the reactor scram, the auxiliary cooling system removes residual heat of the reactor core maintaining the structural integrity of graphite blocks of the reactor core.

We propose analytical simulations on transient behaviors of the reactor and plant during

the loss of off-site electric power of the HTTR as benchmark problems for the IAEA coordinated research program on "Evaluation of HTGR Performance". The objective of the present benchmark problems is to validate analytical codes of participating countries, such as 'ACCORD' code [1.5] of the JAERI, and performance models to actual operating conditions and results of the HTTR.

In this report, an event scenario of transient during the loss of off-site electric power, conditions before and after the startup of the auxiliary cooling system are explained. The core components and reactor internals, main cooling system and residual heat removal system are reviewed. The detailed thermal and nuclear data set (geometry, material, parameter for core dynamics, decay heat, performance of helium circulators, thermophysical properties, correlation of heat transfer coefficient, etc.) are described for solving the benchmark problems. Pre-estimation results of the benchmark problems concerning the loss of off-site electric power simulation of the HTTR by the 'ACCORD' code are presented. In addition, the outline of the 'ACCORD' code is shown in Appendix A.

Table 1.1 Major specifications of the HTTR

Thermal power	30MW
Outlet coolant temperature	850/950°C
Inlet coolant temperature	395°C
Primary coolant pressure	4MPa
Core structure	Graphite
Equivalent core diameter	2.3m
Effective core height	2.9m
Average power density	2.5W/cm^3
Fuel	Low-enriched UO_2
Uranium enrichment	3-10wt% (average 6wt%)
Fuel type	Pin-in-block
Coolant	Helium gas
Direction of coolant flow	Downward flow
Number of fuel assembly	150
Number of fuel columns	30
Plant lifetime	20yr

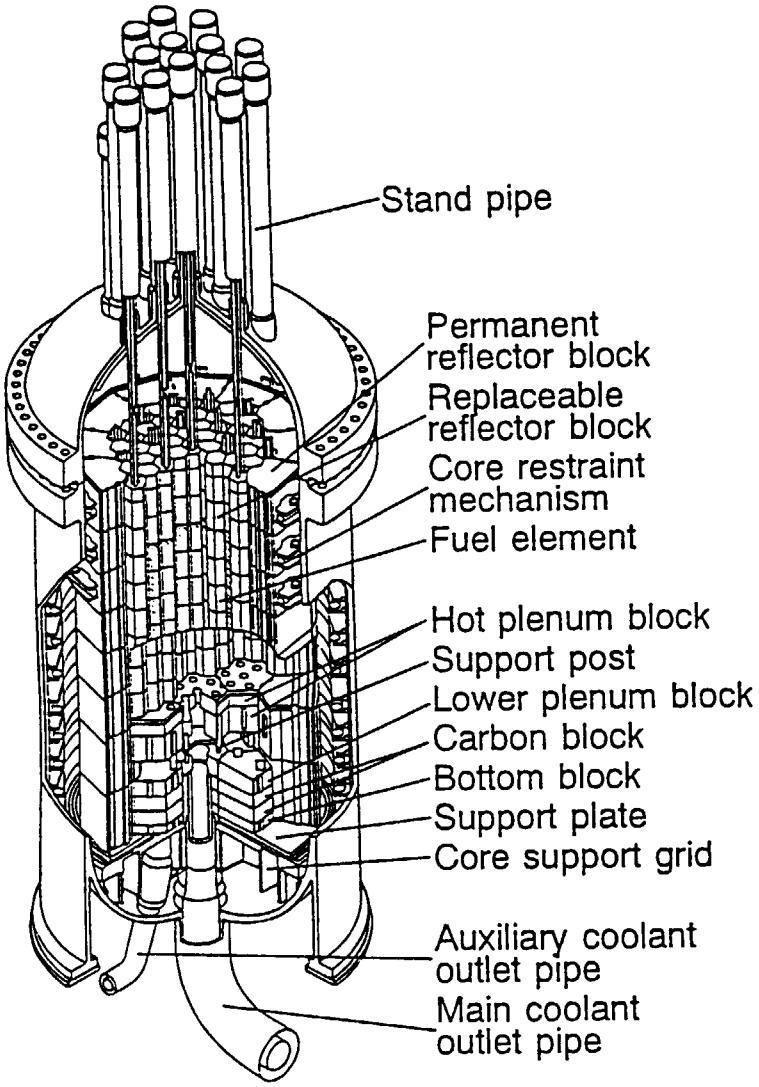

Fig. 1.1 Bird's-eye view of reactor pressure vessel and core

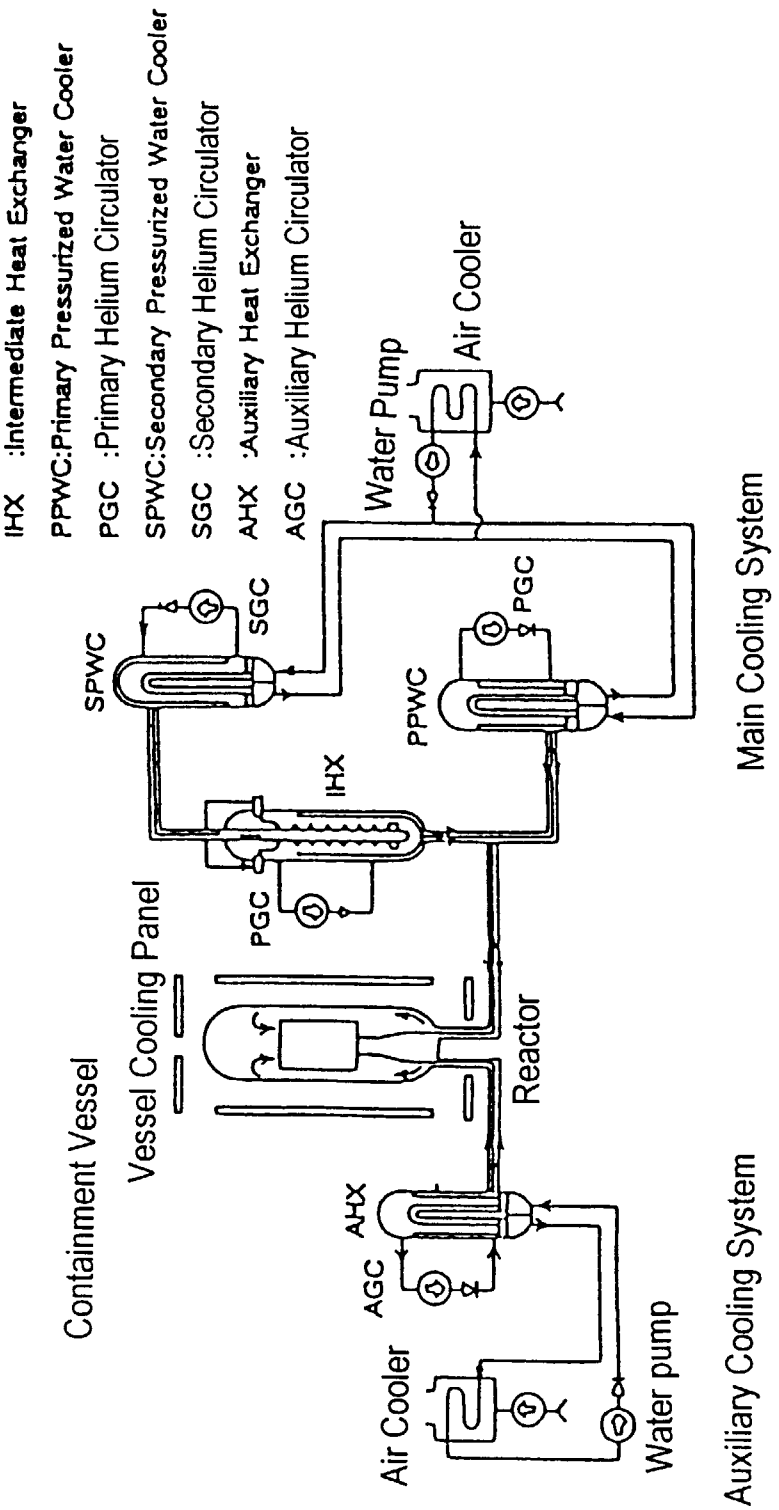

Fig. 1.2 Schematic diagram of reactor cooling system

2. Benchmark problems

We propose the following benchmark problems concerning the loss of off-site electric power simulation designated as HTTR-LP(15MW, 30MW). During the normal operation, called parallel loaded operation, the intermediate heat exchanger, primary and secondary pressurized water coolers are operated simultaneously.

(1) HTTR-LP(15MW)

Analytical simulation on transient behaviors of the reactor and plant during the loss of off-site electric power from the normal operation under 15 MW thermal power

(2) HTTR-LP(30MW)

Analytical simulation on transient behaviors of the reactor and plant during the loss of off-site electric power from the normal operation under 30 MW thermal power

In both simulation cases, estimation items are as follows; transition of (1)hot plenum block temperature, (2)reactor inlet coolant temperature, (3)reactor outlet coolant temperature, (4)primary coolant pressure, (5)reactor power, (6)heat removal of auxiliary heat exchanger. Estimation duration is for 10hr from the beginning of the loss of off-site electric power.

2.1 Event scenario of transient during loss of off-site electric power

Figure 2.1 shows an event scenario of transient during the loss of off-site electric power. The loss of off-site electric power is caused by failure of the power transmission line or the HTTR electrical equipment. All the primary and secondary helium circulators as well as the water pump for the pressurized water cooling system are coasted down immediately after the loss of off-site electric power. Accordingly, flow rates of primary and secondary helium as well as water reduce. Flow rate of primary helium, which is deflected at a hot header and discharged around the heat transfer tubes of the intermediate heat exchanger, decreases to 92% of normal flow rate in 5s after the loss of off-site electric power. In 3.2s after 92% flow rate is reached, the reactor is scrammed by the reactor protection system. In 1s after the reactor scram, breaking stop of all the primary and secondary helium circulators is initiated. The auxiliary cooling system starts up in 50s after the loss of off-site electric power by electricity supplied through the emergency power feeder. The auxiliary cooling system mainly consists of an auxiliary heat exchanger, two auxiliary helium circulators, air cooler and two water pumps. Helium flow rate of the auxiliary cooling system reaches about 1.2kg/s in 20s

after the startup of the auxiliary cooling system. One of the two auxiliary helium circulators is coasted down in 40min after the startup of the auxiliary cooling system to prevent the graphite blocks, composing the reactor core, from overcooling. Then helium flow rate of the auxiliary cooling system decreases to about 0.8kg/s.

2.2 Conditions before startup of auxiliary cooling system

Table 2.1 shows the major process conditions of the reactor core (thermal power, reactor inlet and outlet temperatures, primary coolant pressure and flow rate as well as hot plenum block temperature). Tables 2.2, 2.3, 2.4 and 2.5 show the major process conditions (temperature, pressure and flow rate) of the intermediate heat exchanger, primary and secondary pressurized water coolers as well as the air cooler for the pressurized water cooling system, respectively. Helium and water flow rates of the auxiliary cooling system in standby are fixed to 0.036kg/s and 5.5kg/s, respectively, to prevent the auxiliary heat exchanger from the thermal shock. During the standby of the auxiliary cooling system, the two auxiliary helium circulators are not operated and one of the two water pumps for the auxiliary cooling system is driven. Tables 2.6 and 2.7 show the major process conditions (temperature, pressure and flow rate) of the auxiliary heat exchanger and air cooler for the auxiliary cooling system, respectively.

2.3 Conditions after startup of auxiliary cooling system

Helium flow rate of the auxiliary cooling system reaches about 1.2kg/s in 20s after the startup of the auxiliary cooling system. Helium flow rate of the auxiliary cooling system decreases to about 0.8kg/s in 40min after the startup of the auxiliary cooling system. Water flow rate of the auxiliary cooling system is fixed to about 18.3kg/s all the time after the startup of the auxiliary cooling system.

Table 2.1 Major process conditions of reactor core

Items	HTTR-LP(15MW)	HTTR-LP(30MW)
Thermal power	15MW	30MW
Reactor inlet coolant temperature	About 241°C	395°C
Reactor outlet coolant temperature	About 470°C	850°C
Primary coolant pressure	About 3MPa(abs)	4MPa(abs)
Primary coolant flow rate	12.4kg/s	12.4kg/s
Hot plenum block temperature	About 490°C	About 890°C

Table 2.2 Process conditions of intermediate heat exchanger

Items	HTTR-LP(15MW)	HTTR-LP(30MW)
Primary helium inlet temperature	About 468°C	850°C
Primary helium outlet temperature	About 238°C	395°C
Primary helium pressure	About 3MPa(abs)	4MPa(abs)
Primary helium flow rate	4.1kg/s	4.1kg/s
Secondary helium inlet temperature	About 154°C	About 241°C
Secondary helium outlet temperature	About 431°C	About 783°C
Secondary helium pressure	About 3.1MPa(abs)	4.1MPa(abs)
Secondary helium flow rate	3.6kg/s	3.6kg/s

Table 2.3 Process conditions of primary pressurized water cooler

Items	HTTR-LP(15MW)	HTTR-LP(30MW)
Helium inlet temperature	About 468°C	850°C
Helium outlet temperature	About 242°C	395°C
Helium pressure	About 3MPa(abs)	4MPa(abs)
Helium flow rate	8.3kg/s	8.3kg/s
Water inlet temperature	About 89°C	About 135°C
Water outlet temperature	About 110°C	About 175°C
Water pressure	About 2.6MPa(abs)	3.5MPa(abs)
Water flow rate	115kg/s	115kg/s

Table 2.4 Process conditions of secondary pressurized water cooler

Items	HTTR-LP(15MW)	HTTR-LP(30MW)
Helium inlet temperature	About 430°C	About 782°C
Helium outlet temperature	About 154°C	About 240°C
Helium pressure	About 3.1MPa(abs)	4.1MPa(abs)
Helium flow rate	3.6kg/s	3.6kg/s
Water inlet temperature	About 89°C	About 135°C
Water outlet temperature	About 110°C	About 175°C
Water pressure	About 2.5MPa(abs)	3.4MPa(abs)
Water flow rate	60kg/s	60kg/s

Table 2.5 Process conditions of air cooler for pressurized water cooling system

Items	HTTR-LP(15MW)	HTTR-LP(30MW)
Water inlet temperature	About 110°C	About 175°C
Water outlet temperature	About 58°C	About 80°C
Water pressure	About 2MPa(abs)	3MPa(abs)
Water flow rate	70kg/s	70kg/s
Air inlet temperature	About 33°C	About 33°C
Air outlet temperature	About 58°C	About 81°C
Air pressure	0.1MPa(abs)	0.1 MPa(abs)
Air flow rate	605kg/s	605kg/s

Table 2.6 Process conditions of auxiliary heat exchanger

Items	HTTR-LP(15MW)	HTTR-LP(30MW)
Helium inlet temperature	About 452°C	About 812°C
Helium outlet temperature	About 50°C	About 62°C
Helium pressure	About 3MPa(abs)	4MPa(abs)
Helium flow rate	0.036kg/s	0.036kg/s
Water inlet temperature	About 35°C	About 36°C
Water outlet temperature	About 39°C	About 45°C
Water pressure	About 2MPa(abs)	About 3MPa(abs)
Water flow rate	5.5kg/s	5.5kg/s

Table 2.7 Process conditions of air cooler for auxiliary cooling system

Items	HTTR-LP(15MW)	HTTR-LP(30MW)
Water inlet temperature	About 39°C	About 45°C
Water outlet temperature	About 35°C	About 36°C
Water pressure	About 1MPa(abs)	About 2MPa(abs)
Water flow rate	5.5kg/s	5.5kg/s
Air inlet temperature	About 33°C	About 33°C
Air outlet temperature	About 34°C	About 42°C
Air pressure	0.1MPa(abs)	0.1 MPa(abs)
Air flow rate	106.5kg/s	106.5kg/s

(1) Loss of off-site electric power of HTTR caused by failure of power transmission line or HTTR electrical equipment

↓

(2) Coast down of all primary and secondary helium circulators as well as water pump for pressurized water cooling system

↓

(3) Decrease of flow rate of primary and secondary helium as well as water

↓ 5s after (1)

(4) Decrease to 92% of total primary helium flow rate of intermediate heat exchanger

↓ 3.2s after (4)

(5) Reactor scram by reactor protection system

↓ 1s after (5)

(6) Initiation of breaking stop of all primary and secondary helium circulators

↓ 50s after (1)

(7) Startup of auxiliary cooling system by supplying electricity through emergency power feeder

↓ 40min after (7)

(8) Coast down of one of two auxiliary helium circulators

Fig. 2.1 Event scenario of transient during loss of off-site electric power

3. Core components and reactor internals

The reactor consists of core components, reactor internals, reactor pressure vessel, etc. The reactor pressure vessel of 2 1/4 Cr – 1 Mo steel, 13.2m in height, 5.5m in diameter and 120mm in thickness of cylinder, contains the core components and reactor internals. The core components such as fuel blocks and replaceable reflector blocks are prismatic hexagonal blocks, which are 580mm in height and 360mm in width across the flats. Gap width between the blocks is 2mm in average. The configuration of the fuel element is shown in Fig. 3.1. Tri-isotropic (TRISO) coated fuel particles with low-enriched UO_2 kernel of 6wt% in average enrichment are dispersed in the graphite matrix. The TRISO coating consists of a low density pyrolytic carbon (PyC) buffer layer adjacent to the fuel kernel, surrounded by a high density isotropic PyC layer, a SiC layer and a final PyC coating. The coated fuel particles are incorporated into the fuel compact, which is 10mm in inner diameter, 26mm in outer diameter and 39mm in height. Fourteen fuel compacts are contained in a graphite sleeve forming a fuel rod as shown in Fig. 3.2. The fuel rod is 34mm in outer diameter, 3.875mm in thickness and 577mm in length. The fuel rod is inserted into 31 or 33 vertical holes bored in each hexagonal graphite block as coolant channels. Material of the graphite sleeve and graphite block is IG-110 graphite.

Figure 3.3 shows a vertical view of the reactor core. Top shielding block of 316 stainless steel above the top reflector block is 300mm in height and 360mm in width across the flats. The top shielding blocks and top reflector blocks have coolant channels to fuel blocks below. The active reactor core, 2.9m in height and 2.3m in effective diameter, consists of 30 fuel columns and 7 control rod guide columns. As shown in Fig. 3.4, the active reactor core is surrounded by 12 replaceable reflector columns, 9 control rod guide columns and 3 irradiation test columns. Each fuel column consists of one top shielding block, 2 top replaceable reflector blocks, 5 fuel assemblies and 2 bottom replaceable reflector blocks. Table 3.1 shows the number of the fuel rods at each fuel zone. The fuel element has 33 fuel rods in the fuel zone 1 and 2, while it has 31 fuel rods in the fuel zone 3 and 4. Total number of the fuel rods is 954. Figures 3.5 and 3.6 show structural drawings of the fuel graphite block for 31 and 33 pins fuel element, respectively. Figures 3.7 and 3.8 show structural drawings of the replaceable reflector block in 1st, 2nd and 8th layer of 31 and 33 pins fuel columns, respectively. Figure

3.9 shows the replaceable reflector block in 9th layer of the fuel columns. Figures 3.10 and 3.11 show the replaceable reflector block in 1st – 8th and 9th layer of the replaceable reflector columns, respectively.

The reactor internals are composed of graphite and metallic core support structures as well as shielding blocks as shown in Fig. 3.12. The graphite core support structures mainly consist of permanent reflector blocks, hot plenum blocks, lower plenum block and bottom block, which are made of PGX graphite. The permanent reflector blocks of PGX graphite, surrounding the replaceable reflector blocks of IG-110 graphite, are fixed by the core restraint mechanism. Width across the flats including the permanent reflector blocks is 4250mm as shown in Fig. 3.13. Height of the permanent reflector blocks in 1st – 5th and 6th layer are 904 and 1000mm, respectively. The support posts located between the hot plenum block and core bottom structures provide a hot plenum space where the hot coolant is mixed uniformly.

As shown in Fig. 3.3, coolant flow in the reactor pressure vessel is as follows.

1. Coolant enters into the reactor pressure vessel through the annular path between the inner tube of the concentric hot gas duct and the helium nozzle placed at the bottom of the vessel (Fig. 3.3a).
2. Coolant flows upward in the two annular paths between the reactor pressure vessel and the side shielding blocks as well as between side shielding blocks and permanent reflector blocks (Fig. 3.3b).
3. Coolant turns at the top of the reactor core (Fig. 3.3c).
4. Coolant flows downward in the annular gap between vertical holes in the hexagonal graphite block and the fuel rods to remove heat by fission and gamma heating. The top and bottom replaceable reflector blocks above and below the active reactor core have the same arrangement of coolant channels as the fuel blocks within the identical columns. The side replaceable reflector blocks adjacent to the core have the same envelope dimensions as the fuel blocks (Fig. 3.3d).
5. The bottom replaceable reflector block below fuel blocks provides transition of coolant channels to a single large channel, which gets together with other coolant channels within the hot plenum blocks (Fig. 3.3e).
6. Coolant flows inside the liner of the concentric hot gas duct (Fig. 3.3f).

Reactivity is controlled by control rods, which are individually supported by mechanisms located in standpipes connected with the hemispherical top head closure of the reactor pressure vessel. Ratio of reactivity by the control rods at their inserting time will be described in Section 6.1(Table 6.3). The control rods compensate the reactivity change due to variations of the temperature, concentration change of ^{135}Xe, and burnup of ^{235}U and burnable poisons.

Table 3.1 Number of fuel rods at each fuel zone

Fuel zone number*			
1	2	3	4
33	33	31	31

* Fuel zone number is shown in Fig. 3.4.

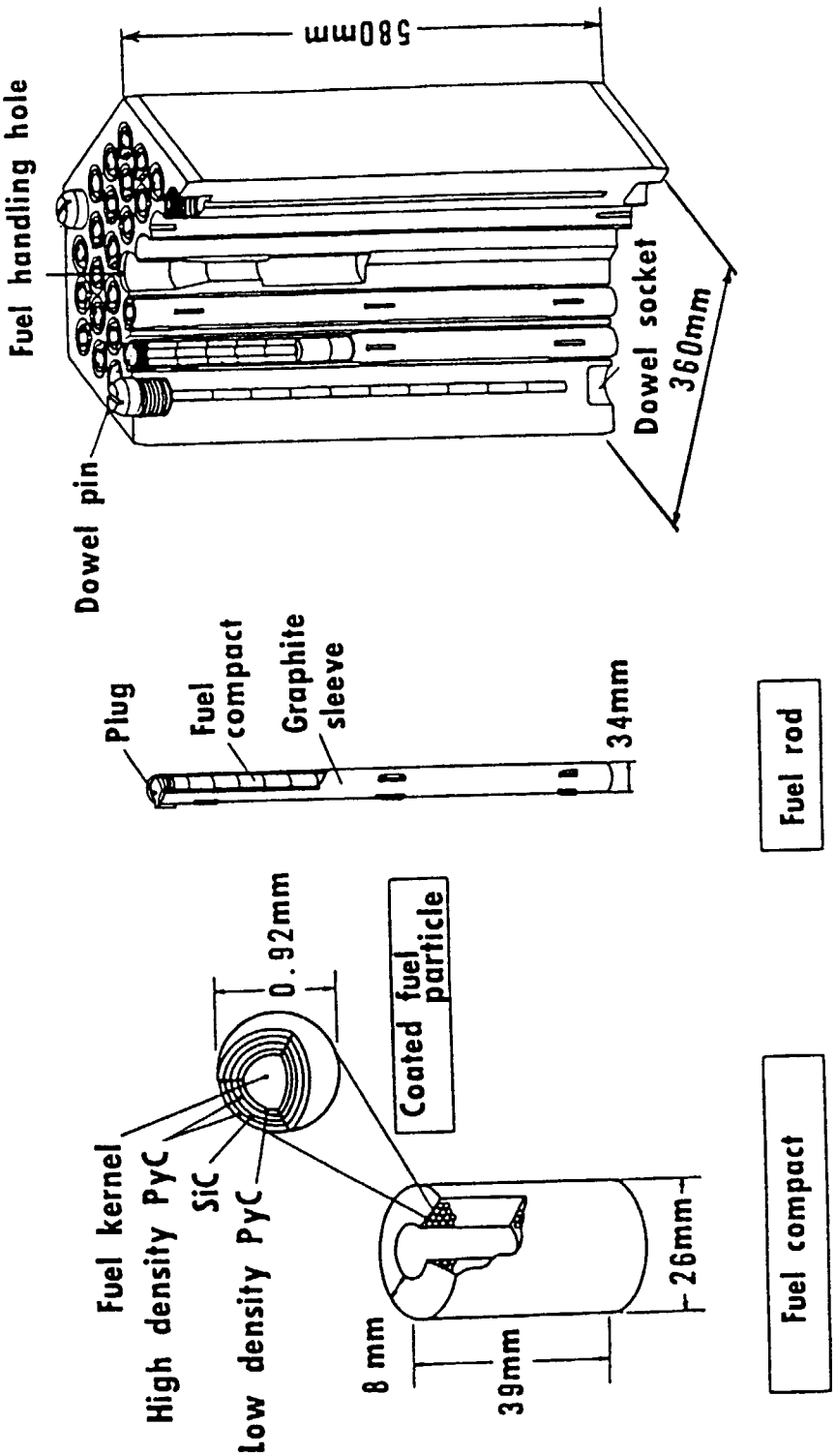

Fig. 3.1 Configuration of fuel element

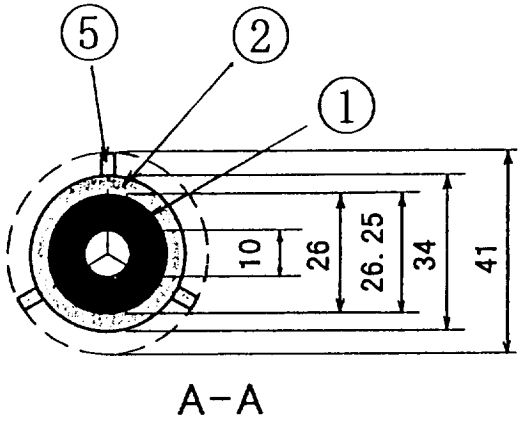

	Name	Number
①	Fuel compact	14
②	Graphite sleeve	1
③	Buffer plate	2
④	Graphite plug	2
⑤	Spacer	9

Note:We recommend to regard buffer plates as void region

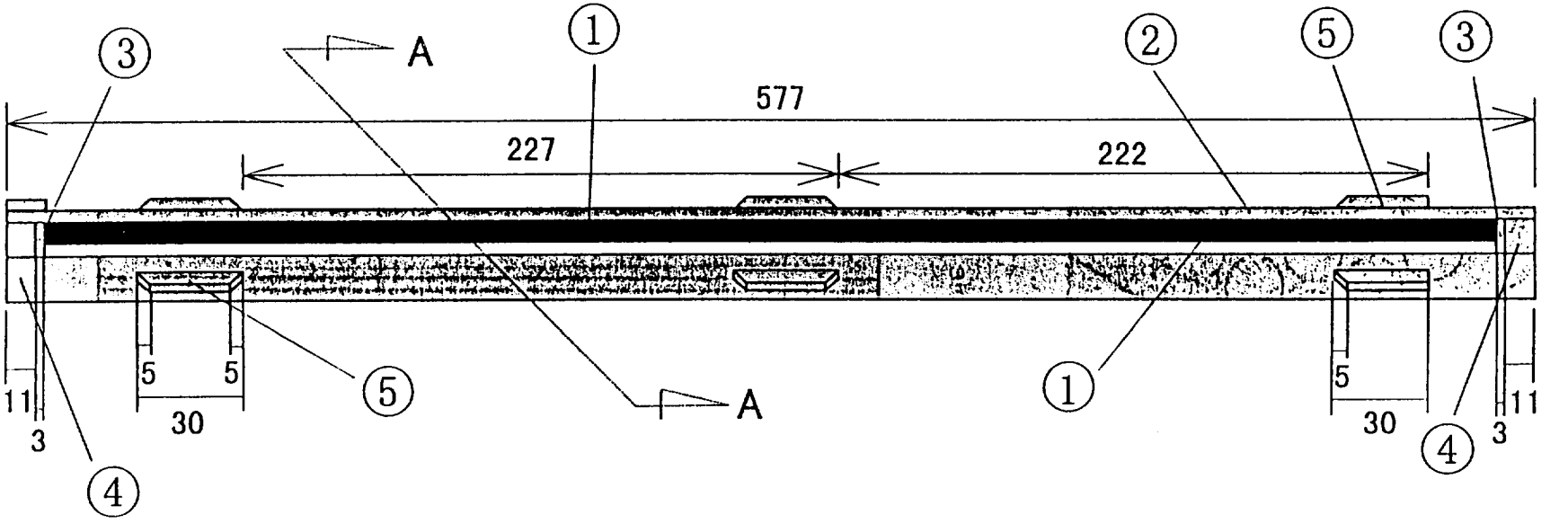

Unit (mm)

Fig. 3.2 Structural drawing of fuel rod

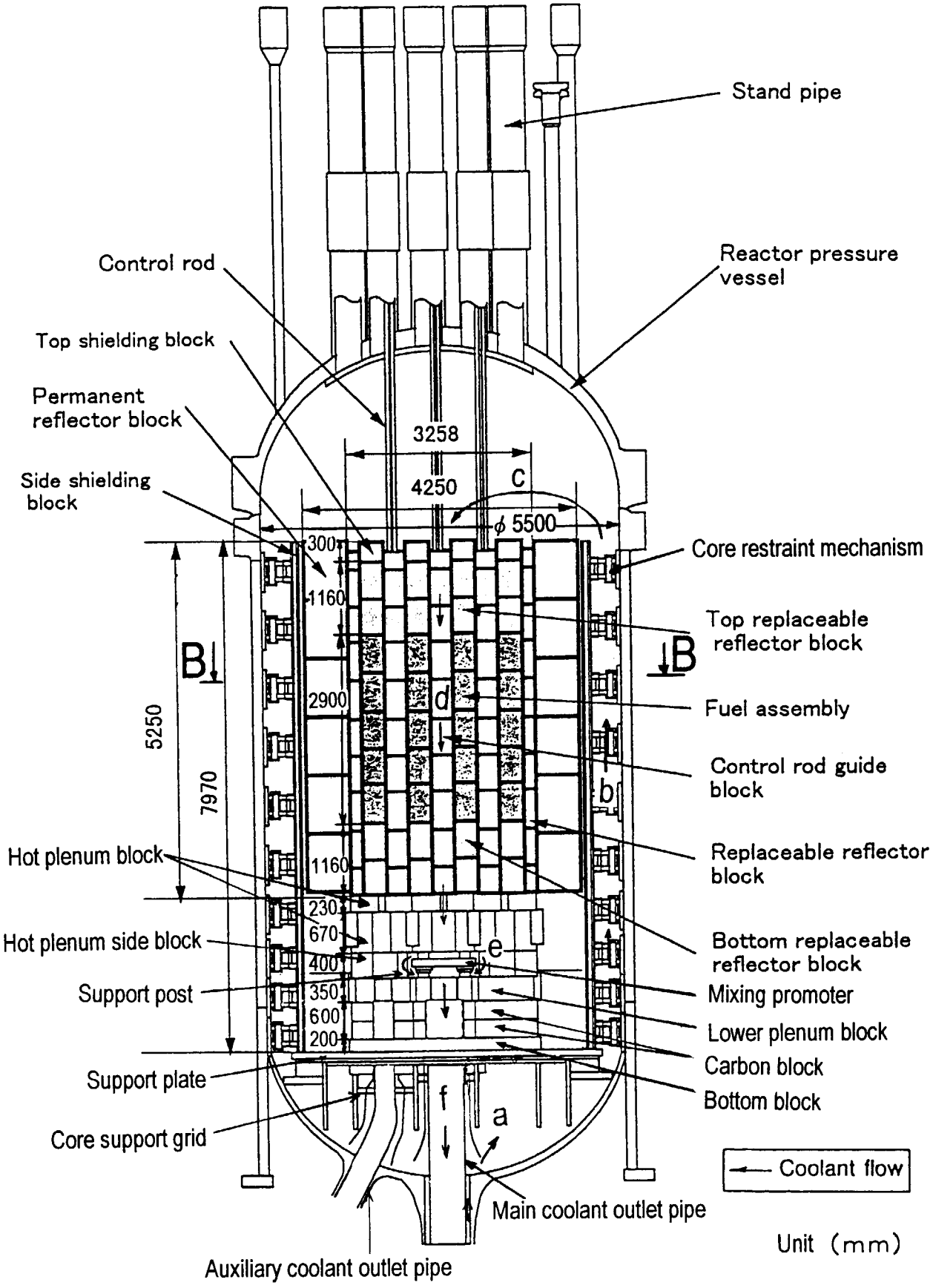

Fig. 3.3 Vertical view of reactor core

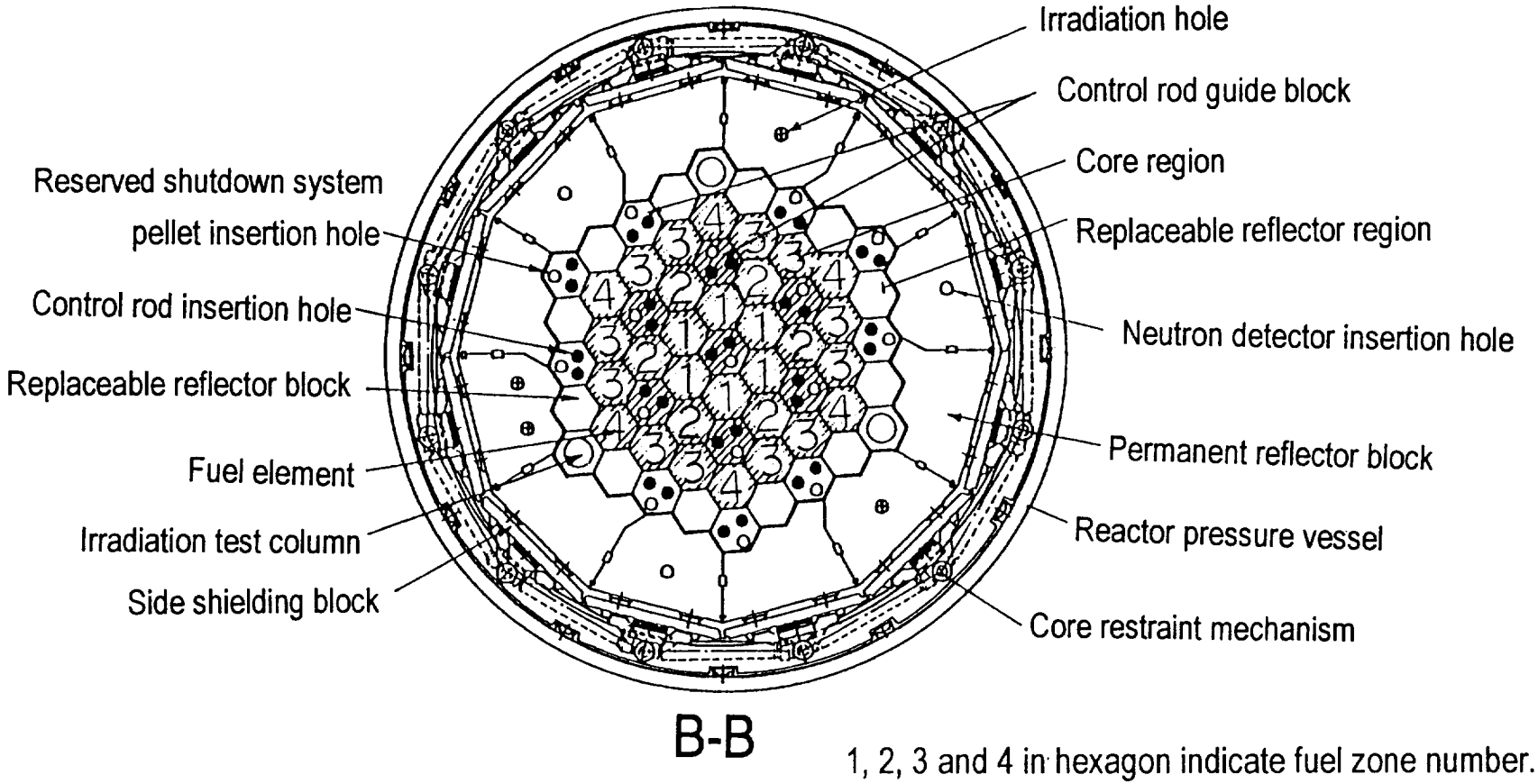

Fig. 3.4 Horizontal arrangement of reactor core

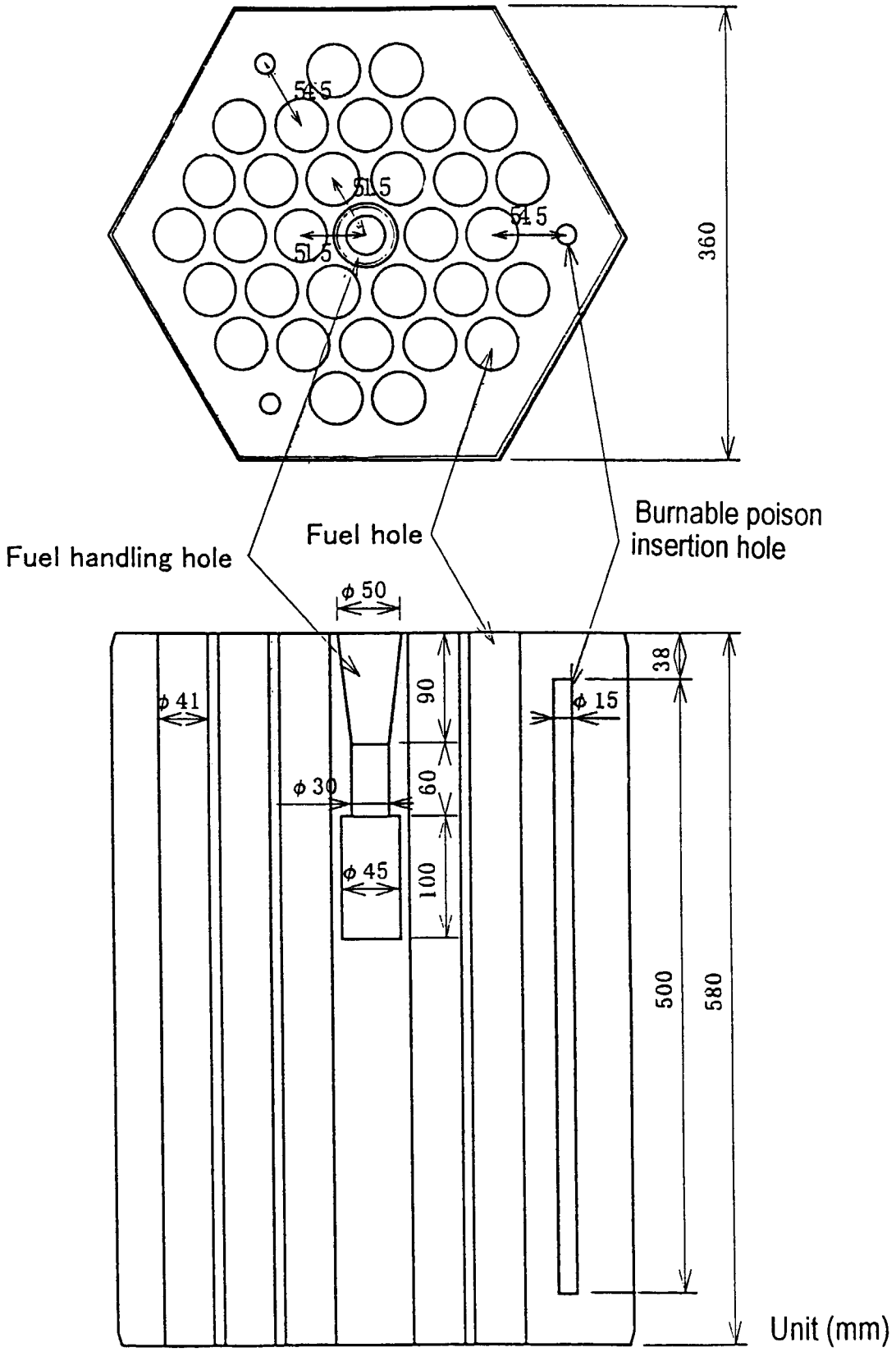

Fig. 3.5 Structural drawing of fuel graphite block for 31 pins fuel element

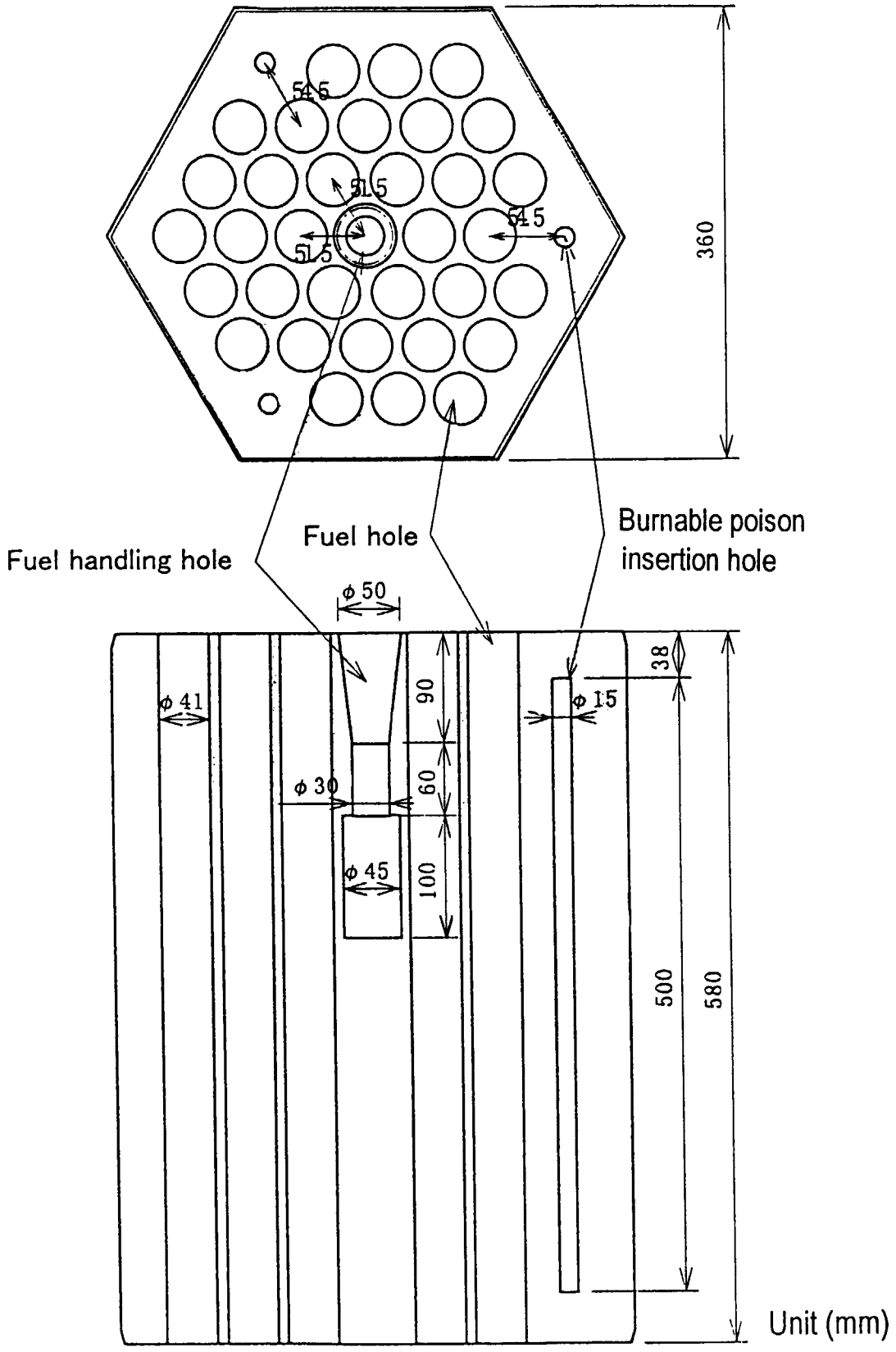

Fig. 3.6 Structural drawing of fuel graphite block for 33 pins fuel element

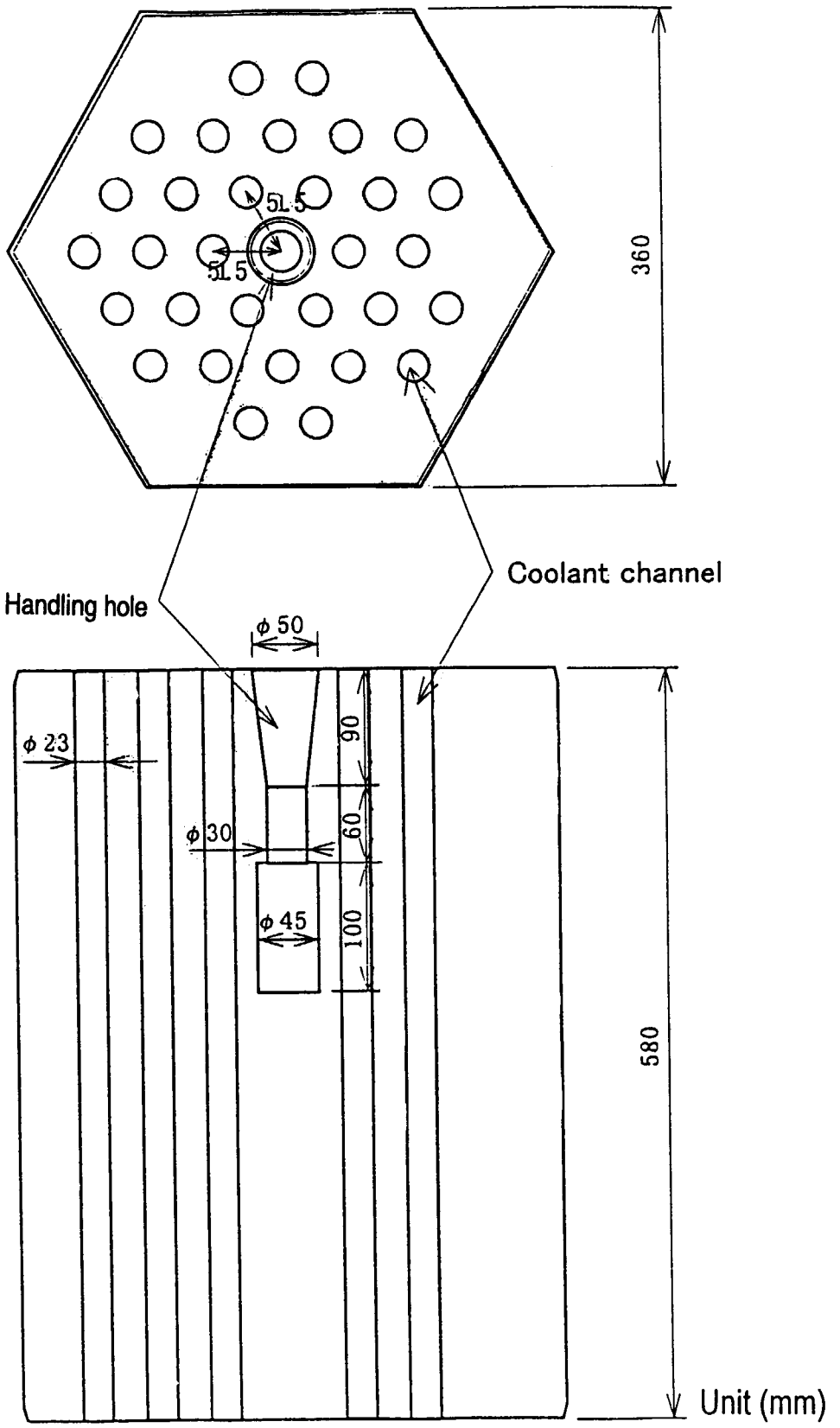

Fig. 3.7 Structural drawing of replaceable reflector block in 1st, 2nd and 8th layer of 31 pins fuel columns

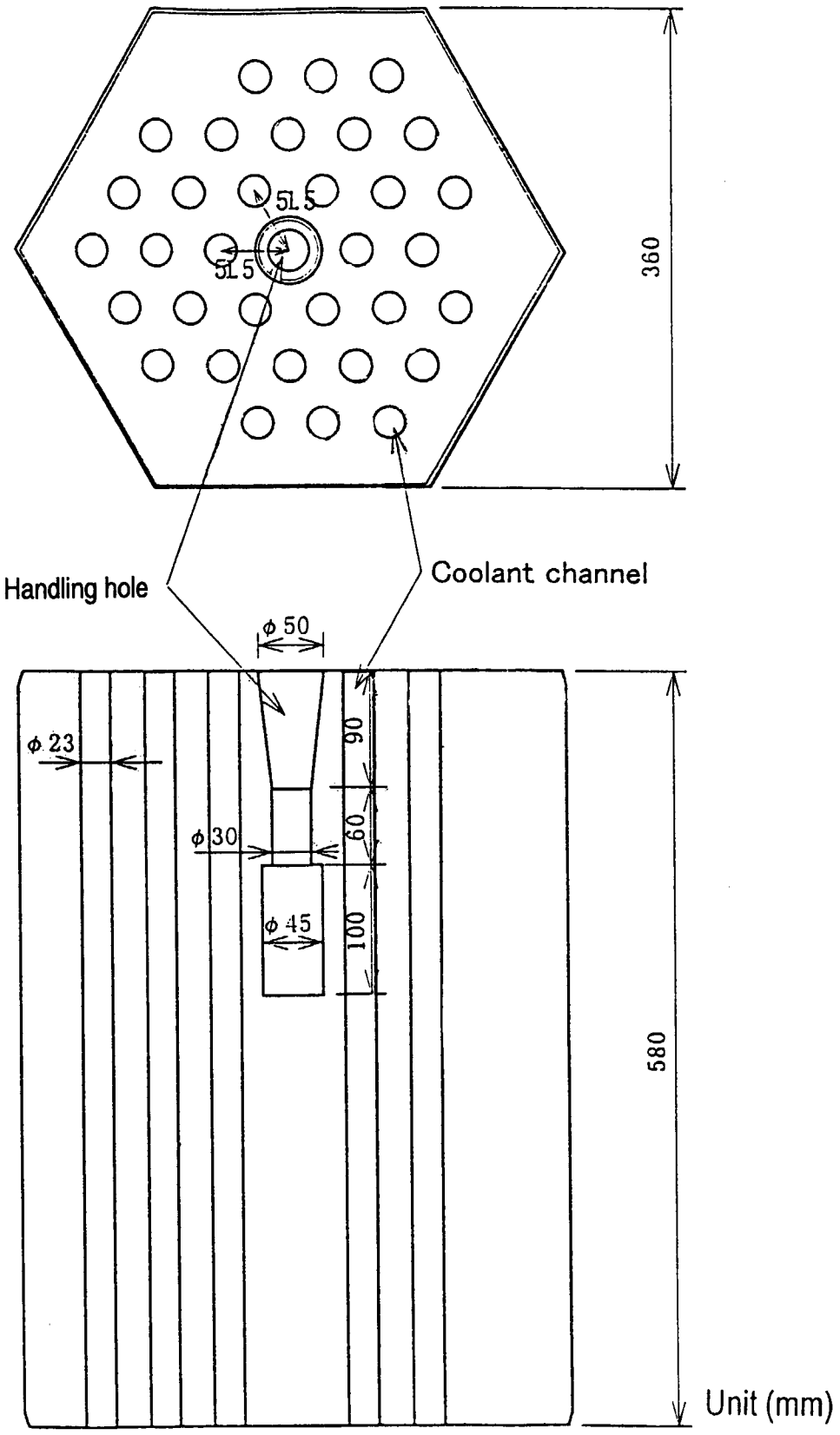

Fig. 3.8 Structural drawing of replaceable reflector block in 1st, 2nd and 8th layer of 33 pins fuel columns

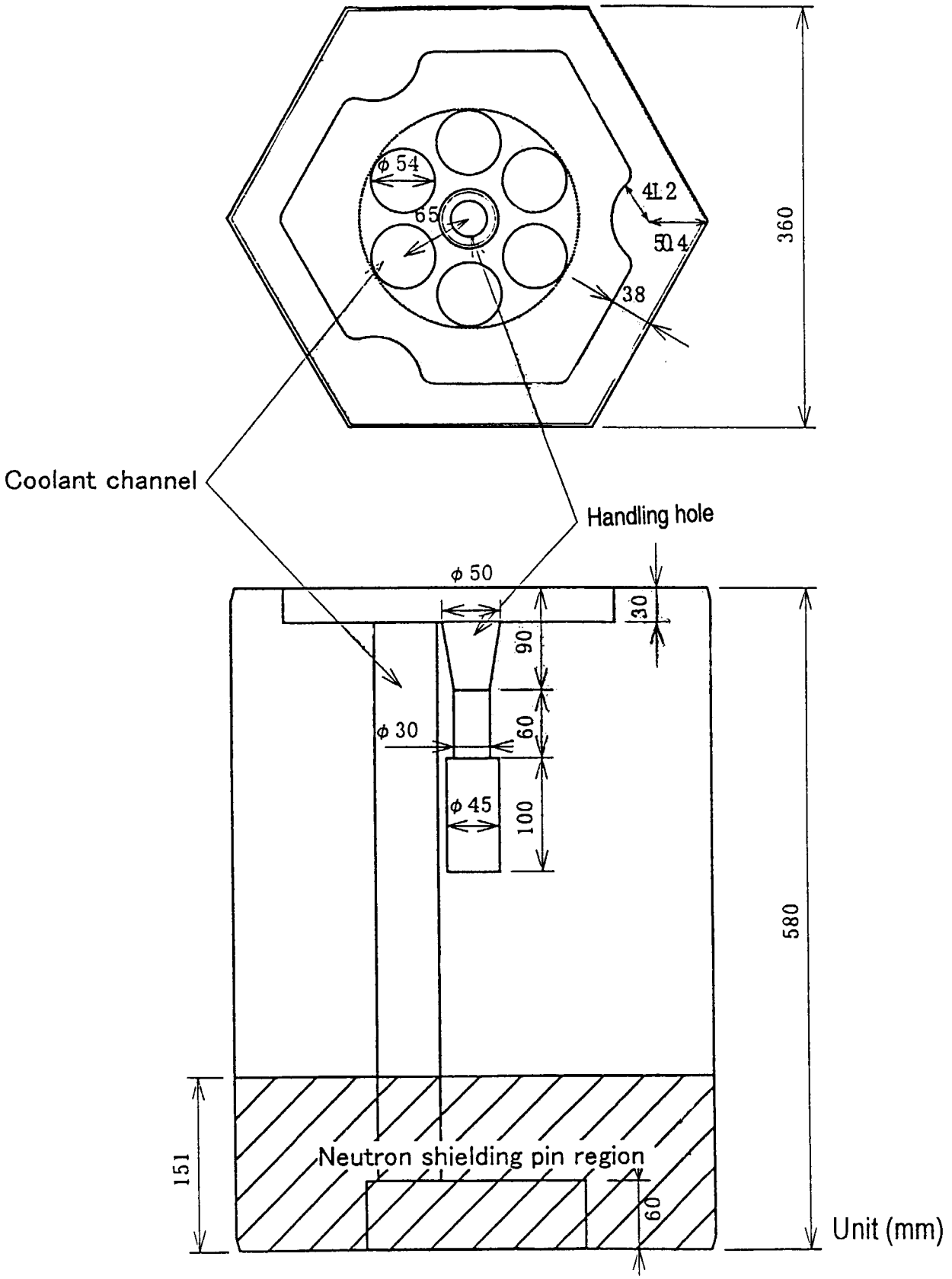

Fig. 3.9 Structural drawing of replaceable reflector block in 9 th layer of fuel columns

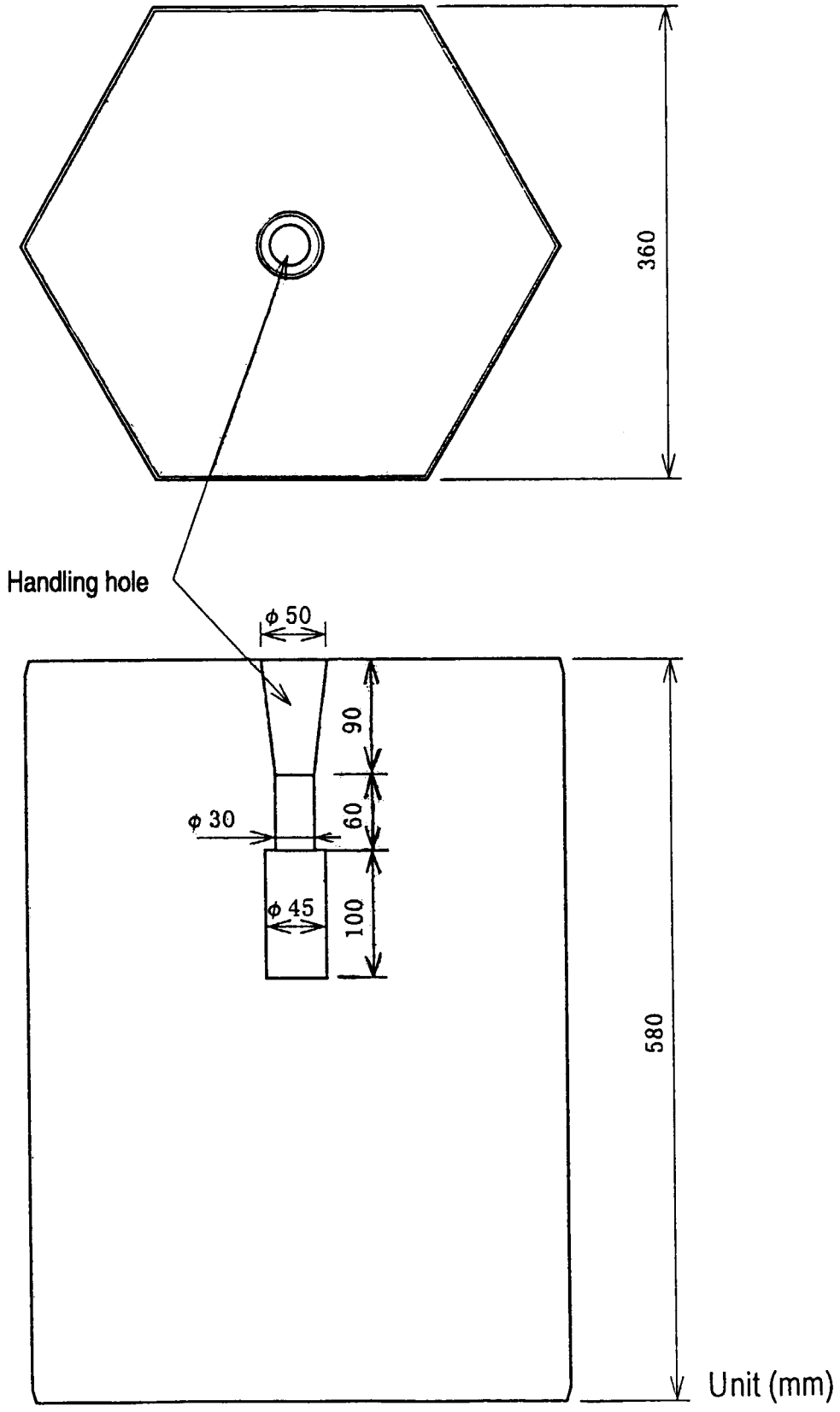

Fig. 3.10 Structural drawing of replaceable reflector block in 1st – 8th layer of replaceable reflector columns

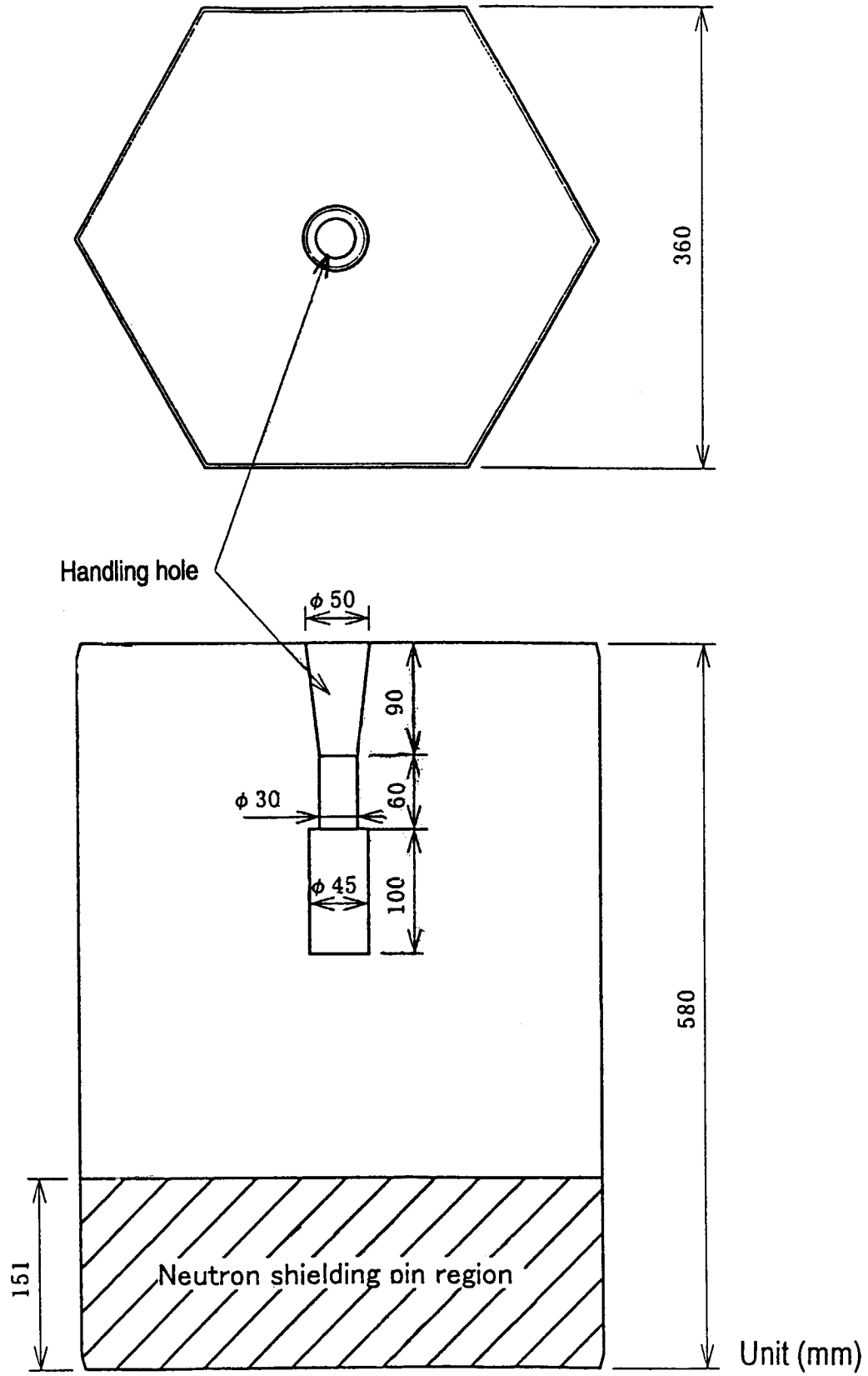

Fig. 3.11 Structural drawing of replaceable reflector block in 9th layer of replaceable reflector columns

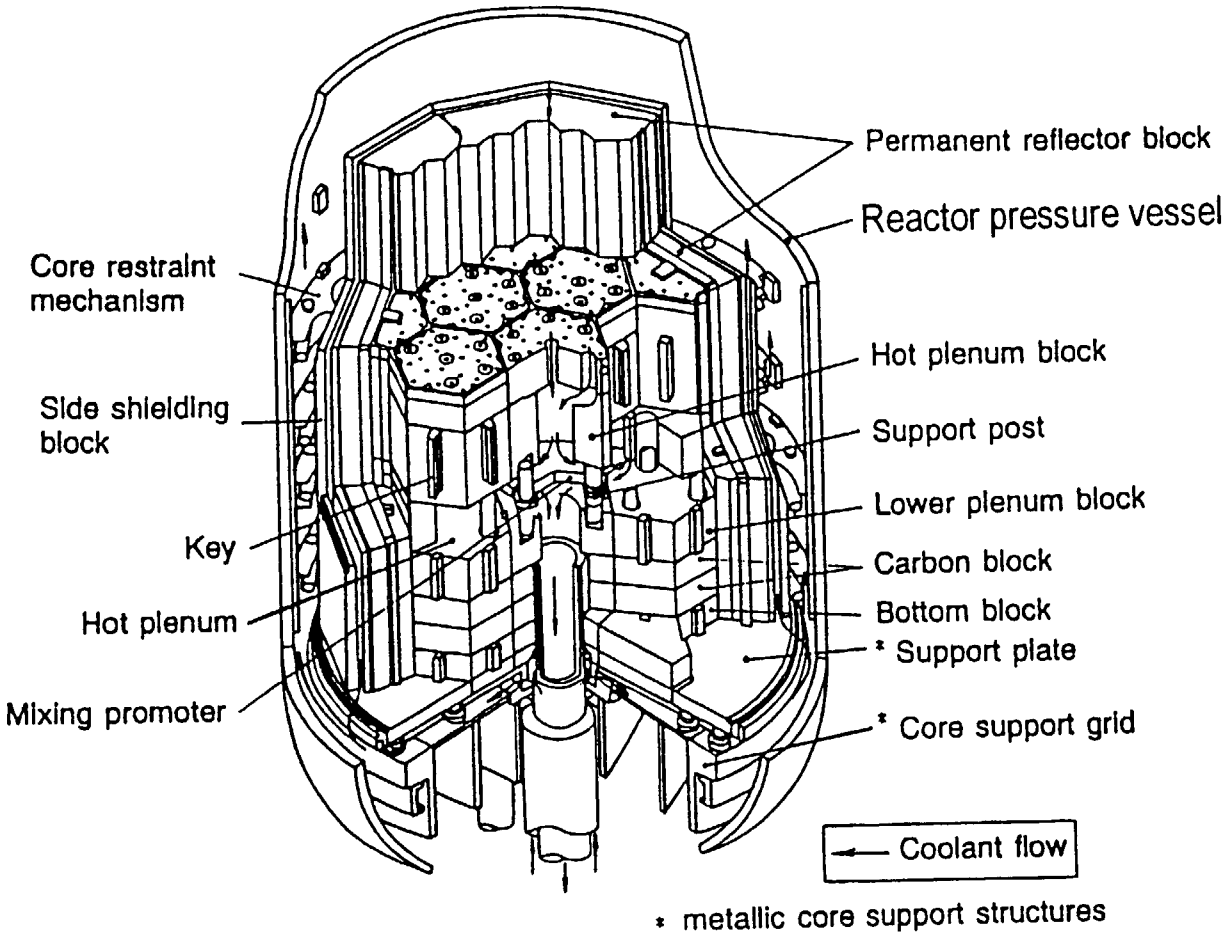

Fig. 3.12 Bird's-eye view of reactor internals

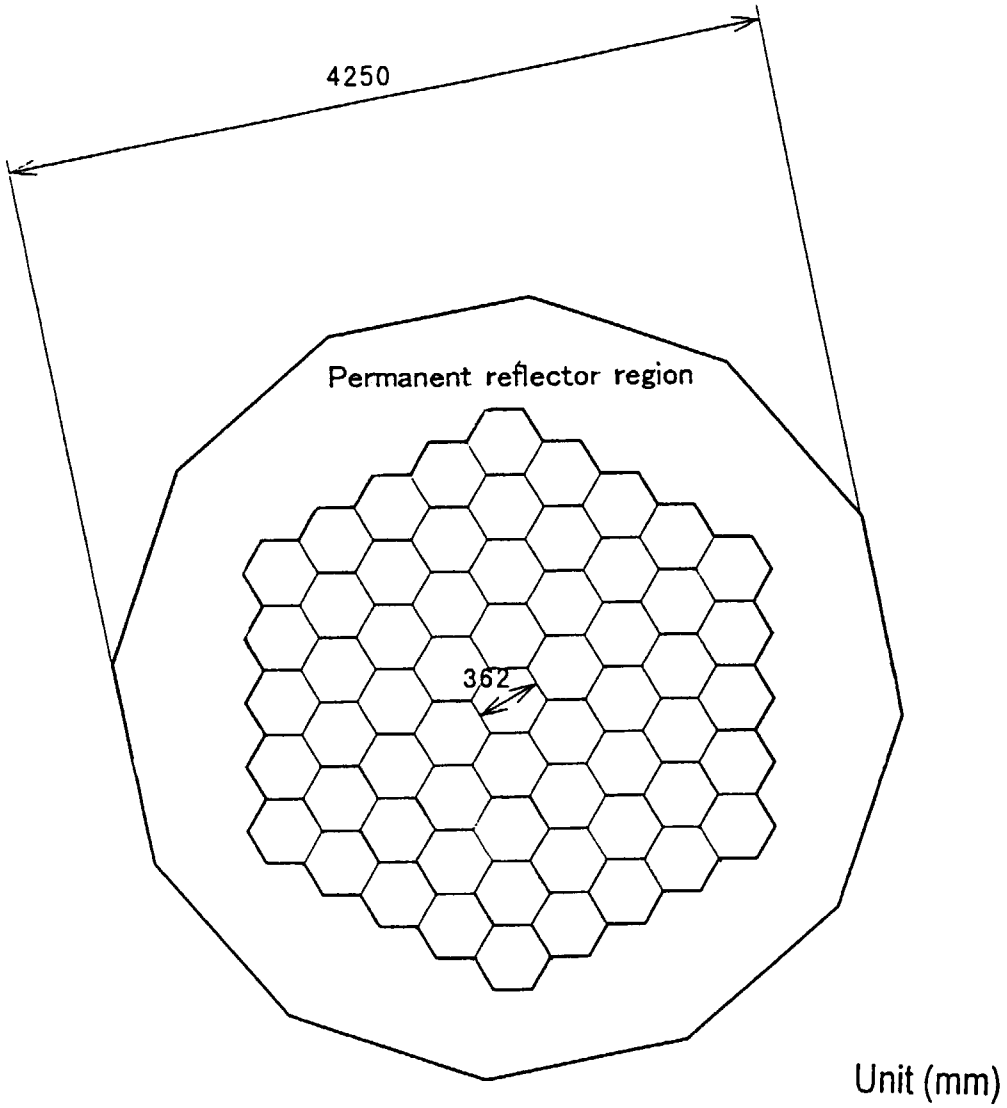

Fig. 3.13 Horizontal view of permanent reflector region

4. Main cooling system

The main cooling system consists of the primary cooling system, secondary helium cooling system and pressurized water cooling system.

4.1 Primary cooling system

Primary coolant is transported from the reactor core to the primary pressurized water cooler and intermediate heat exchanger through the primary concentric hot gas duct. The primary cooling system consists of the primary pressurized water cooler, intermediate heat exchanger, primary concentric hot gas duct and primary helium piping.

4.1.1 Primary pressurized water cooler

The primary pressurized water cooler is a vertical inverse-U-tube type heat exchanger as shown in Figs. 4.1 and 4.2. Hot primary helium from the inlet nozzle flows horizontally between the baffle plates, and cools the outer surface of the heat transfer tubes. It once goes out via the outlet nozzle to the primary helium circulators and goes back to the annular path between the inner and outer shells. The honeycomb plate is installed in the front of the heat transfer tubes to make helium flow uniform around the tubes. The baffle plates not only promote the heat transfer of helium but also keep the heat transfer tubes from the flow-induced vibration. Water from the water inlet nozzle flows into the inlet side of the water chamber and goes upward inside the heat transfer tubes. It turns downward at the inverse U bend portion and flows into the outlet side of the water chamber. Thermal insulator is installed inside the inner shell. Major specifications of the primary pressurized water cooler are given in Table 4.1.

4.1.2 Intermediate heat exchanger

The intermediate heat exchanger is a vertical helically-coiled type heat exchanger as shown in Figs. 4.3 and 4.4. Primary helium flows on the shell side, while secondary helium goes into the tube side. Primary helium is deflected at a hot header and discharged around the heat transfer tubes transferring the heat to the secondary helium cooling system. It flows to the primary helium circulator via the upper outlet nozzle and goes back to the annular path between the inner and outer shells. On the contrary, secondary helium flows downward inside

the heat transfer tubes and goes upward inside the central hot gas duct through the hot header. Thermal insulator is installed inside the inner shell. Major specifications of the intermediate heat exchanger are given in Table 4.2.

4.1.3 Primary helium circulator

The primary helium circulator is a centrifugal and dynamic gas bearing type circulator as shown in Fig. 4.5. Three helium circulators for the primary pressurized water cooler and one for the intermediate heat exchanger are installed in the primary cooling system. Helium from the inlet nozzle flows horizontally between filters and goes downward to impeller unit. A variable speed motor using a frequency converter controls primary helium flow rate. The casing prevents primary helium from leaking into the atmosphere.

4.1.4 Primary concentric hot gas duct

The primary concentric hot gas duct consists of a pressure tube, inner tube, liner and thermal insulator as shown in Fig. 4.6. Hot primary helium goes inside the liner, while lower temperature primary helium flows in annular path between the pressure and inner tubes. The pressure tube can contain high pressure helium. The inner tube separates the hot and lower temperature primary helium paths. The liner located inside the inner tube forms hot primary helium boundary. Lagging material covers the primary concentric hot gas duct. Major specifications of the primary concentric hot gas duct are given in Table 4.3. Major length, inner diameter and elevation of primary helium piping are given in Table 4.4 and Fig. 4.7.

4.2 Secondary helium cooling system

The secondary helium cooling system removes heat from the primary helium through the intermediate heat exchanger. Heat is transported to the pressurized water cooling system through the secondary pressurized water cooler. The secondary helium cooling system consists of the secondary pressurized water cooler, secondary helium circulator, secondary concentric hot gas duct and secondary helium piping. As shown in Fig. 4.8, the secondary pressurized water cooler is a vertical inverse-U-tube type heat exchanger, similar to the primary pressurized water cooler. One secondary helium circulator for the secondary pressurized water cooler is a centrifugal and dynamic gas bearing type circulator. The

secondary concentric hot gas duct consists of a pressure tube, inner tube, liner and thermal insulator as shown in Fig. 4.9. Lagging material covers the secondary concentric hot gas duct. Major specifications of the secondary pressurized water cooler and secondary concentric hot gas duct are given in Tables 4.5 and 4.6, respectively. Major length, inner diameter and elevation of secondary helium piping are given in Table 4.7 and Fig. 4.10.

4.3 Pressurized water cooling system

The pressurized water cooling system consists of an air cooler (Fig. 4.11), water pump and water piping. The air cooler with fins cools water in the primary and secondary pressurized water coolers and transfers heat from the reactor core to the final heat sink of atmosphere. Air flowing into the shell side of the air cooler through its fans cools the outer surface of the heat transfer tubes in which water flows. The water pump is a horizontal and centrifugal type pump. Major specifications of the air cooler for the pressurized water cooling system are given in Table 4.8. Major length, inner diameter and elevation of water piping for the pressurized water cooling system are given in Table 4.9 and Fig. 4.12.

Table 4.1 Major specifications of primary pressurized water cooler

1. Number of heat transfer tubes	136
2. Outer diameter of heat transfer tube	25.4mm
3. Thickness of heat transfer tube	2.6mm
4. Number of rows of heat transfer tubes	8
5. Effective axial length of flow path of primary helium	2.49m
6. Average cross section of flow path of primary helium	0.7114m^2
7. Total heat transfer area	54m^2
8. Material of inner and outer shells	2 1/4 Cr-1 Mo steel
9. Material of heat transfer tubes	321TB stainless steel

Table 4.2 Major specifications of intermediate heat exchanger

1. Number of heat transfer tubes	96
2. Outer diameter of heat transfer tube	31.8mm
3. Thickness of heat transfer tube	3.5mm
4. Number of rows of heat transfer tubes	6
5. Effective axial length of flow path of primary helium	4.87m
6. Average cross section of flow path of primary helium	0.173m^2
7. Total heat transfer area	244m^2
8. Length of flow path of secondary helium	22.4m
9. Material of inner and outer shells	2 1/4 Cr-1 Mo steel
10.Material of heat transfer tubes	Hastelloy XR

Table 4.3 Major specifications of primary concentric hot gas duct

Unit(m)

Flow path	Length	Liner**	Therm*	Inner tube**		Pressure tube**		Lagg*
		ID*	ID*	ID*	OD*	ID*	OD*	OD*
①	9.846	0.436	0.45	0.6304	0.6604	0.7796	0.8636	1.1636
②	0.924	0.436	0.45	0.6304	0.6604	0.7796	0.8636	1.1636
③	6.081	0.206	0.22	0.6304	0.6604	0.7796	0.8636	1.1636

①;Duct from reactor to T junction
②;Duct from primary pressurized water cooler to T junction
③;Duct from intermediate heat exchanger to T junction

* Therm; Thermal insulator, Lagg; Lagging material, ID;Inner diameter, OD;Outer diameter
** Material of pressure tube and inner tube; 2 1/4Cr-1 Mo steel, Liner; Hastelloy XR

Table 4.4 Major length, inner diameter and elevation of primary helium piping

Line*	Length	ID**	Point*	Elevation
G1*1	0.924m	0.436m	P1	14.55m
G2*2	10.099m	0.032m	P2	14.35m
G3	8.8m	0.254m	P3	17.649m
G4*2	2.099m	0.19m	P4	16.449m
G5*1	0.924m	0.1192m	P5	14.35m
G6*1	6.081m	0.1192m	P6	14.55m
G7*5	6.115m	0.06m	P7	17.935m
G8	6.5m	0.254m	P8	24.05m
G9*5	8.195m	0.047m	P9	25.6m
G10*1	6.081m	0.206m	P10	18.15m
G11*1	9.846m	0.436m	P11	20.05m
G12*3	6.318m	0.155m	P12	14.55m
G13*4	6.65m	0.095m	P13	17.45m
G14	5.85m	0.1654m	P14	14.3m
G15*4	2m	0.115m	P15	14.55m
G16*3	6.318m	0.071m	P16	18.575m
G17*1	9.846m	0.1192m		

* Flow line G1-G17 and pressure point P1-P6 are shown in Fig. 4.7.
** ID;Inner diameter
*1 Primary concentric hot gas duct
*2 Primary pressurized water cooler
*3 Auxiliary concentric hot gas duct
*4 Auxiliary heat exchanger
*5 Intermediate heat exchanger

Table 4.5 Major specifications of secondary pressurized water cooler

1. Number of heat transfer tubes	104
2. Outer diameter of heat transfer tube	25.4mm
3. Thickness of heat transfer tube	2.6mm
4. Number of rows of heat transfer tubes	9
5. Effective axial length of heat transfer tube	3.32m
6. Average cross section of flow path of secondary helium	0.3884m^2
7. Total heat transfer area	55m^2
8. Material of inner and outer shells	2 1/4 Cr-1 Mo steel
9. Material of heat transfer tubes	321TB stainless steel

Table 4.6 Major specifications of secondary concentric hot gas duct

Unit(m)

Flow path	length	Liner**	Therm*	Inner tube**		Pressure tube**		Lagg*
		ID*	ID*	ID*	OD*	ID*	OD*	OD*
①	5.15	0.240	0.250	0.381	0.4064	0.5028	0.5588	0.7988

①;Duct from intermediate heat exchanger to secondary pressurized water cooler
* Therm; Thermal insulator, Lagg; Lagging material, ID;Inner diameter, OD;Outer diameter
** Material of pressure tube and inner tube; 2 1/4Cr-1 Mo steel, Liner; Hastelloy XR

Table 4.7 Major length, inner diameter and elevation of secondary helium piping

Line*	Length	ID**	Point*	Elevation
G1	5.15m	0.0964m	P1	28.695m
G2*1	22.4m	0.0248m	P2	26.7m
G3*2	5.15m	0.24m	P3	26.7m
G4*3	10.801m	0.41m	P4	28.695m
G5	3.7m	0.254m	P5	25.944m
G6*3	1.926m	0.2m	P6	26.769m

* Flow line G1-G6 and pressure point P1-P6 are shown in Fig. 4.9.
** ID;Inner diameter
*1 Intermediate heat exchanger
*2 Secondary concentric hot gas duct
*3 Secondary pressurized water cooler

Table 4.8 Major specifications of air cooler for pressurized water cooling system

1. Number of heat transfer tubes	504
2. Outer diameter of heat transfer tube	25.4mm
3. Thickness of heat transfer tube	2.77mm
4. Number of fins of heat transfer tubes	10 per 25.4mm
5. Effective axial length of heat transfer tube	11.975m
6. Average cross section of flow path of air	219.8m^2
7. Material of heat transfer tubes	2 1/4 Cr-1 Mo steel

Table 4.9 Major length, inner diameter and elevation of water piping for pressurized water cooling system

Line*	Length	ID**	Point*	Elevation
G1	62m	0.2488m	P1	23.2m
G2*1	4.98m	0.0202m	P2	11.005m
G3	37m	0.2488m	P3	11.005m
G4	26m	0.151m	P4	24.2011m
G5	2m	0.2488m	P5	25.1m
G6	10m	0.2488m	P6	25.1m
G7	60m	0.2488m	P7	53.6m
G8*2	24m	0.01986m	P8	53.6m
G9	68m	0.2488m	P9	26.5m
G10	60m	0.2488m	P10	24.05m
G11	46m	0.151m	P11	24.05m
G12*3	6.62m	0.0202m		
G13	30m	0.151m		

* Flow line G1-G13 and pressure point P1-P11 are shown in Fig. 4.11.
** ID;Inner diameter
*1 Primary pressurized water cooler
*2 Air cooler
*3 Secondary pressurized water cooler

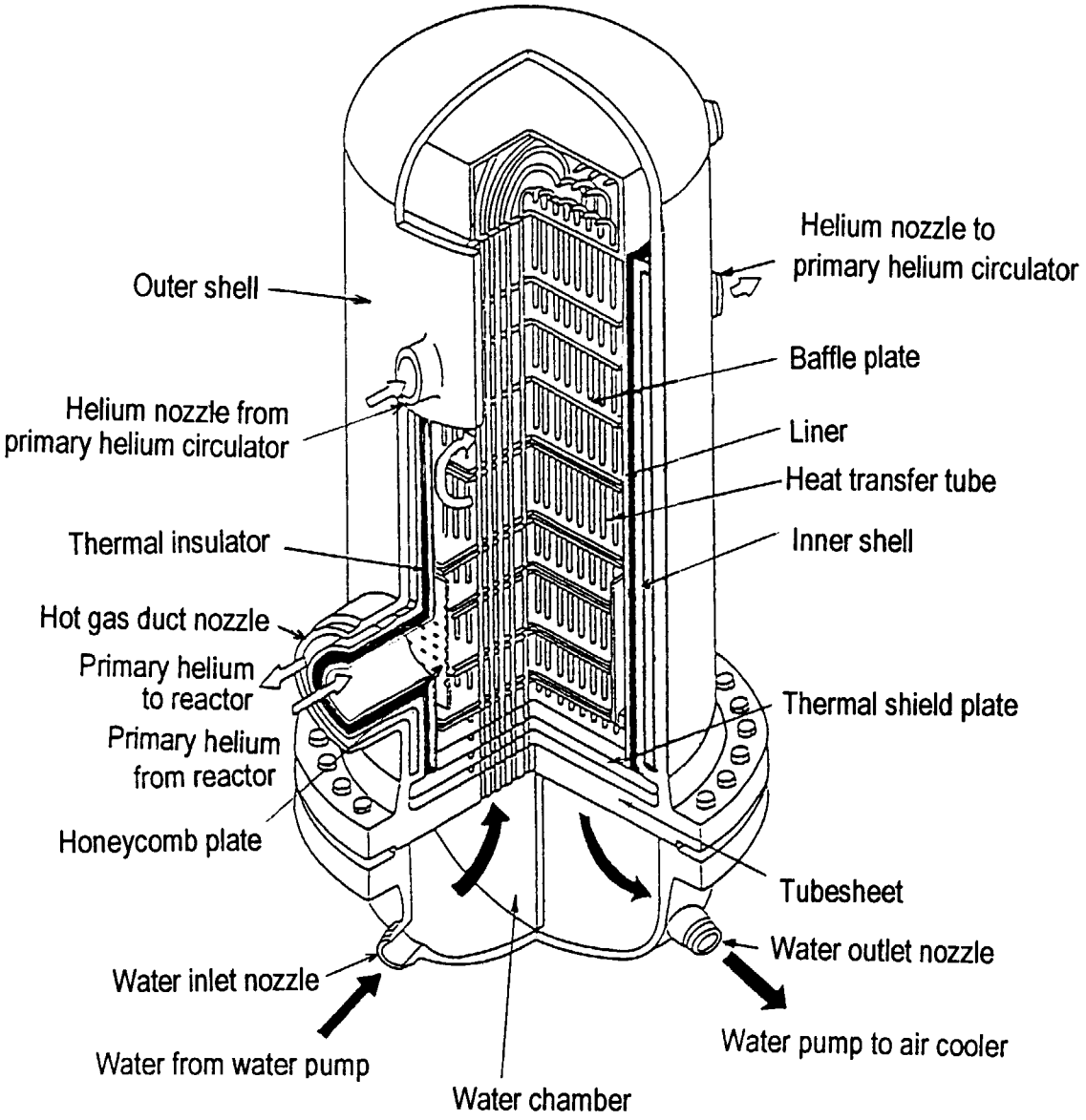

Fig. 4.1 Bird's-eye view of primary pressurized water cooler

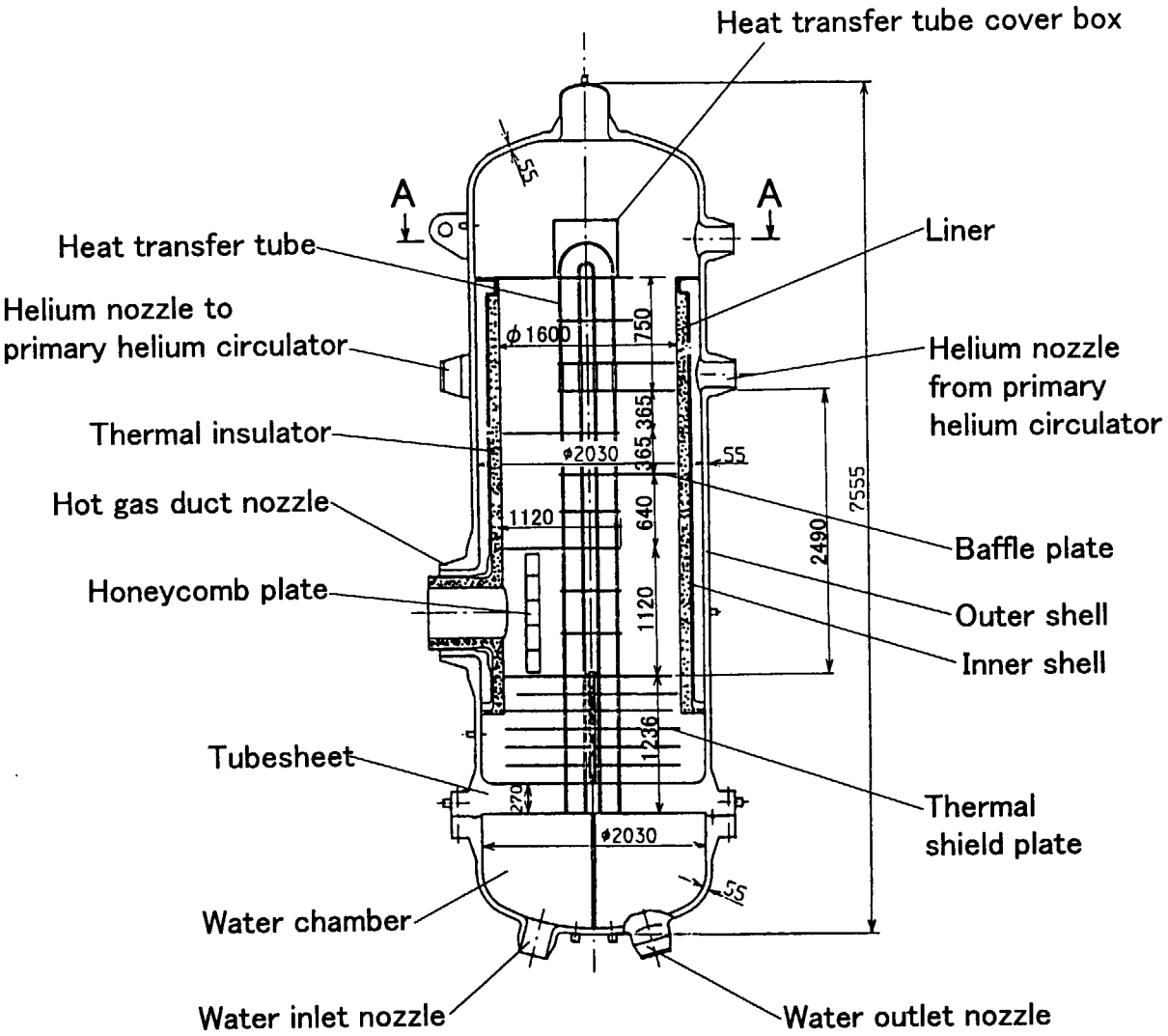

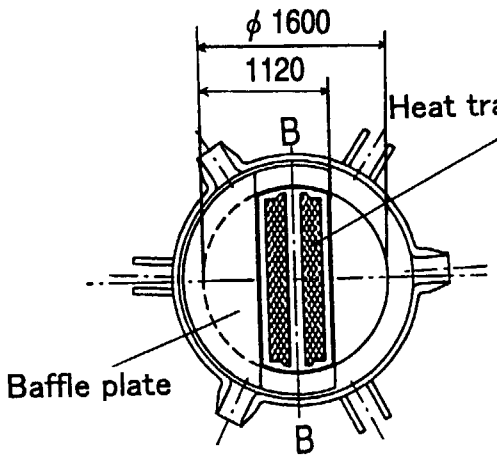

Section A–A

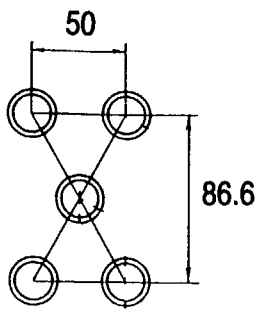

Tube arrangement

	Num*3	Dis*4
1st row*1	18	64mm
2nd row	17	89mm
3rd row	18	114mm
4th row	17	139mm
5th row	16	164mm
6th row	17	189mm
7th row	16	214mm
8th row*2	17	239mm

*1 Inner side
*2 Outer side
*3 Number of tubes
*4 Distance from Line B-B to center of tubes

Fig. 4.2 Structural drawing of primary pressurized water cooler

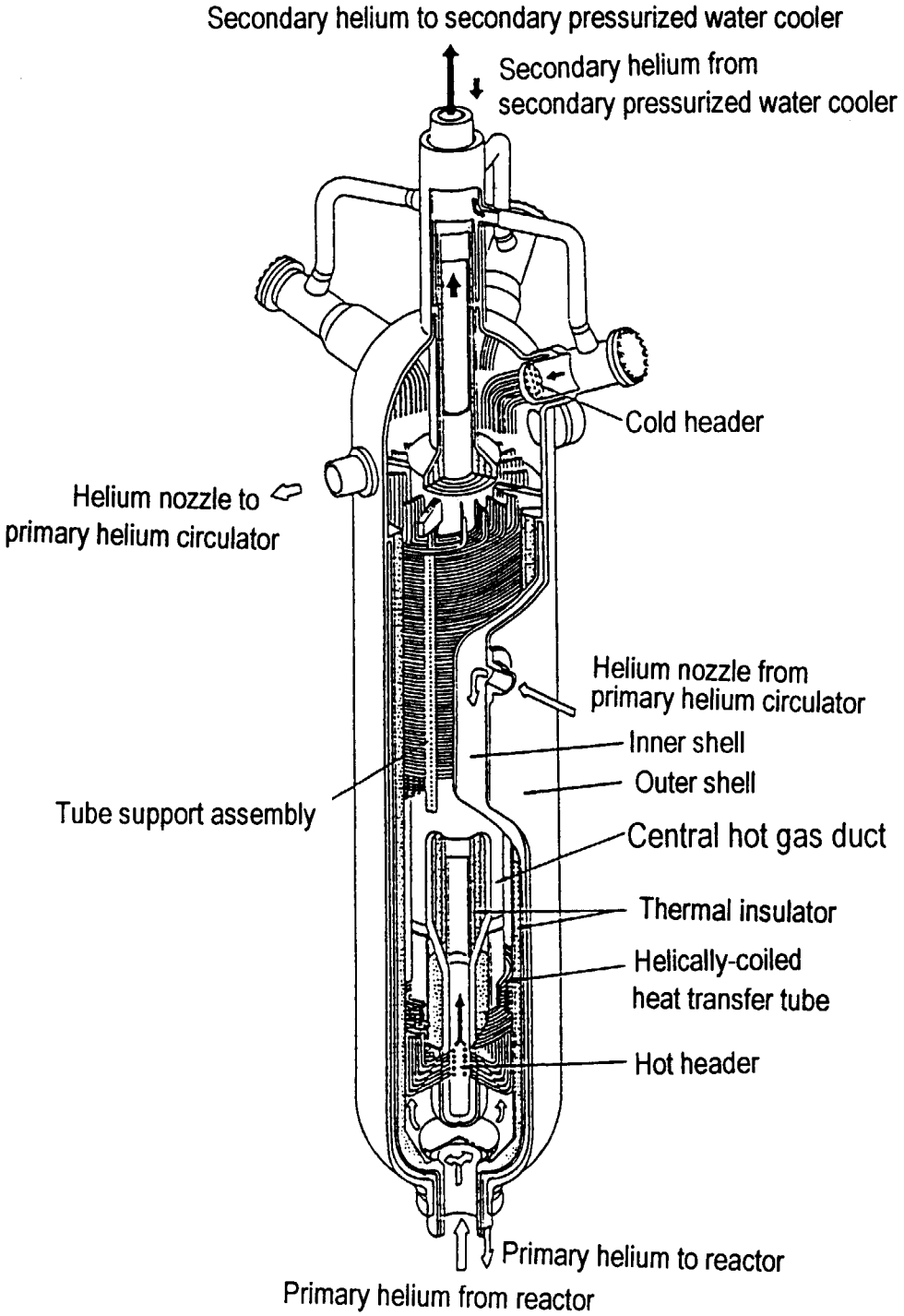

Fig. 4.3 Bird's-eye view of intermediate heat exchanger

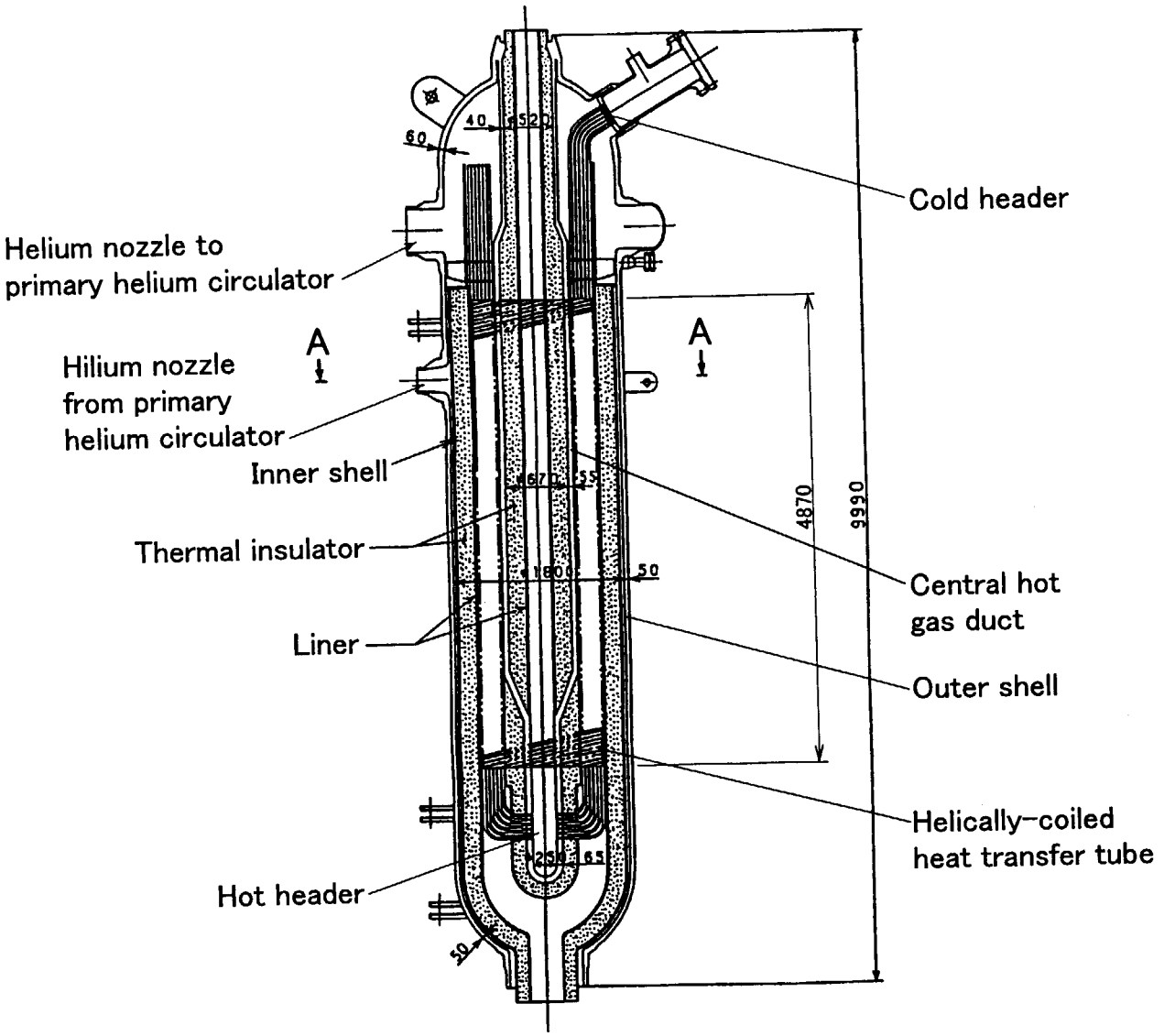

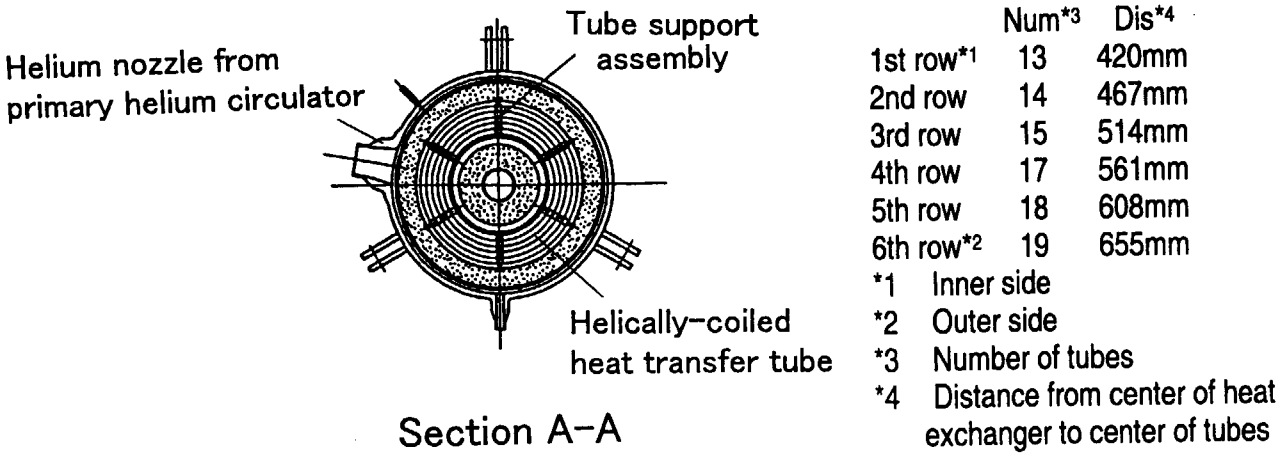

	Num*3	Dis*4
1st row*1	13	420mm
2nd row	14	467mm
3rd row	15	514mm
4th row	17	561mm
5th row	18	608mm
6th row*2	19	655mm

*1 Inner side
*2 Outer side
*3 Number of tubes
*4 Distance from center of heat exchanger to center of tubes

Fig. 4.4 Structural drawing of intermediate heat exchanger

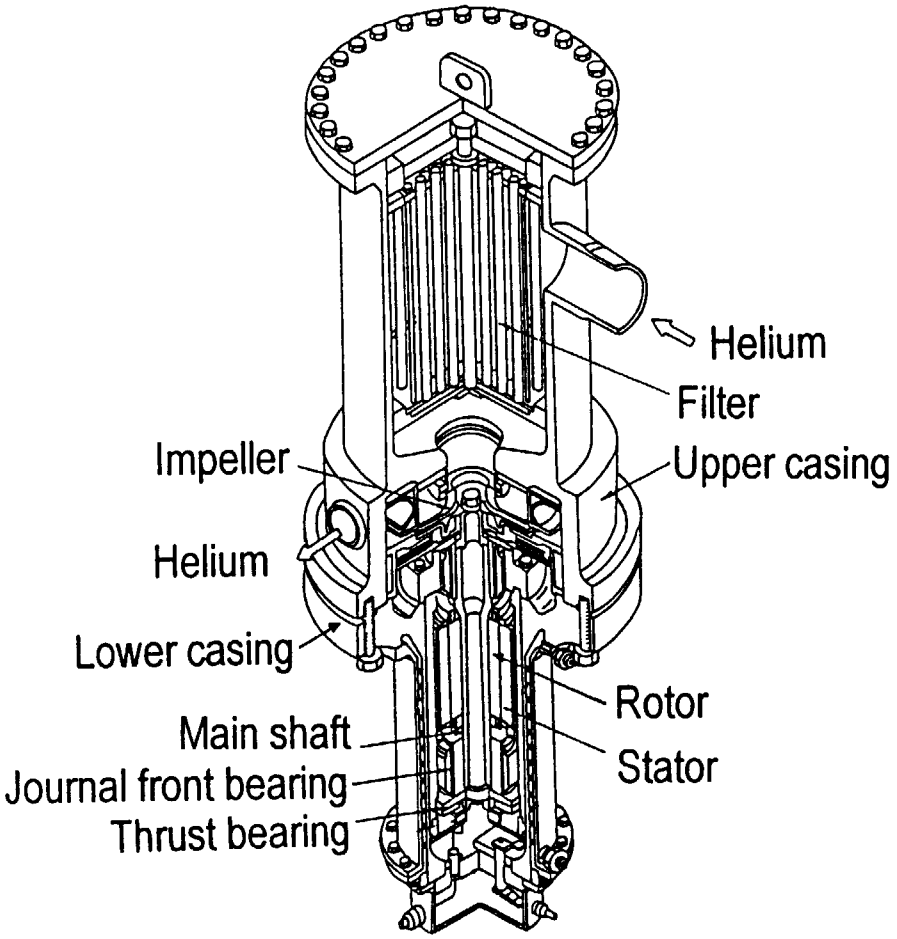

Fig. 4.5 Bird's-eye view of helium circulator

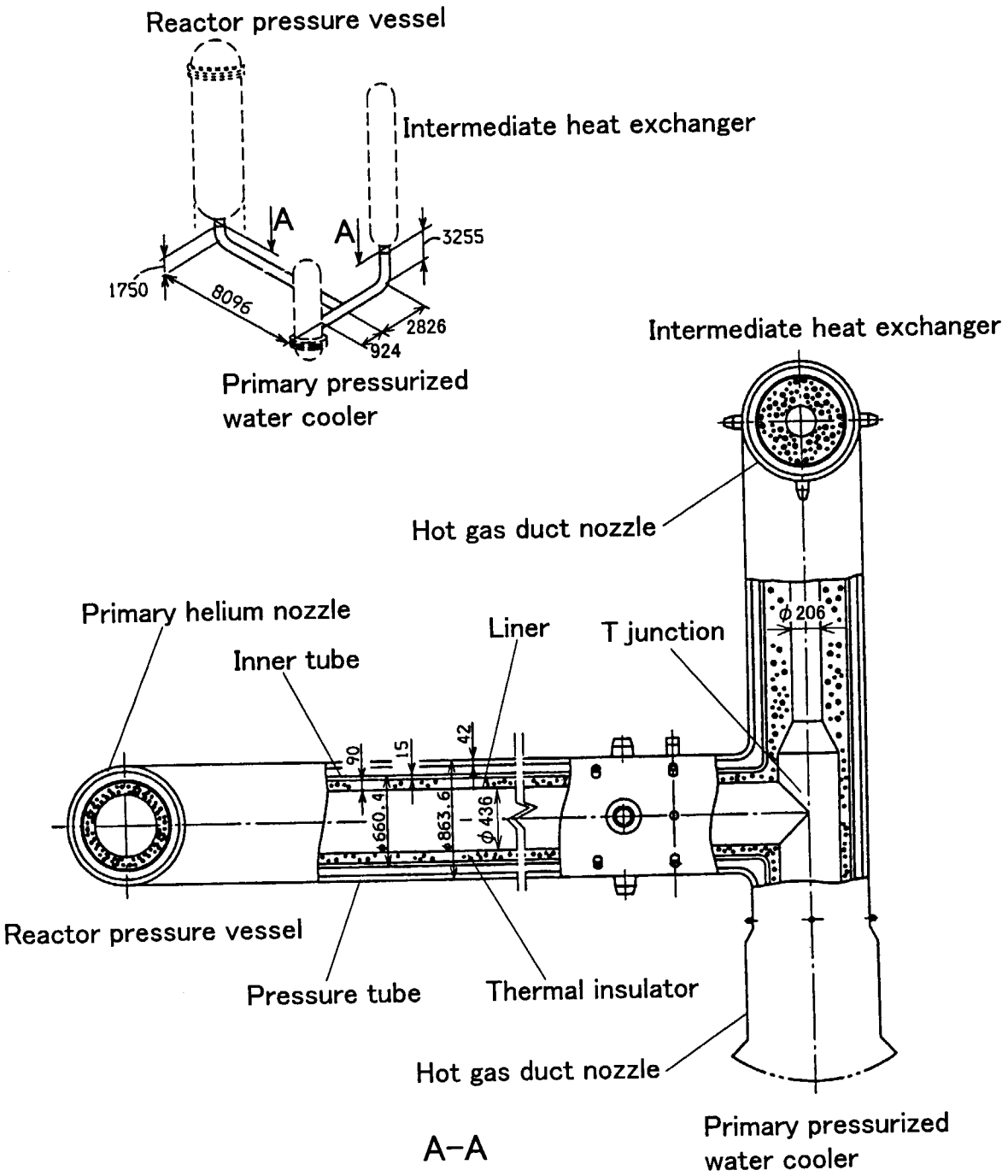

Fig. 4.6 Cross-sectional view of primary concentric hot gas duct

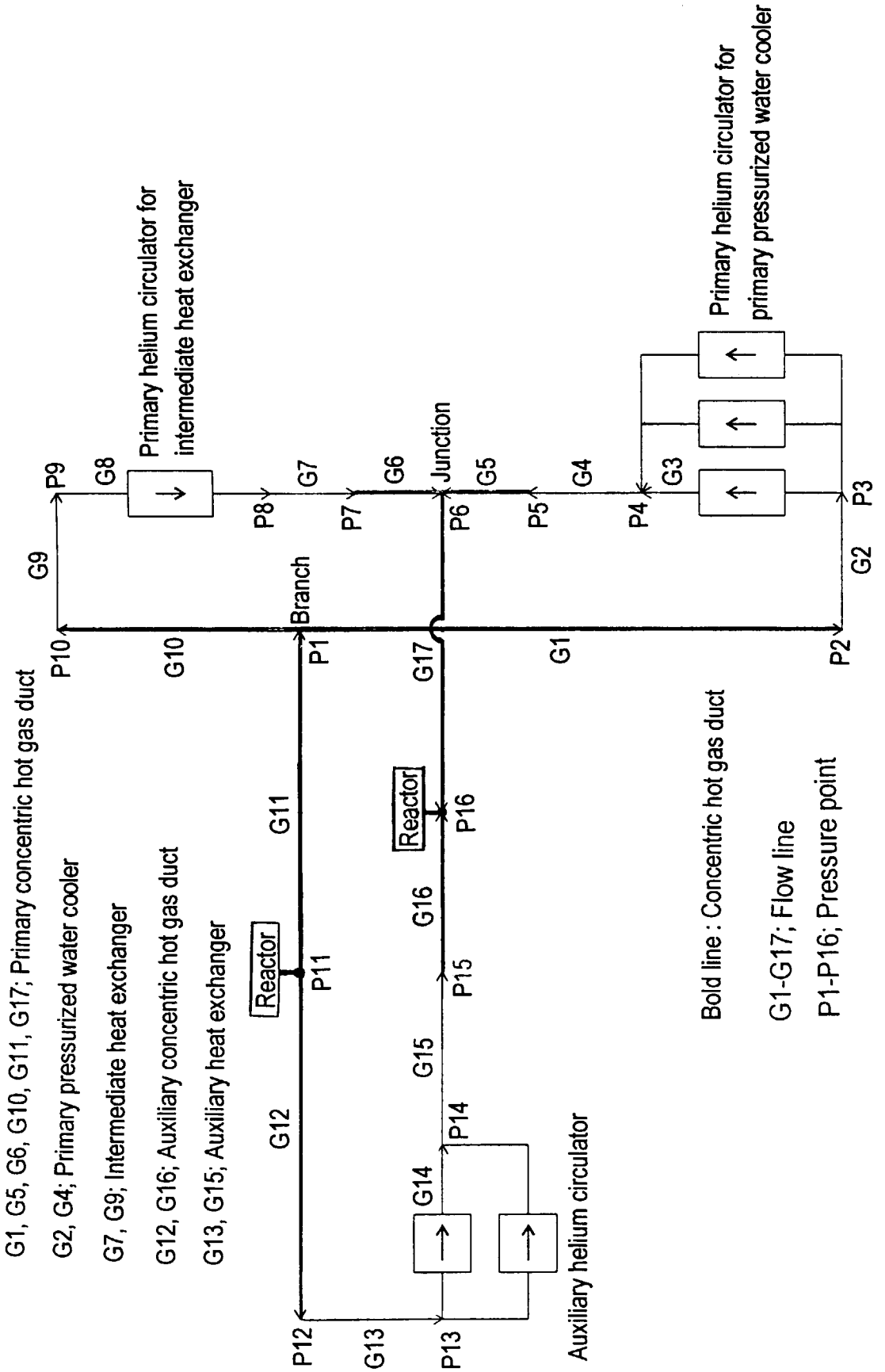

Fig. 4.7 Flow network diagram of primary helium piping

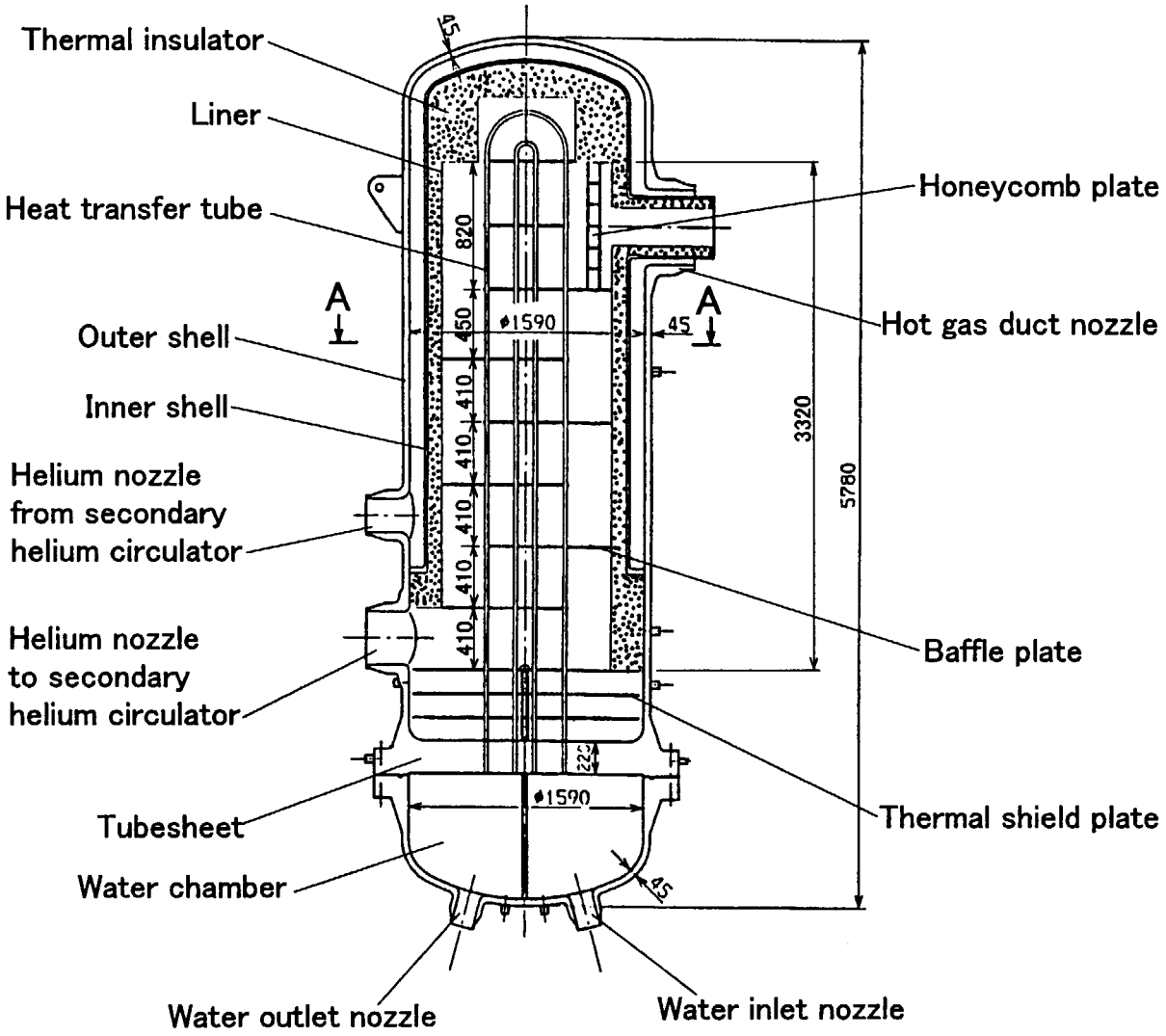

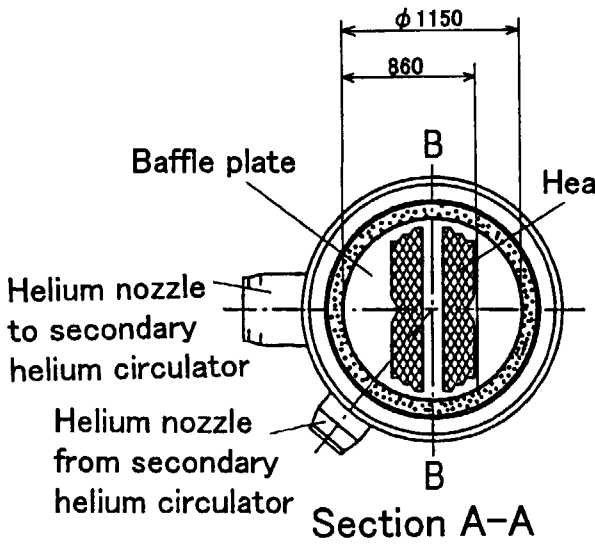

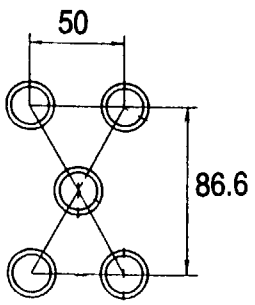

	Num*3	Dis*4
1st row*1	13	64mm
2nd row	12	89mm
3rd row	13	114mm
4th row	12	139mm
5th row	11	164mm
6th row	12	189mm
7th row	11	214mm
8th row	10	239mm
9th row*2	10	264mm

*1 Inner side
*2 Outer side
*3 Number of tubes
*4 Distance from Line B-B to center of tubes

Fig. 4.8 Structural drawing of secondary pressurized water cooler

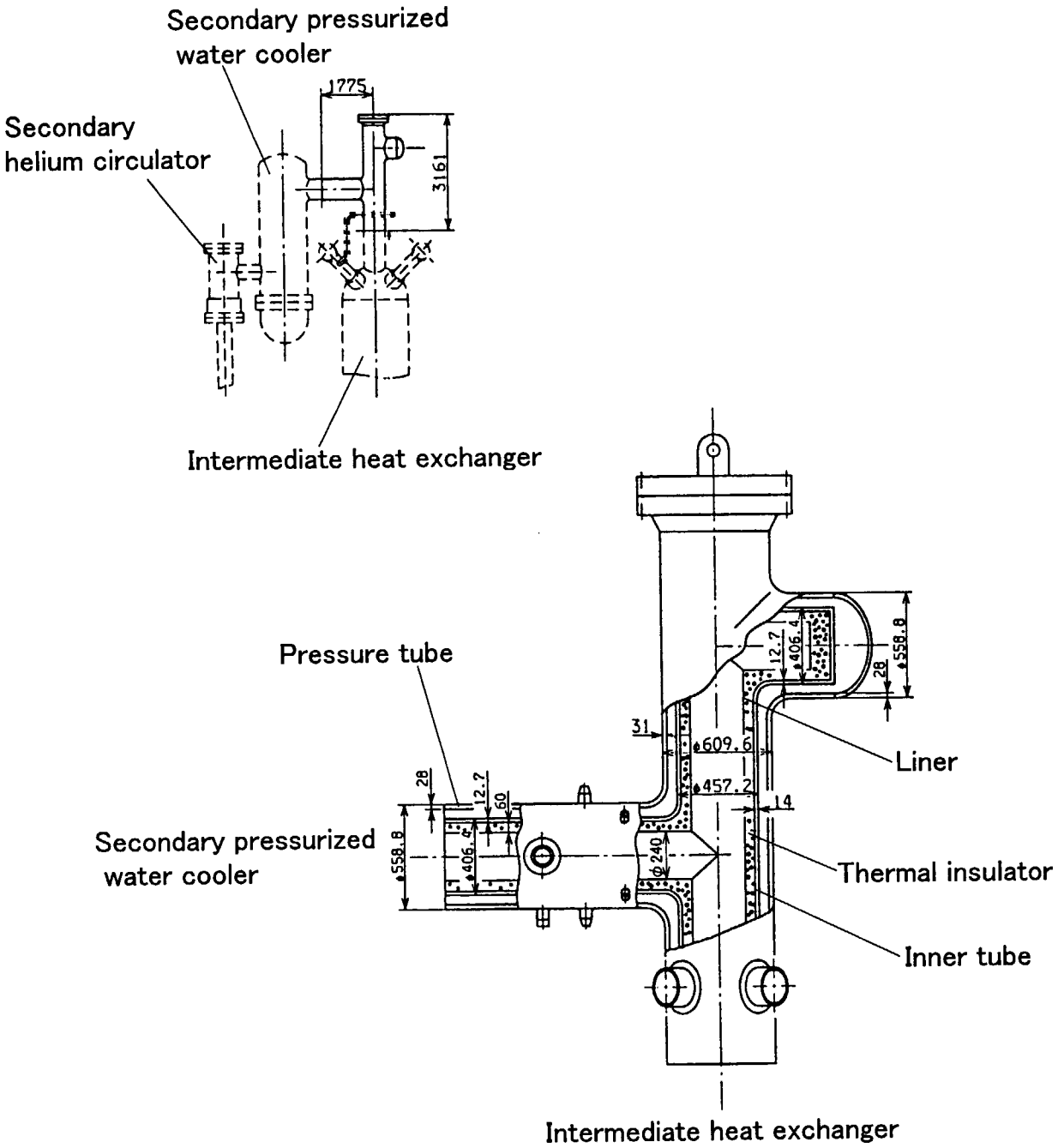

Fig. 4.9 Cross-sectional view of secondary concentric hot gas duct

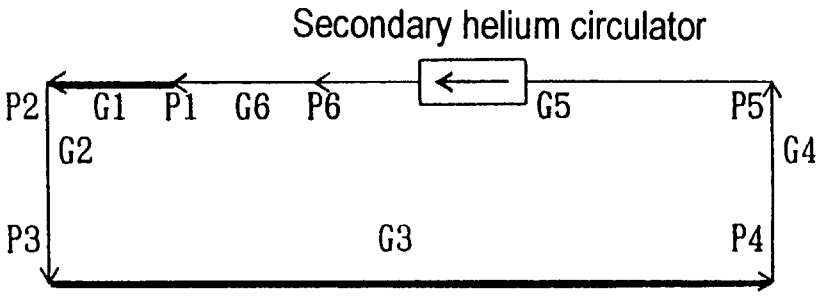

G2; Intermediate heat exchanger

G4, G6; Secondary pressurized water cooler

Bold line : Concentric hot gas duct

G1-G6; Flow line

P1-P6; Pressure point

Fig. 4.10 Flow network diagram of secondary helium piping

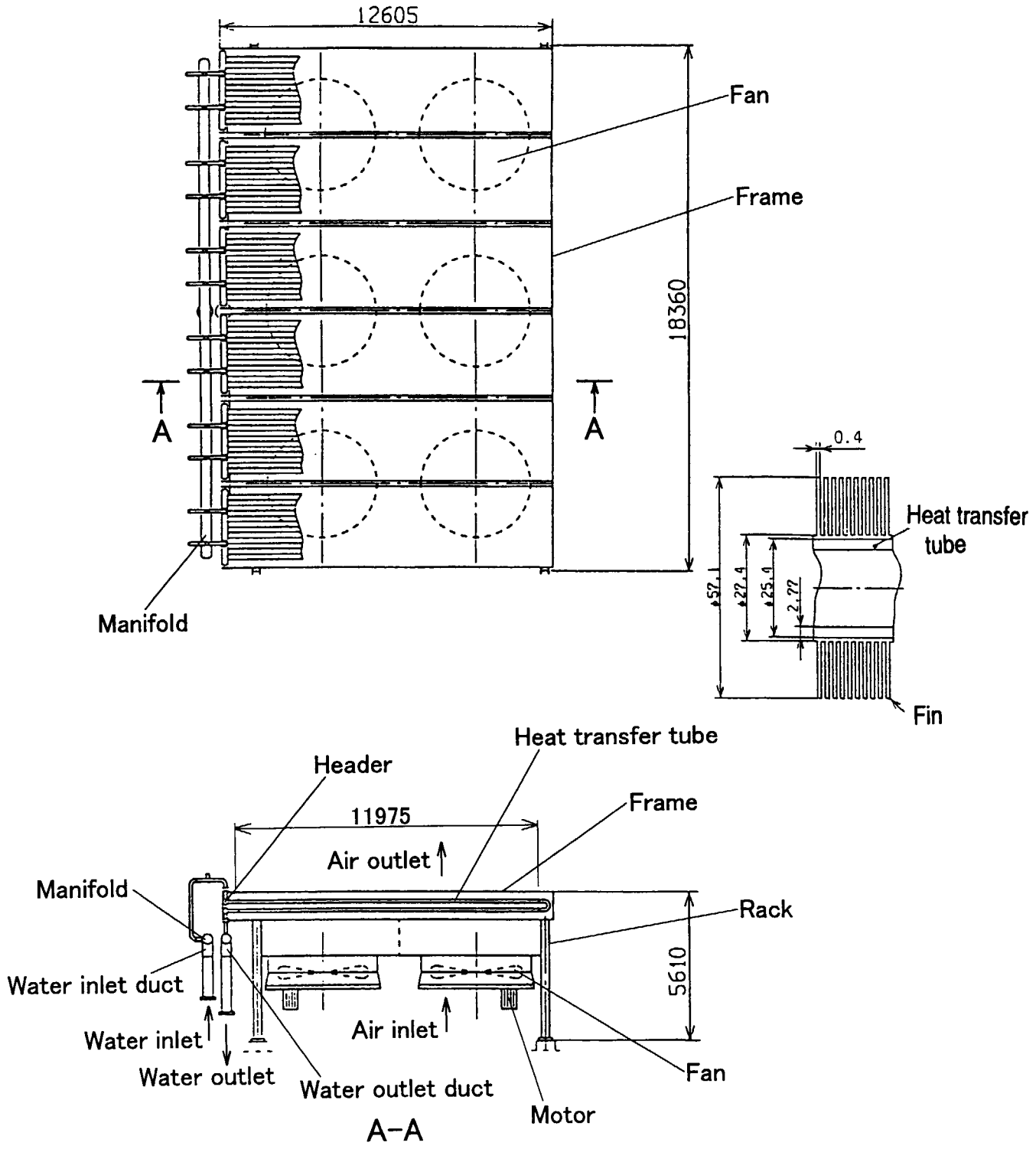

Fig. 4.11 Structural drawing of air cooler for pressurized water cooling system

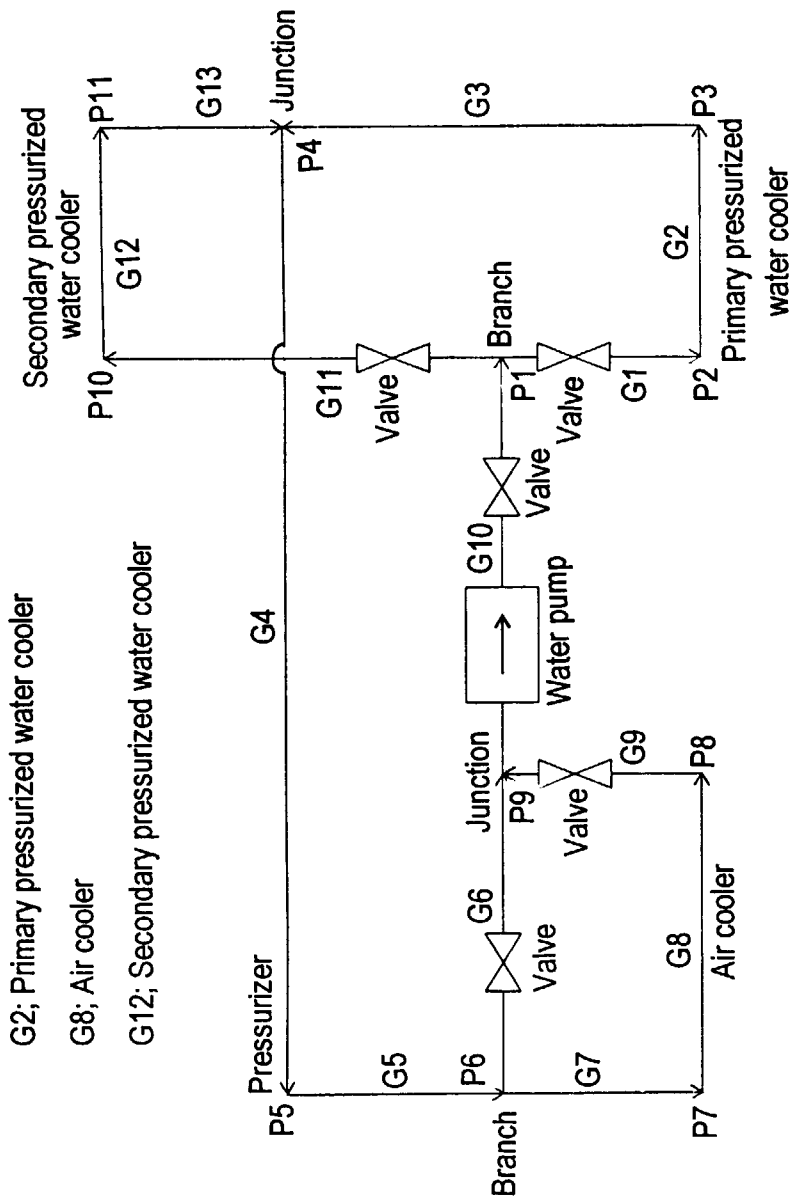

G1-G13; Flow line
P1-P11; Pressure point

Fig. 4.12 Flow network diagram of water piping for pressurized water cooling system

5. Residual heat removal system

The HTTR has two residual heat removal systems; the auxiliary cooling system and vessel cooling system as shown in Fig. 5.1.

5.1 Auxiliary cooling system

The auxiliary cooling system is in standby during the normal operation and automatically starts up when the reactor is scrammed in an accident. The auxiliary cooling system consists of an auxiliary heat exchanger, two auxiliary helium circulators, auxiliary concentric hot gas duct, air cooler, two water pumps and water piping. As shown in Figs. 5.2 and 5.3, the auxiliary heat exchanger is a vertical inverse-U-tube type heat exchanger, similar to the primary and secondary pressurized water coolers. During the standby of the auxiliary cooling system, small amount of hot primary coolant from the reactor core flows inside the liner of the auxiliary heat exchanger. It once goes out via the nozzle to the purification system and goes back to the annular path between the inner and outer shells. Then helium flow rate is 0.036kg/s. The two auxiliary helium circulators for the auxiliary heat exchanger are centrifugal and dynamic gas bearing type circulators. The auxiliary concentric hot gas duct consists of a pressure tube, inner tube, liner and thermal insulator as shown in Fig. 5.4. Lagging material covers the auxiliary concentric hot gas duct. The air cooler with fins (Fig. 5.5) cools water in the auxiliary heat exchanger and transports residual heat from the reactor core to the final heat sink of atmosphere. The water pumps are horizontal and centrifugal type pumps. Major specifications of the auxiliary heat exchanger, auxiliary concentric hot gas duct and air cooler for the auxiliary cooling system are given in Tables 5.1, 5.2 and 5.3, respectively. Major length, inner diameter and elevation of water piping for the auxiliary cooling system are given in Table 5.4 and Fig. 5.6.

5.2 Vessel cooling system

The vessel cooling system operates to cool the biological concrete shield during the normal operation and removes residual heat in an accident in which forced circulation of the primary coolant cannot be maintained. As shown in Fig. 5.7, the vessel cooling system consists of upper, lower and side cooling panels as well as heat removal adjustment panels around the reactor pressure vessel. The cooling panels cool the reactor pressure vessel by radiation and natural convection, as will be described in Section 9.3 (1). Height of the reactor pressure vessel is 13.2m. Width between the reactor pressure vessel and vessel cooling system is 0.988m. Temperature of the side cooling panels of the vessel cooling system is about 60°C under 30MW thermal power. The amount of the heat removal of the vessel cooling system is adjusted to more than 0.3MW under 30MW thermal power.

Table 5.1 Major specifications of auxiliary heat exchanger

1. Number of heat transfer tubes	33
2. Outer diameter of heat transfer tube	25.4mm
3. Thickness of heat transfer tube	2.6mm
4. Number of rows of heat transfer tubes	5
5. Effective axial length of heat transfer tube	2.6m
6. Average cross section of flow path of primary helium	0.09112m^2
7. Total heat transfer area	13m^2
8. Material of inner and outer shells	2 1/4 Cr-1 Mo steel
9. Material of heat transfer tubes	321TB stainless steel

Table 5.2 Major specifications of auxiliary concentric hot gas duct

Unit(m)

Flow path	Length	Liner**	Therm*	Inner tube**		Pressure tube**		Lagg*
		ID*	ID*	ID*	OD*	ID*	OD*	OD*
①	6.318	0.155	0.165	0.357	0.381	0.452	0.508	0.748

①;Duct from reactor to auxiliary heat exchanger

* Therm; Thermal insulator, Lagg; Lagging material, ID;Inner diameter, OD;Outer diameter

** Material of pressure tube and inner tube; 2 1/4Cr-1 Mo steel, Liner; Hastelloy XR

Table 5.3 Major specifications of air cooler for auxiliary cooling system

1. Number of heat transfer tubes	40
2. Outer diameter of heat transfer tube	25.4mm
3. Thickness of heat transfer tube	2.3mm
4. Number of fins of heat transfer tubes	10 per 25.4mm
4. Effective axial length of heat transfer tube	6.5m
5. Average cross section of flow path of air	17.6m^2
6. Material of heat transfer tubes	2 1/4 Cr-1 Mo steel

Table 5.4 Major length, inner diameter and elevation of water piping for auxiliary cooling system

Line*	Length	ID**	Point*	Elevation
G1	40m	0.0889m	P1	24.2m
G2	10m	0.0889m	P2	24.2m
G3	50m	0.0889m	P3	12.9m
G4*1	4.94m	0.0202m	P4	12.9m
G5	47.3m	0.0889m	P5	12.9m
G6	3.2m	0.0889m	P6	12.9m
G7	50.1m	0.0889m	P7	12.9m
G8*2	13m	0.0208m	P8	50.7m
G9	23.2m	0.0889m	P9	50.7m

* Flow line G1-G9 and pressure point P1-P9 are shown in Fig. 5.5.

** ID;Inner diameter

*1 Auxiliary heat exchanger

*2 Air cooler

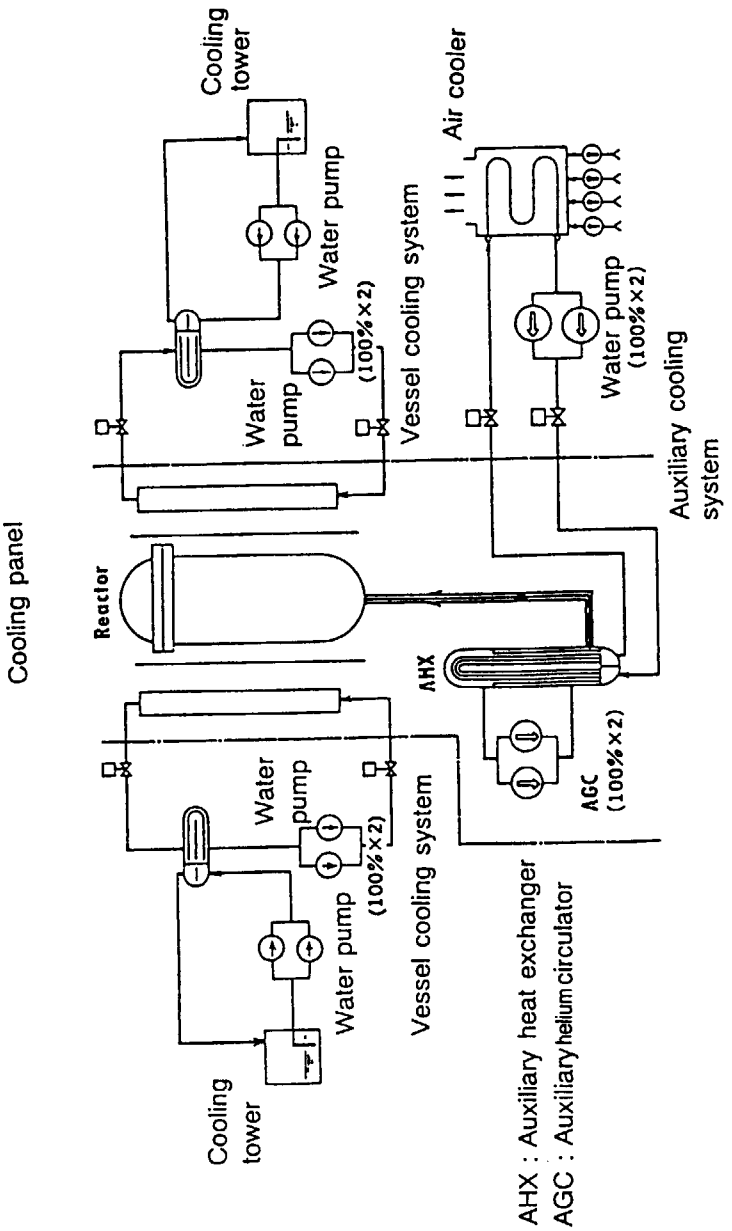

Fig. 5.1 Flow diagram of residual heat removal system

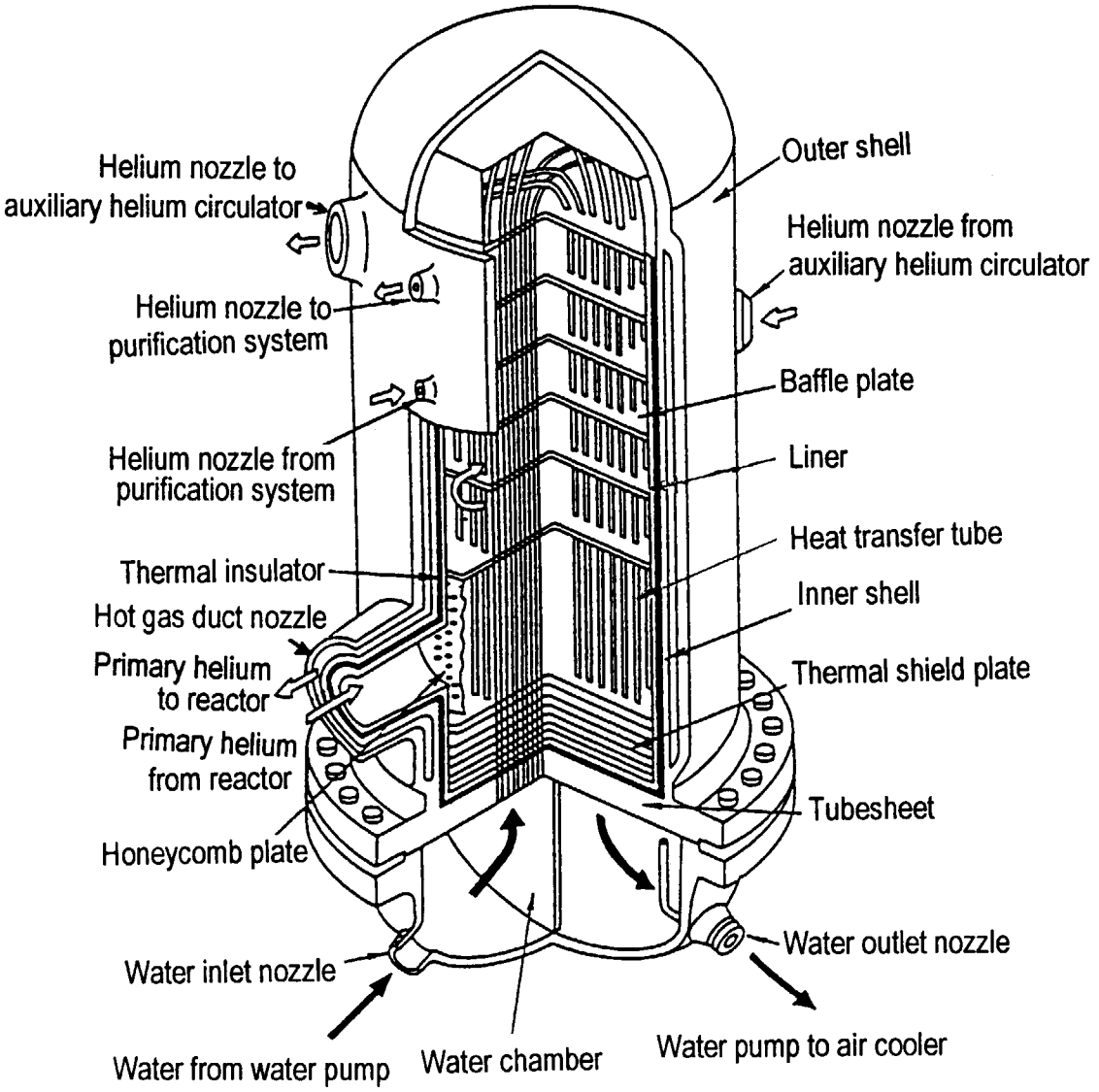

Fig. 5.2 Bird's-eye view of auxiliary heat exchanger

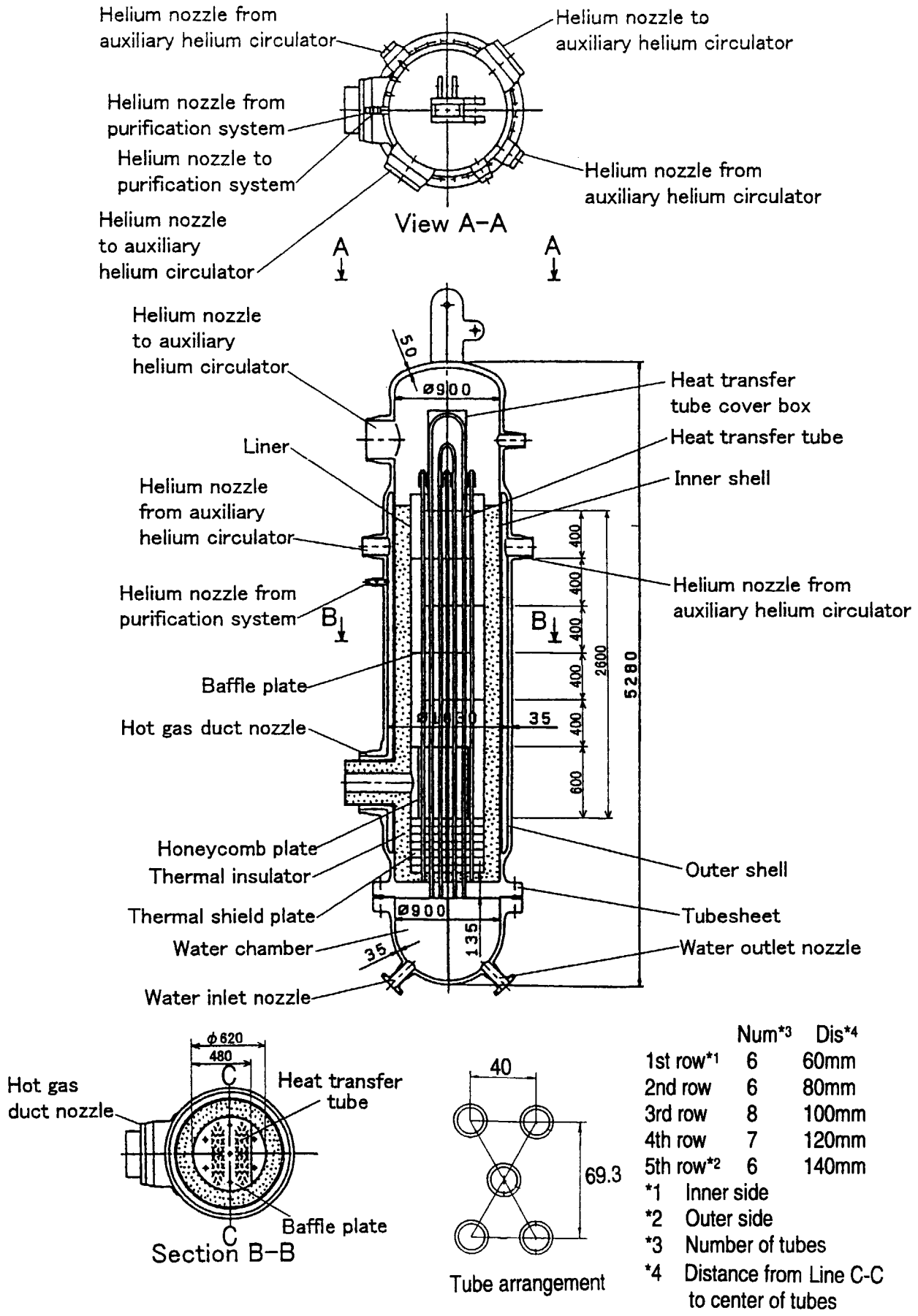

Fig. 5.3 Structural drawing of auxiliary heat exchanger

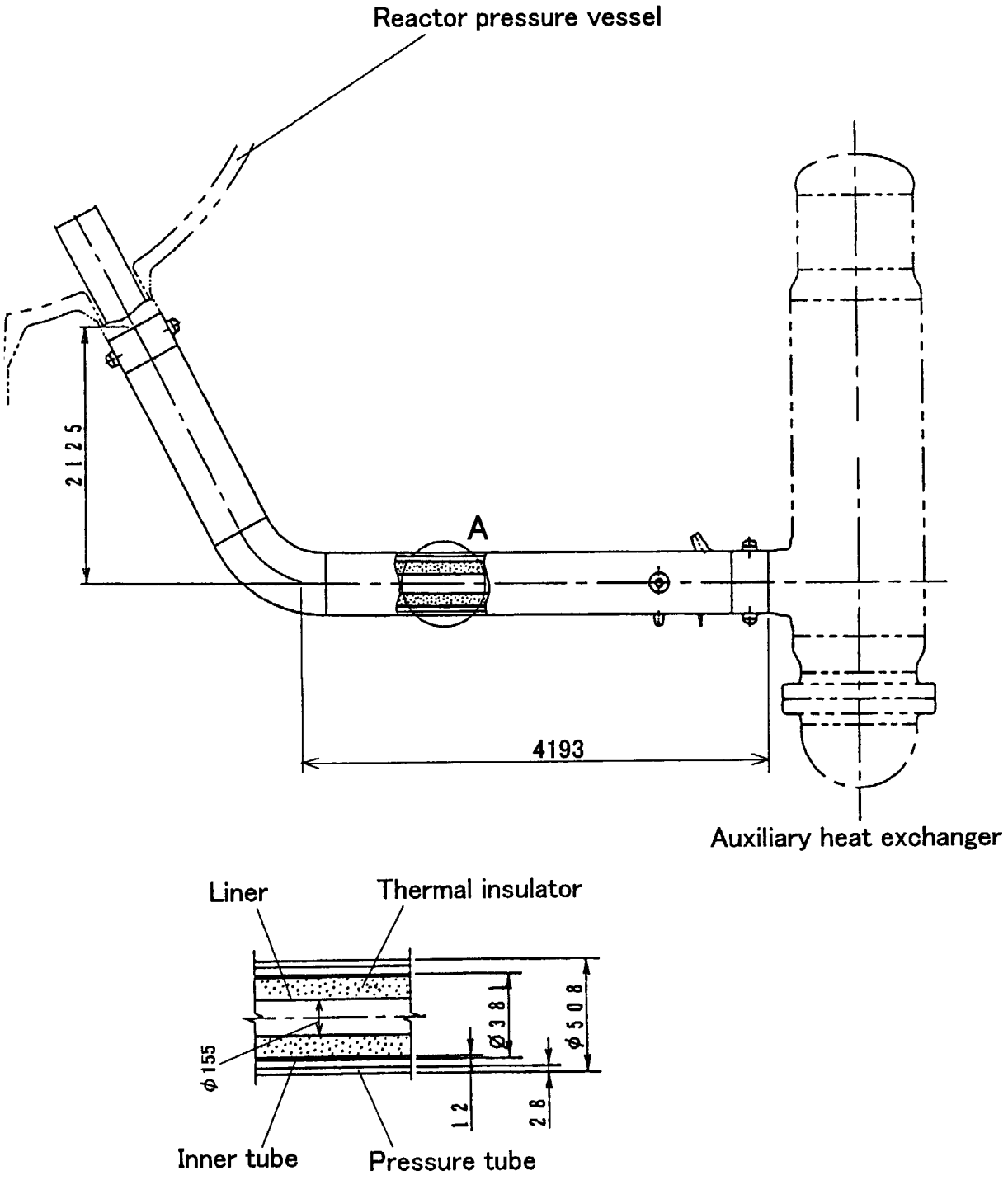

Fig. 5.4 Cross-sectional view of auxiliary concentric hot gas duct

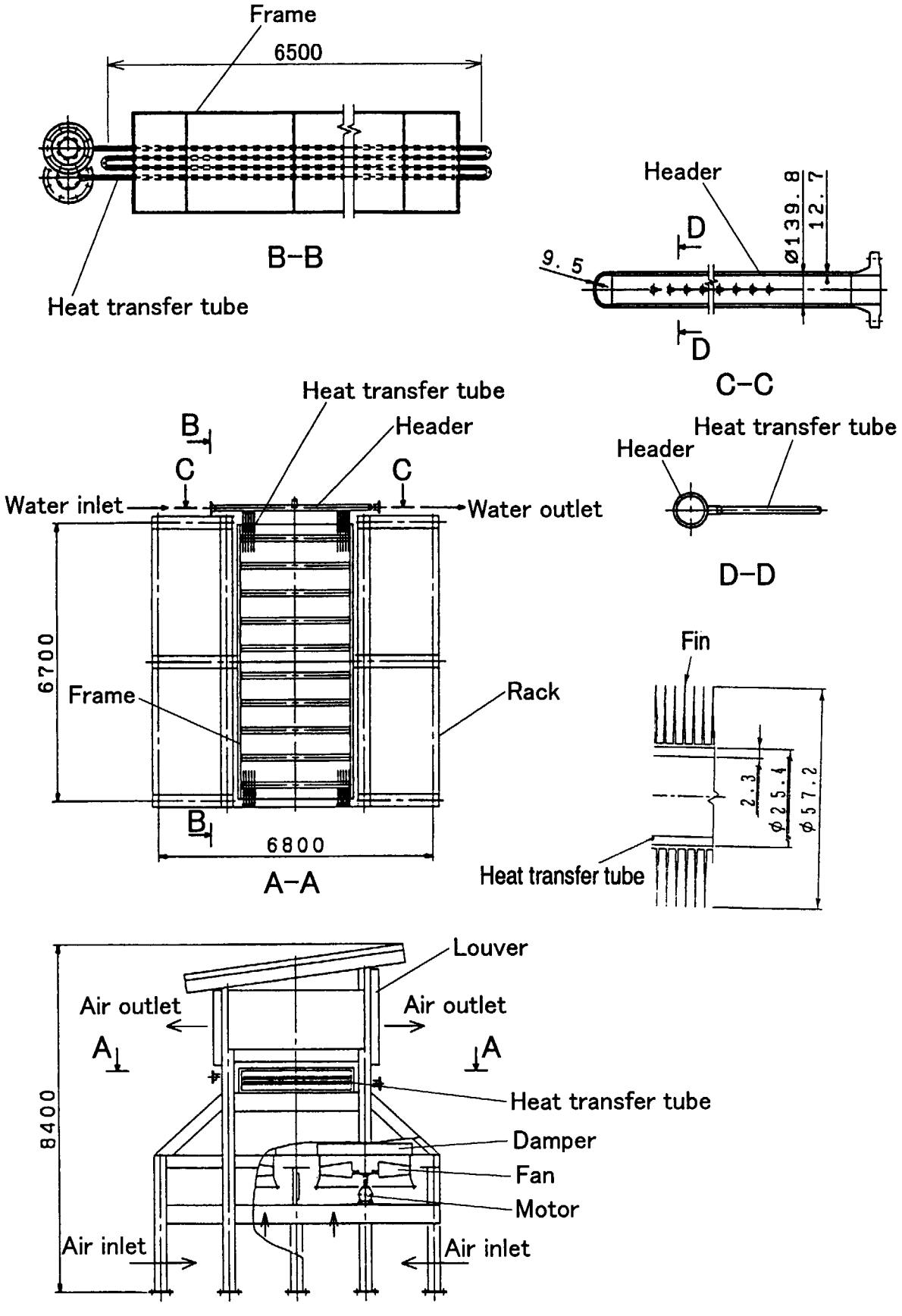

Fig. 5.5 Structural drawing of air cooler for auxiliary cooling system

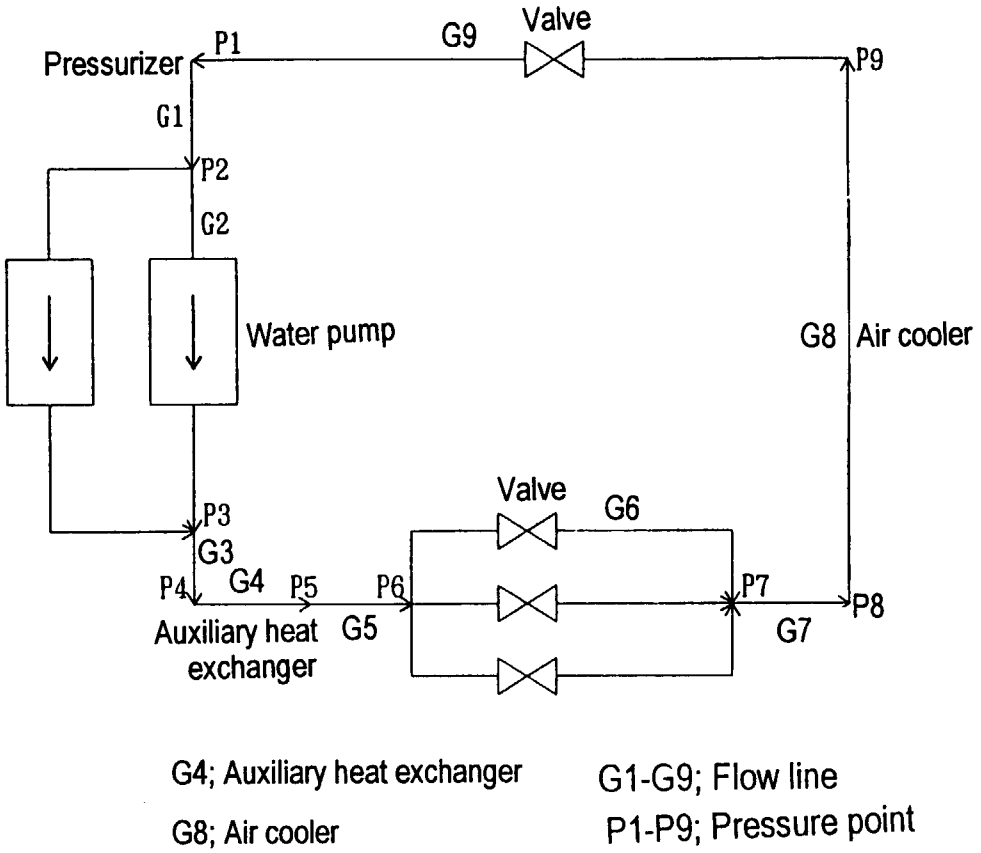

Fig. 5.6 Flow network diagram of water piping for auxiliary cooling system

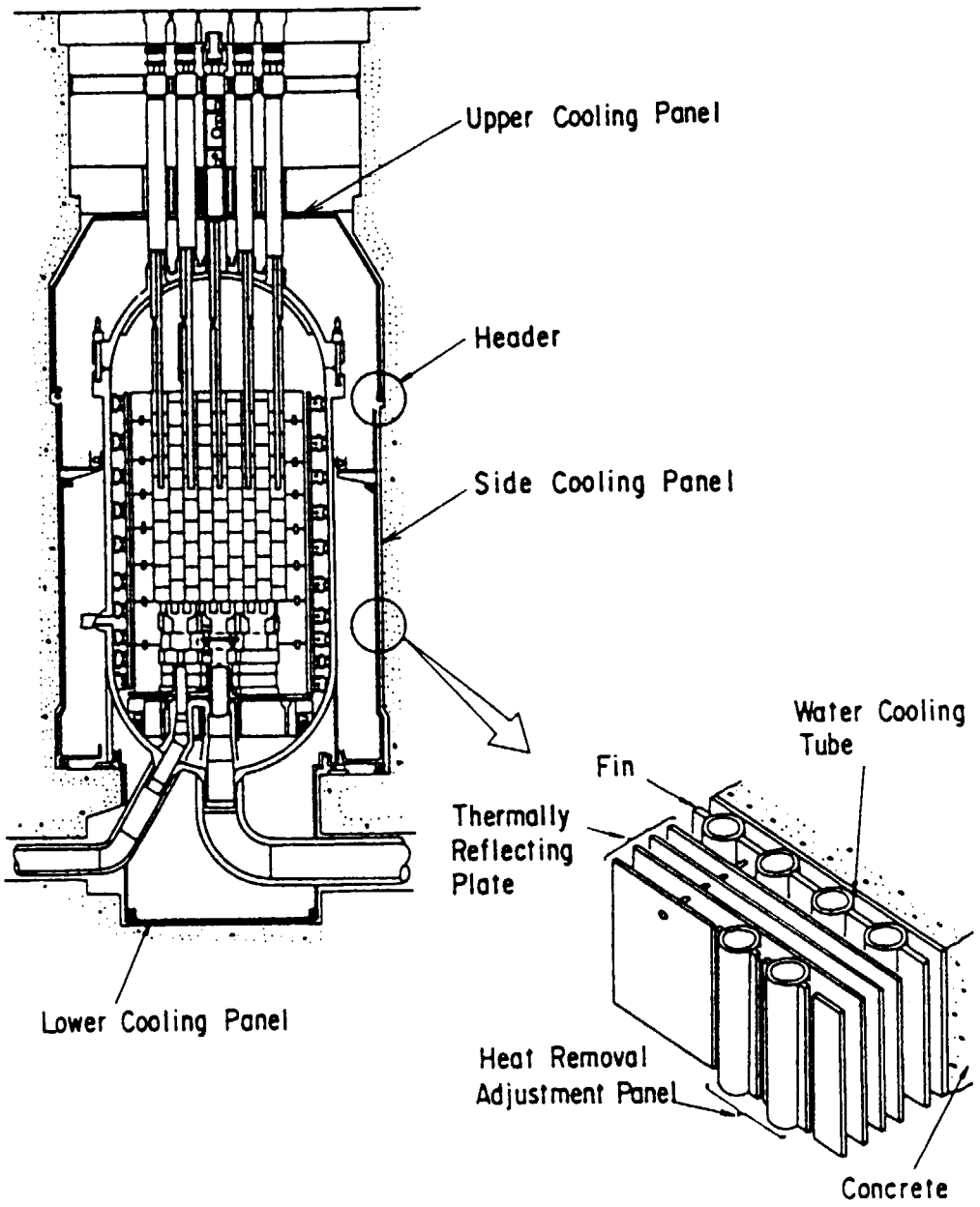

Fig. 5.7 Cross-sectional view of vessel cooling system

6. Parameter for core dynamics and decay heat

6.1 Parameter for core dynamics

Core dynamics parameters in the beginning of life are shown in Table 6.1[6.1]. Total reactivity is calculated by a balance of feedback reactivity due to fuel and moderator temperatures with additional reactivity caused by insertion of the control rods after the reactor scram. Scram reactivity at full insertion of the control rods is $4\times10^{-2}\triangle k/k$. Table 6.2 shows the relationship among the fuel and moderator temperatures and their reactivity [6.2]. Table 6.3 shows the relationship between the ratio of scram reactivity by the control rods and their inserting time [1.1]. Axial power distributions of five layers of fuel blocks are as shown in Table 6.4 [6.3]. Flow rate of helium flowing in the coolant channel of the fuel columns of the reactor core is about 90.2% of total primary and auxiliary helium flow rate [6.3].

6.2 Decay heat

Decay heat of fission products after the reactor scram is estimated by Shure's formula [6.4] and decay heat of actinide [6.5].

$Pd/Po=A\cdot t^{-B}/200$

$Pact/Po=\{F29(t)+F39(t)\}/Q$

$F29(t)=E29\cdot R\cdot\exp(-\lambda u\cdot t)$

$F39(t)=E39\cdot R\cdot\{\lambda u/(\lambda u-\lambda np)\cdot\exp(-\lambda np\cdot t)-\lambda np/(\lambda u-\lambda np)\cdot\exp(-\lambda u\cdot t)\}$

Where

Po	Reactor power at operation (W)
Pd	Decay heat (W)
Pact	Decay heat of actinide (W)
t	Elapsed time after reactor scram (s)
Q	Released average energy per one fission (MeV)(=200 MeV)
E29	Released average energy by decay of ^{239}U (MeV)(=0.474 MeV)
E39	Released average energy by decay of ^{239}Np (MeV)(=0.419 MeV)
λu	Decay constant of ^{239}U (s^{-1})($=4.91\times10^{-4}\ s^{-1}$)
λnp	Decay constant of ^{239}Np (s^{-1})($=3.41\times10^{-6}\ s^{-1}$)
R	Generation ratio of ^{239}U during reactor operation (=0.636)

Parameters of A and B dependent on elapsed time of t (s) are shown in Table 6.5.

Table 6.1 Core dynamics parameters

Prompt neutron lifetime; 7.32×10^{-4} s
Decay constants of delayed neutron precursor $\lambda_{1\text{-}6}$;
$\lambda_1=3.88\ s^{-1}$, $\lambda_2=1.40\ s^{-1}$, $\lambda_3=0.311\ s^{-1}$, $\lambda_4=0.116\ s^{-1}$, $\lambda_5=0.0317\ s^{-1}$, $\lambda_6=0.0127\ s^{-1}$
Production ratio of delayed neutron $\beta_{1\text{-}6}$;
$\beta_1=1.74\times10^{-4}$, $\beta_2=8.39\times10^{-4}$, $\beta_3=2.65\times10^{-3}$,
$\beta_4=1.22\times10^{-3}$, $\beta_5=1.37\times10^{-3}$, $\beta_6=2.46\times10^{-4}$

Table 6.2 Fuel and moderator temperatures versus their reactivity

Temperature(°C)	Doppler reactivity(△k/k)	Moderator reactivity(△k/k)
27	0.0	0.0
77	-0.0019	-0.00295
177	-0.0056	-0.00935
277	-0.0089	-0.01595
377	-0.0119	-0.02295
477	-0.0147	-0.02975
577	-0.0170	-0.03655
677	-0.0190	-0.04335
777	-0.0208	-0.05025
877	-0.0229	-0.05775
977	-0.0248	-0.06555
1077	-0.0267	-0.07335
1177	-0.0285	-0.08165

Table 6.3 Ratio of scram reactivity by control rods versus their inserting time

Time (s)	0.0	0.96	2.07	2.63	3.19	3.75
Ratio*	0.0	0.0069	0.0386	0.069	0.109	0.1614
Time (s)	4.86	7.09	9.32	11.55	13.78	
Ratio*	0.2828	0.5641	0.8207	0.9641	1.0	

* relative value to reactivity of 4×10^{-2}△k/k at full insertion of control rods

Table 6.4 Axial power distributions of fuel blocks
(relative value to power density of 1 st layer of fuel block)

1st layer*		2nd layer		3rd layer		4th layer		5th layer*	
Upper	Lower	Upper	Lower	Upper	Lower	Upper	Lower	Upper	Lower
1	1.76	2.01	2.28	1.99	1.92	1.44	1.25	1.02	0.83

* Top fuel block is 1st layer, while bottom fuel block is 5th layer.

Table 6.5 Decay heat parameters in Shure's formula

t(s)	A	B
$0.1 \leqq t < 10$	12.05	0.0639
$10 \leqq t < 150$	15.31	0.1807
$150 \leqq t < 4.0 \times 10^6$	26.02	0.2834
$4.0 \times 10^6 \leqq t < \infty$	53.18	0.335

7. Performance of helium circulators

Figure 7.1 shows a Q-H characteristic of the primary and secondary helium circulators [7.1]. Pressure ratio of outlet to inlet of the helium circulator is denoted as functions of invariant rotation and invariant flow rate based on similarity law for fluid machinery. All the primary and secondary helium circulators as well as the water pump for the pressurized water cooling system are coasted down immediately after the loss of off-site electric power. Tables 7.1-7.6 show the relationships between the elapsed time and ratio of rotation of all the primary and secondary helium circulators as well as the water pump for the pressurized water cooling system after the loss of off-site electric power. Reactor is scrammed in about 8s after the loss of off-site electric power, that is 3.2s after primary helium flow rate reduces to 92% of normal flow rate, which occurs in 5s after the loss of off-site electric power. In 1s after reactor scram, breaking stop of all the primary and secondary helium circulators is initiated. Table 7.7 shows the relationship between the elapsed time and ratio of rotation of all the primary and secondary helium circulators after the reactor scram. Figure 7.2 shows a Q-H characteristic of the auxiliary helium circulator [7.1]. One of the two auxiliary helium circulators is coasted down in 40min after the startup of the auxiliary cooling system. Table 7.8 shows the relationship between the elapsed time and ratio of rotation of the auxiliary helium circulator during coasting down.

Table 7.1 Elapsed time versus ratio of rotation of helium circulator (A) for primary pressurized water cooler during coasting down

Time (s)	0.0	2.5	5.0	7.5	10.0	12.5	15.0
Ratio	1.0	0.881	0.679	0.603	0.527	0.473	0.422

Table 7.2 Elapsed time versus ratio of rotation of helium circulator (B) for primary pressurized water cooler during coasting down

Time (s)	0.0	2.5	5.0	7.5	10.0	12.5	15.0
Ratio	1.0	0.815	0.689	0.597	0.521	0.462	0.416

Table 7.3 Elapsed time versus ratio of rotation of helium circulator (C) for primary pressurized water cooler during coasting down

Time (s)	0.0	2.5	5.0	7.5	10.0	12.5	15.0
Ratio	1.0	0.815	0.685	0.592	0.521	0.458	0.416

Table 7.4 Elapsed time versus ratio of rotation of helium circulator for intermediate heat exchanger during coasting down

Time (s)	0.0	2.5	5.0	7.5	10.0	12.5	15.0
Ratio	1.0	0.774	0.624	0.527	0.452	0.398	0.355

Table 7.5 Elapsed time versus ratio of rotation of helium circulator for secondary pressurized water cooler during coasting down

Time (s)	0.0	1.8	4.8	7.8	10.8	13.8	16.8
Ratio	1.0	0.880	0.699	0.585	0.497	0.432	0.388

Table 7.6 Elapsed time versus ratio of rotation of water pump for pressurized water cooling system during coasting down

Time (s)	0.0	0.5	1.47	7.8	10.8	13.8	16.8
Ratio	1.0	0.874	0.8	0.585	0.497	0.432	0.388

Table 7.7 Elapsed time versus ratio of rotation of all primary and secondary helium circulators after reactor scram

Time (s)	0.0	1.0	2.0	3.0	4.0	5.0
Ratio	1.0	0.901	0.819	0.696	0.585	0.491
Time (s)	6.0	7.0	8.0	8.5	8.8	9.0
Ratio	0.398	0.292	0.175	0.082	0.012	0.0

Table 7.8 Elapsed time versus ratio of rotation of auxiliary helium circulator during coasting down

Time (s)	0.0	15	20	25	83	147
Ratio	1.0	0.689	0.521	0.416	0.118	0.0

Invariant flow rate = [flow rate (kg/h)] · [inlet temperature (K)]$^{0.5}$/[inlet pressure (kg/cm^{2}a)]

Invariant rotation = [rotation (min^{-1})]/[inlet temperature (K)]$^{0.5}$

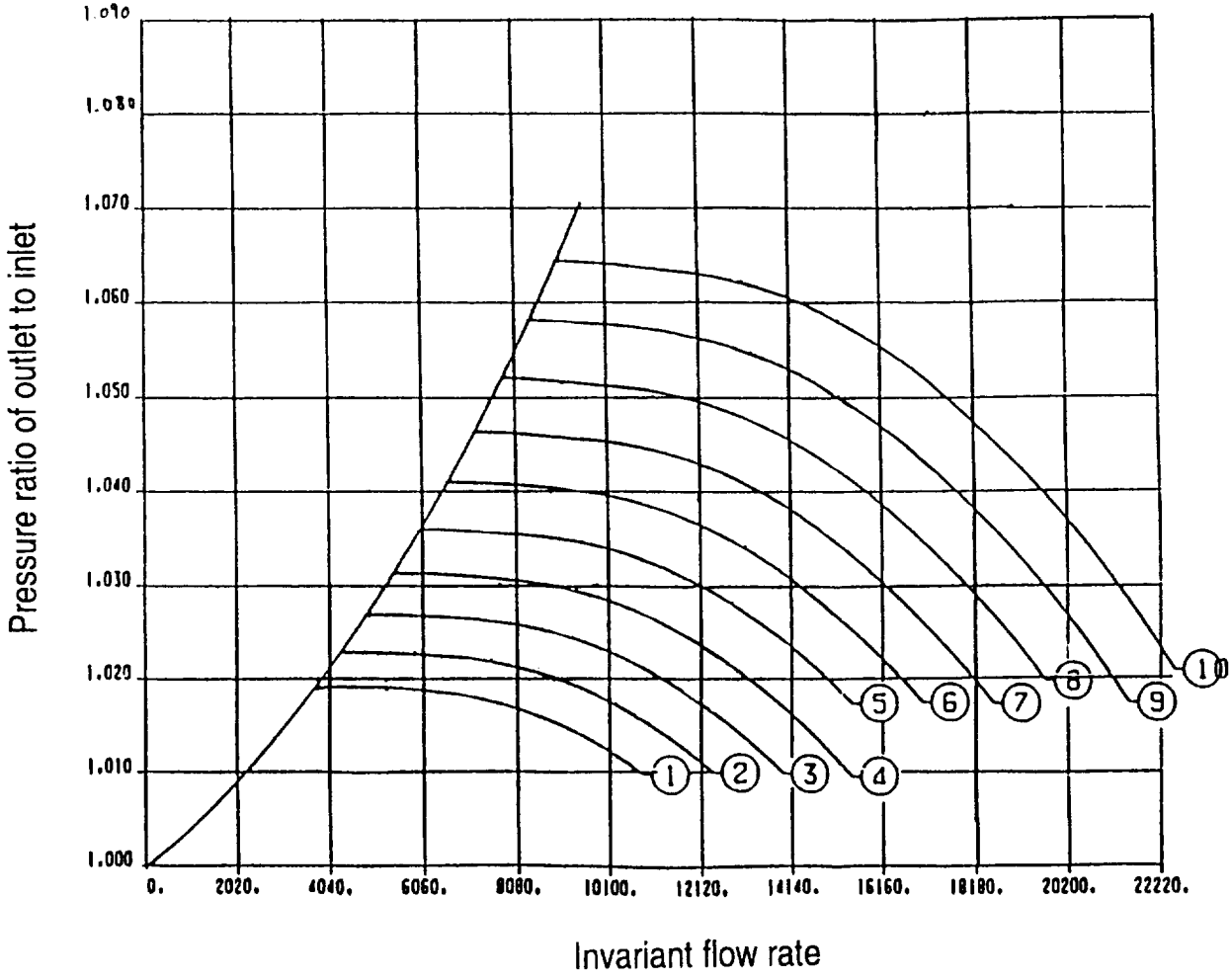

Fig. 7.1 Q-H characteristic of primary and secondary helium circulators

Invariant flow rate = [flow rate (kg/h)] · [inlet temperature (K)]$^{0.5}$/[inlet pressure (kg/cm^{2}a)]

Invariant rotation = [rotation (min^{-1})]/[inlet temperature (K)]$^{0.5}$

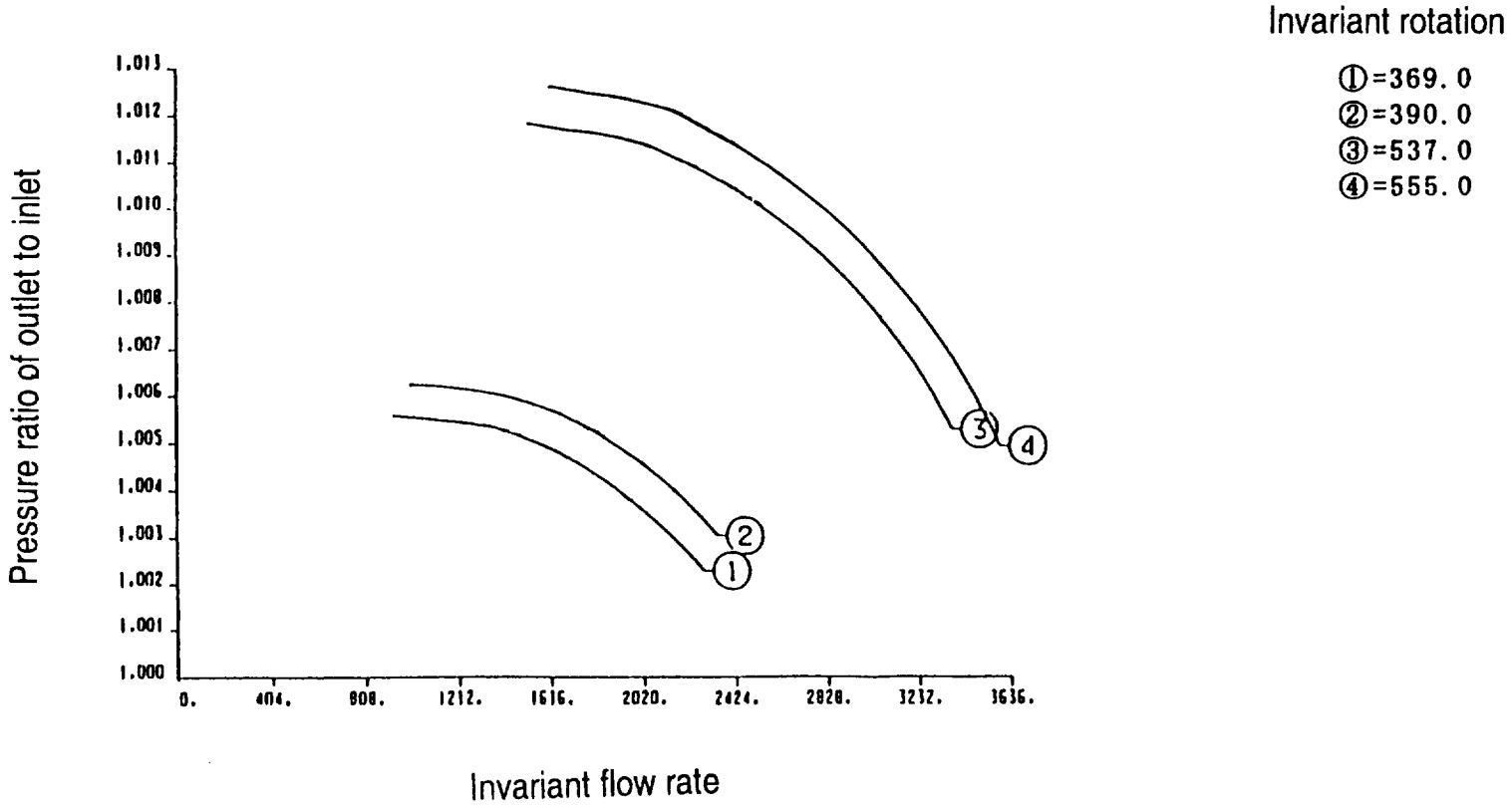

Fig. 7.2 Q-H characteristic of auxiliary helium circulator

8. Thermophysical properties

This chapter describes thermophysical properties used in the 'ACCORD' code.

8.1 Thermophysical properties of components

Thermophysical properties (density, specific heat and thermal conductivity) of components are as follows. The density of ρ (kg/m^3), specific heat of Cp (J/(kg・K)) and thermal conductivity of λ (W/(m・K)) are presented as parameters of ambient temperature of T(K).

(1) IG-110 graphite of reactor core

Following values are applied to those of graphite sleeve, graphite block as well as replaceable reflector block of reactor core.

ρ =1.75E3

Cp=4.187E3・(5.4212E-1-2.42667E-6・T-9.02725E1・T^{-1}-4.34493E4・T^{-2}
+1.59309E7・T^{-3}-1.43688E9・T^{-4})

λ =4.187E3・3E-2・{1.02748-1.35887E-3・(T-273.15)+1.11271E-6・(T-273.15)^2
-4.76484E-10・(T-273.15)^3+8.69490E-14・(T-273.15)^4}

(2) Fuel compact of reactor core

ρ =2.46E3

Cp=4.187E3・{1.15689E-1-5.38719E-4・(T-273.15)-6.27977E-7・(T-273.15)^2
+3.82411E-10・(T-273.15)^3-1.12556E-13・(T-273.15)^4+1.27705E-17・(T-273.15)^5}

λ =1.88E1

(3) PGX graphite of reactor core

Following values are applied to those of permanent reflector block, hot plenum block, lower plenum block and bottom block of reactor core.

ρ =1.73E3

Cp=4.187E3・(5.4212E-1-2.42667E-6・T-9.02725E1・T^{-1}-4.34493E4・T^{-2}
+1.59309E7・T^{-3}-1.43688E9・T^{-4})

λ =4.187E3・{2.41693E-2-2.26769E-5・(T-273.15)+1.10893E-8・(T-273.15)^2
-1.85727E-2・(T-273.15)^3}

(4) Carbon block of reactor core

ρ =1.65E3

Cp=4.187E3・(5.08433E-1+9.60852E1・T^{-1}-2.13944E5・T^{-2}+7.37673E7・T^{-3}-8.13649E9・T^{-4})

λ =4.187E3・1.96E-3・{9.88315E-1+7.28178E-4・(T-273.15)

-4.66499E-7・$(T-273.15)^2$+1.04522E-10・$(T-273.15)^3$}

(5) Hastelloy XR [8.1][8.2]

Following values are applied to those of heat transfer tubes of intermediate heat exchanger and liner of concentric hot gas duct.

ρ =8.23E3

Cp=4.187E3・{5.8713E-5・(T-273.15)+1.0499E-1}

λ =1.163・{1.7166E-2・(T-273.15)+7.6496}

(6) 316 stainless steel of reactor core

Following values are applied to those of top shielding block of reactor core.

ρ =-4.0183E-1・(T-273.15)+8.0471E3

Cp=4.187E3・{5.3241E-5・(T-273.15)+1.022E-1}

λ =1.163・{1.2286E-2・(T-273.15)+1.2885E1}

(7) 2 1/4 Cr-1 Mo steel

Following values are applied to those of reactor pressure vessel, heat transfer tubes of air coolers for pressurized water cooling system and auxiliary cooling system.

ρ =-3.3098E-1・(T-273.15)+7.8221E3

Cp=4.187E3・{1.1294E-4・(T-273.15)+9.9174E-2}

λ =1.163・{-2.7091E-3・(T-273.15)+2.824E1}

(8) Lagging material covered concentric hot gas duct

ρ =2E2

Cp=8.374E2

λ =7.85E-2

(9) Thermal insulator of concentric hot gas duct

ρ =2.2E2

Cp=1.067E3

λ =5.815E-1

(10) 321TB stainless steel

Following values are applied to those of heat transfer tubes of primary and secondary pressurized water coolers as well as auxiliary heat exchanger.

ρ =-4.0183E-1·(T-273.15)+7.9374E3

Cp=4.187E3·{5.324E-5·(T-273.15)+1.1675E-1}

λ =1.163·{1.1782E-2·(T-273.15)+1.3086E1}

8.2 Thermophysical properties of helium

Thermophysical properties (density, specific heat, thermal conductivity and viscosity) of helium are as follows. The density of ρ (kg/m^3), specific heat of Cp (J/(kg·K)), thermal conductivity of λ (W/(m·K)) and viscosity of η (Pa·s) are presented as parameters of ambient temperature of T(K) and ambient pressure of P (MPa abs).

$\rho = A(T,P)\cdot\{2\cdot B(T)\}^{-1}$

$A(T,P)=[1+\{4\cdot P\cdot B(T)\}\cdot(2.07723E\text{-}3\cdot T)^{-1}]^{0.5}-1$

$B(T)=4.5E\text{-}4+5.42\cdot(1.89E3+T)^{-1}$

Cp=5.192E3

$\lambda = 2.97E\text{-}3\cdot T^{0.69}+\{9.23E9\cdot(T-273.15)\}\cdot\{(T-273.15)^5+4.29E14\}^{-1}+2.33E\text{-}4\cdot\rho+2.39E\text{-}6\cdot\rho^2$

$\eta = 3.78E\text{-}7\cdot T^{0.69}+5E\text{-}7\cdot(5.2E\text{-}1+T\cdot 5.696E2^{-1})^{-1}+2.67E\text{-}10\cdot\rho^2$

8.3 Thermophysical properties of water

Thermophysical properties (density, specific heat, thermal conductivity and viscosity) of water are as follows. The density (kg/m^3), specific heat (J/(kg·K)), thermal conductivity (W/(m·K)) and viscosity (μ Pa·s) are presented as parameters of ambient temperature (K) and ambient pressure (MPa abs) as shown in Tables 8.1, 8.2, 8.3 and 8.4, respectively.

Table 8.1 Density of water as parameters of ambient temperature and pressure

Unit(kg/m³)

MPa (abs)	300K	320K	340K	380K	420K	460K	500K
0.1	996.66	989.47	979.48				
0.5	996.84	989.65	979.65	953.26	919.74		
1	997.07	989.86	979.88	953.51	920.02		
2	997.51	990.31	980.33	954	920.6	880.14	
3	997.95	990.74	980.77	954.49	921.18	880.86	831.91
4	998.4	991.17	981.21	954.98	921.74	881.56	832.86

Table 8.2 Specific heat of water as parameters of ambient temperature and pressure

Unit(J/(kg·K))

MPa (abs)	300K	320K	340K	380K	420K	460K	500K
0.1	4179	4180	4188				
0.5	4178	4179	4187	4223	4302		
1	4176	4178	4186	4222	4300		
2	4174	4176	4184	4220	4297	4431	
3	4171	4173	4182	4218	4294	4427	4658
4	4168	4171	4179	4215	4291	4422	4649

Table 8.3 Thermal conductivity of water as parameters of ambient temperature and pressure

Unit(W/(m·K))

MPa (abs)	300K	320K	340K	380K	420K	460K	500K
0.1	0.6104	0.6369	0.6569				
0.5	0.6106	0.6372	0.6571	0.6802	0.684		
1	0.6109	0.6374	0.6574	0.6805	0.6844		
2	0.6114	0.6379	0.6579	0.6811	0.6851	0.6718	
3	0.612	0.6385	0.6584	0.6817	0.6858	0.6727	0.6427
4	0.6125	0.639	0.6589	0.6822	0.6864	0.6735	0.6438

Table 8.4 Viscosity of water as parameters of ambient temperature and pressure

Unit(μPa·s)

MPa (abs)	300K	320K	340K	380K	420K	460K	500K
0.1	854.4	577.2	422.5				
0.5	854.3	577.3	422.6	263.1	186.2		
1	854.2	577.4	422.7	263.2	186.3		
2	854.1	577.5	423	263.5	186.6	143.8	
3	853.9	577.6	423.2	263.8	186.8	144	117.3
4	853.8	577.8	423.4	264	187.1	144.3	117.5

9. Correlation of heat transfer coefficient

This chapter describes correlation of heat transfer coefficient employed in the 'ACCORD' code.

9.1 Correlation of heat transfer coefficient of helium

(1) Flow in annular path

Following correlation [9.1][9.2] is applied to flow in regions of top shielding block and top replaceable reflector block, annular path between graphite sleeve and block, reactor side part, annular path between pressure and inner tubes of concentric hot gas duct.

$$Nu=\max(Nul, Nut)$$

$$Nul=C(\alpha)\cdot(Tb/Tw)^{0.5}$$

$$C(\alpha)=-4.8268\cdot\alpha^{3}+12.7516\cdot\alpha^{2}-12.2505\cdot\alpha+9.7170$$

$$Nut=0.020\cdot\alpha^{-0.16}\cdot Re^{0.8}\cdot Pr^{0.4}\cdot(Tb/Tw)^{0.5}$$

Where

Nu	Nusselt number(=h·k/De)
h	Heat transfer coefficient (W/(m²·K))
k	Thermal conductivity (W/(m·K))
De	Equivalent diameter (=do-di) (m)
di	Inner diameter of annular path (m)
do	Outer diameter of annular path (m)
α	Ratio of inner to outer diameter of annular path (=di/do)
Re	Reynolds number (=De·ui/ν)
ui	Average velocity of flow in annular path (m/s)
ν	Kinematic viscosity (m²/s)
Pr	Prandtl number (=Cp·μ/k)
Cp	Specific heat (J/(kg·K))
μ	Viscosity (kg/(m·s))
Tb	Bulk temperature (K)
Tw	Wall temperature (K)

(2) Flow in circular tube

Following correlation [9.3] is applied to flow in regions of bottom replaceable reflector block and hot plenum block as well as flow inside liner of concentric hot gas duct.

$Nu=max(Nul, Nut)$

$Nul=4.36 \cdot (Tb/Tw)^{0.5}$

$Nut=0.020 \cdot Re^{0.8} \cdot Pr^{0.4} \cdot (Tb/Tw)^{0.5}$

Where

Nu	Nusselt number(=h・k/di)
h	Heat transfer coefficient (W/(m²・K))
k	Thermal conductivity (W/(m・K))
di	Inner diameter of annular path (m)
Re	Reynolds number (=di・ui/ ν)
ui	Average velocity of flow in circular tubes (m/s)
ν	Kinematic viscosity (m²/s)
Pr	Prandtl number (=Cp・ μ /k)
Cp	Specific heat (J/(kg・K))
μ	Viscosity (kg/(m・s))
Tb	Bulk temperature (K)
Tw	Wall temperature (K)

(3) Flow inside heat transfer tubes of helically-coiled type heat exchanger

Following correlation [9.4] is applied to flow inside heat transfer tubes of intermediate heat exchanger.

$Nu=max(Nul, Nut)$

$Nul=0.64528 \cdot Dean^{0.5}/(1-1.813 \cdot Dean^{-0.5})$

$Nut=0.0223 \cdot Re^{0.83} \cdot di^* \cdot Pr/(Pr^{0.6}-0.057) \cdot \{1+0.0615/(Re \cdot di^{*2.5})^{0.17}\}$

Where

Nu	Nusselt number(=h・k/di)
h	Heat transfer coefficient (W/(m²・K))
k	Thermal conductivity (W/(m・K))
di	Inner diameter of heat transfer tube (m)
Dean	Dean number (=Re・di*0.5)
Re	Reynolds number (=di・ui/ ν)
ui	Average velocity of flow in heat transfer tubes (m/s)
ν	Kinematic viscosity (m²/s)
di*	di/Dm
Dm	Average diameter of helically-coils (m)(=0.537m)

Pr Prandtl number (=Cp・μ/k)
Cp Specific heat (J/(kg・K))
μ Viscosity (kg/(m・s))

(4) Flow outside heat transfer tubes of helically-coiled type heat exchanger

Following correlation [9.5][9.6] is applied to flow outside heat transfer tubes of intermediate heat exchanger.

$Nuo=0.297 \cdot Reo^{0.6} \cdot Pr^{0.3}$ $(Reo \geqq 7000)$

$Nuo=\max(Nuol, Nuot)$ $(Reo < 7000)$

$Nuol=4$

$Nuot=0.047595 \cdot \max(800, Reo)^{0.8} \cdot Pr^{0.4}$

Where

Nuo Nusselt number(=h・k/De)
h Heat transfer coefficient (W/(m²・K))
k Thermal conductivity (W/(m・K))
De Equivalent diameter (m)
Reo Reynolds number (=De・uo/ν)
uo Average velocity of flow outside heat transfer tubes (m/s)
ν Kinematic viscosity (m²/s)
Pr Prandtl number (=Cp・μ/k)
Cp Specific heat (J/(kg・K))
μ Viscosity (kg/(m・s))

(5) Flow outside heat transfer tubes of baffle-tube type heat exchanger

Following correlation [9.7] is applied to flow outside heat transfer tubes of primary and secondary pressurized water coolers as well as auxiliary heat exchanger.

$Nu=0.222 \cdot Re^{0.6} \cdot Pr^{0.33}$

Where

Nu Nusselt number(=h・k/De)
h Heat transfer coefficient (W/(m²・K))
k Thermal conductivity (W/(m・K))
De Equivalent diameter (m)
Re Reynolds number (=De・uo/ν)
uo Average velocity of flow outside heat transfer tubes (m/s)

ν Kinematic viscosity (m^2/s)
Pr Prandtl number ($=Cp \cdot \mu / k$)
Cp Specific heat ($J/(kg \cdot K)$)
μ Viscosity ($kg/(m \cdot s)$)

9.2 Correlation of heat transfer coefficient of water

Following correlation [9.8] is applied to flow inside heat transfer tubes of primary and secondary pressurized water coolers as well as air coolers for the pressurized water cooling system and auxiliary cooling system.

$$Nu=0.023 \cdot Re^{0.8} \cdot Pr^{0.4}$$

Where

Nu Nusselt number($=h \cdot k/De$)
h Heat transfer coefficient ($W/(m^2 \cdot K)$)
k Thermal conductivity ($W/(m \cdot K)$)
De Equivalent diameter (m)
Re Reynolds number ($=De \cdot uo/\nu$)
uo Average velocity of flow outside heat transfer tubes (m/s)
ν Kinematic viscosity (m^2/s)
Pr Prandtl number ($=Cp \cdot \mu / k$)
Cp Specific heat ($J/(kg \cdot K)$)
μ Viscosity ($kg/(m \cdot s)$)

9.3 Correlation of heat transfer coefficient of air

(1) Flow in annular path

Following correlation [9.9] is applied to flow in annular path between reactor pressure vessel and vessel cooling system.

$$hrv=hr+hn$$

$$hr=\sigma \cdot F \cdot (Tr+Tv) \cdot (Tr^2+Tv^2)$$

$$Nun=0.36 \cdot Pr^{0.051} \cdot (H/W)^{-0.11} \cdot Ra^{0.25} \qquad (10^7 < Ra < 4 \times 10^9)$$

$$Nun=0.084 \cdot Pr^{0.051} \cdot Ra^{0.3} \qquad (4 \times 10^9 < Ra < 2 \times 10^{12})$$

$$Nun=0.039 \cdot Ra^{0.33} \qquad (2 \times 10^{12} < Ra)$$

Where

hrv	Equivalent heat transfer coefficient (W/(m^2・K))
hr	Heat transfer coefficient for radiation (W/(m^2・K))
hn	Heat transfer coefficient for natural convection (W/(m^2・K))
σ	Stefan-Boltzmann's constant (=5.6687×10^{-8} W/(m^2・K^4))
F	Configulation factor (={(2/ ε)-1}$^{-1}$)
ε	Emissivity (=0.2353)
Tr	Temperature of reactor pressure vessel (K)
Tv	Temperature of vessel cooling system (K) (=333K)
Nun	Nusselt number for natural convection(=hn・kn/De)
kn	Thermal conductivity (W/(m・K))
De	Equivalent diameter (m)
Pr	Prandtl number (=Cp・μ /kn)
Cp	Specific heat (J/(kg・K))
μ	Viscosity (kg/(m・s))
H	Height (m)(=13.22m)
W	Width (m)(=0.988m)
Ra	Reyleigh number (=Pr・Gr)
Gr	Grashof number (=g・β ・H^3・(Tv-Ta)/ ν ^{2})
g	Accelation due to gravity (m/s^2)(=9.8m/s^2)
β	Coefficient of volume expansion (1/K)(=1/Ta)
Ta	Temperature of air in annular path between reactor pressure vessel and vessel cooling system(=(Tv+Tr)/2) (K)
ν	Kinematic viscosity (m^2/s)

(2) Flow outside heat transfer tubes of fin-tube type heat exchanger

Following correlation [9.10] is applied to flow outside heat transfer tubes of air coolers for the pressurized water cooling system and auxiliary cooling system.

$$h=459.77 \cdot G^{0.5} \cdot 1.163$$

Where

h	Heat transfer coefficient (W/m^2・K)
G	Mass flow rate per unit of heat transfer area (kg/(m^2・s))

10. Pre-estimation results by 'ACCORD' code

This chapter describes pre-estimation results of the benchmark problems concerning the loss of off-site electric power simulation of the HTTR by the 'ACCORD' code. The estimation items are the transition of the hot plenum block temperature, reactor inlet and outlet coolant temperatures, primary coolant pressure, reactor power and heat removal of the auxiliary heat exchanger. The estimation duration is for 3600s from the beginning of the loss of off-site electric power. Figures 10.1-10.3 and 10.4-10.6 show analytical results of transient behaviors of the reactor and plant during the loss of off-site electric power from the normal operation under 15 and 30MW thermal power by the 'ACCORD' code, respectively.

In the transient, primary helium flow rate on the shell side of the intermediate heat exchanger decreases to 92% of normal flow rate in 5s after the loss of off-site electric power. In 3.2s after 92% flow rate is reached, the reactor is scrammed. The auxiliary cooling system starts up in 50s after the loss of off-site electric power. One of the two auxiliary helium circulators is coasted down in 40min after the startup of the auxiliary cooling system. As helium flow rate of the auxiliary heat exchanger reduces, the reactor inlet and outlet coolant temperatures, primary coolant pressure and heat removal of the auxiliary heat exchanger decrease. The decreasing rate of the reactor inlet coolant temperature is greater than that of the reactor outlet coolant temperature. The maximum heat removal of the auxiliary heat exchanger during the operation of the two auxiliary helium circulators under the loss of off-site electric power from 15 and 30MW will be approximately 1.5 and 3MW, respectively.

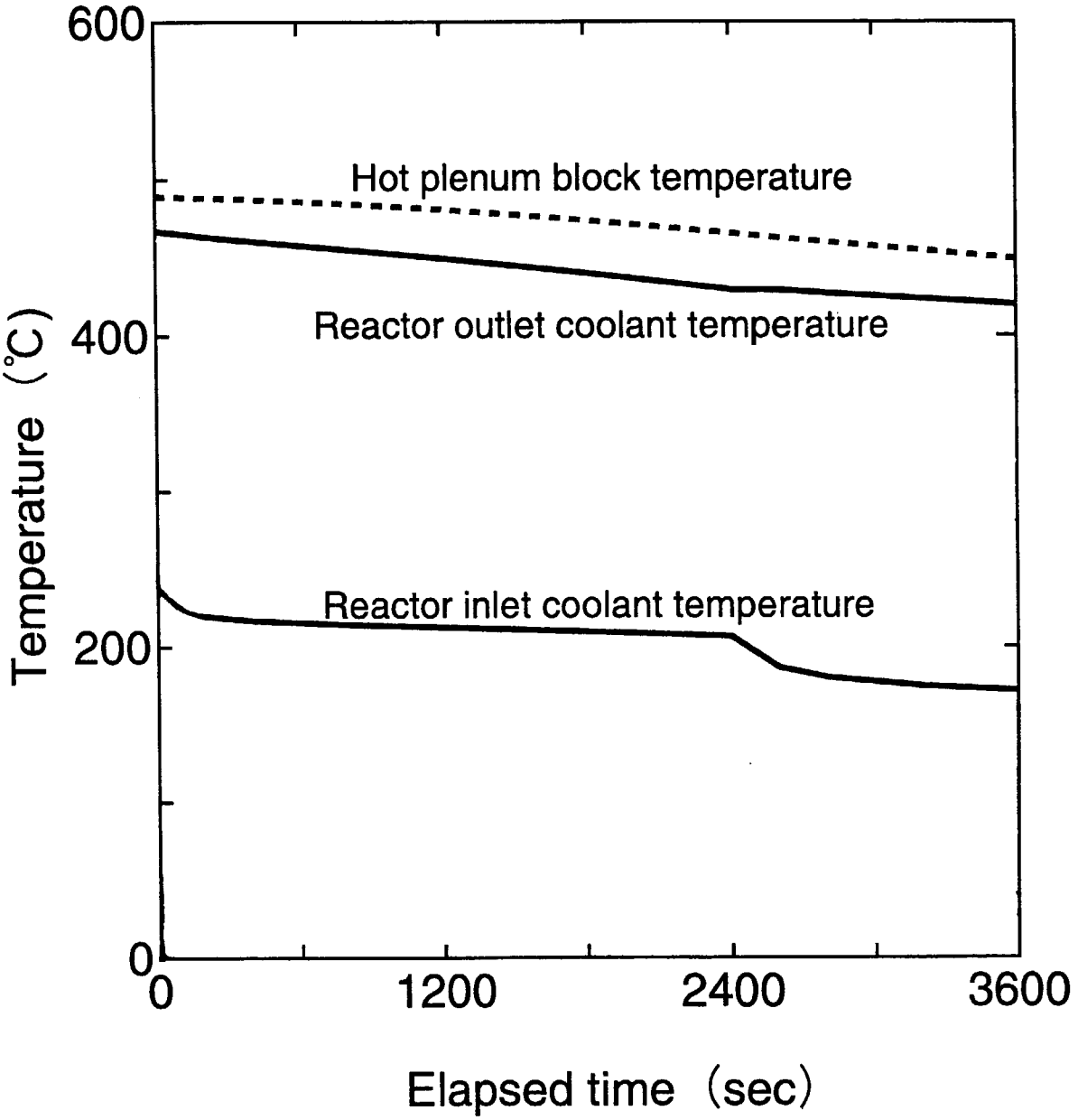

Fig. 10.1 Analytical results of transient behaviors of reactor and plant during loss of off-site electric power from normal operation under 15MW thermal power by 'ACCORD' code (1/3)

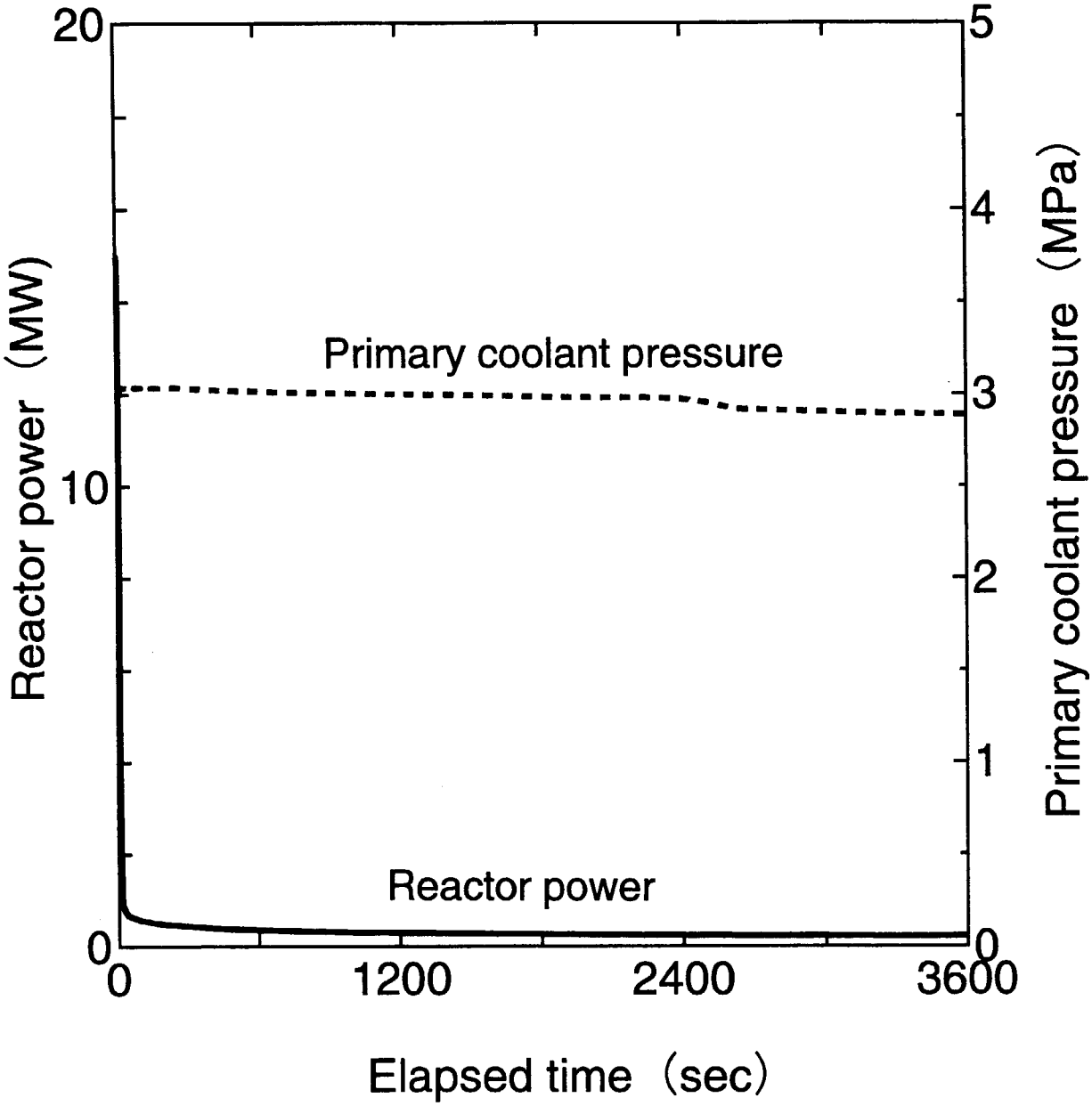

Fig. 10.2 Analytical results of transient behaviors of reactor and plant during loss of off-site electric power from normal operation under 15MW thermal power by 'ACCORD' code (2/3)

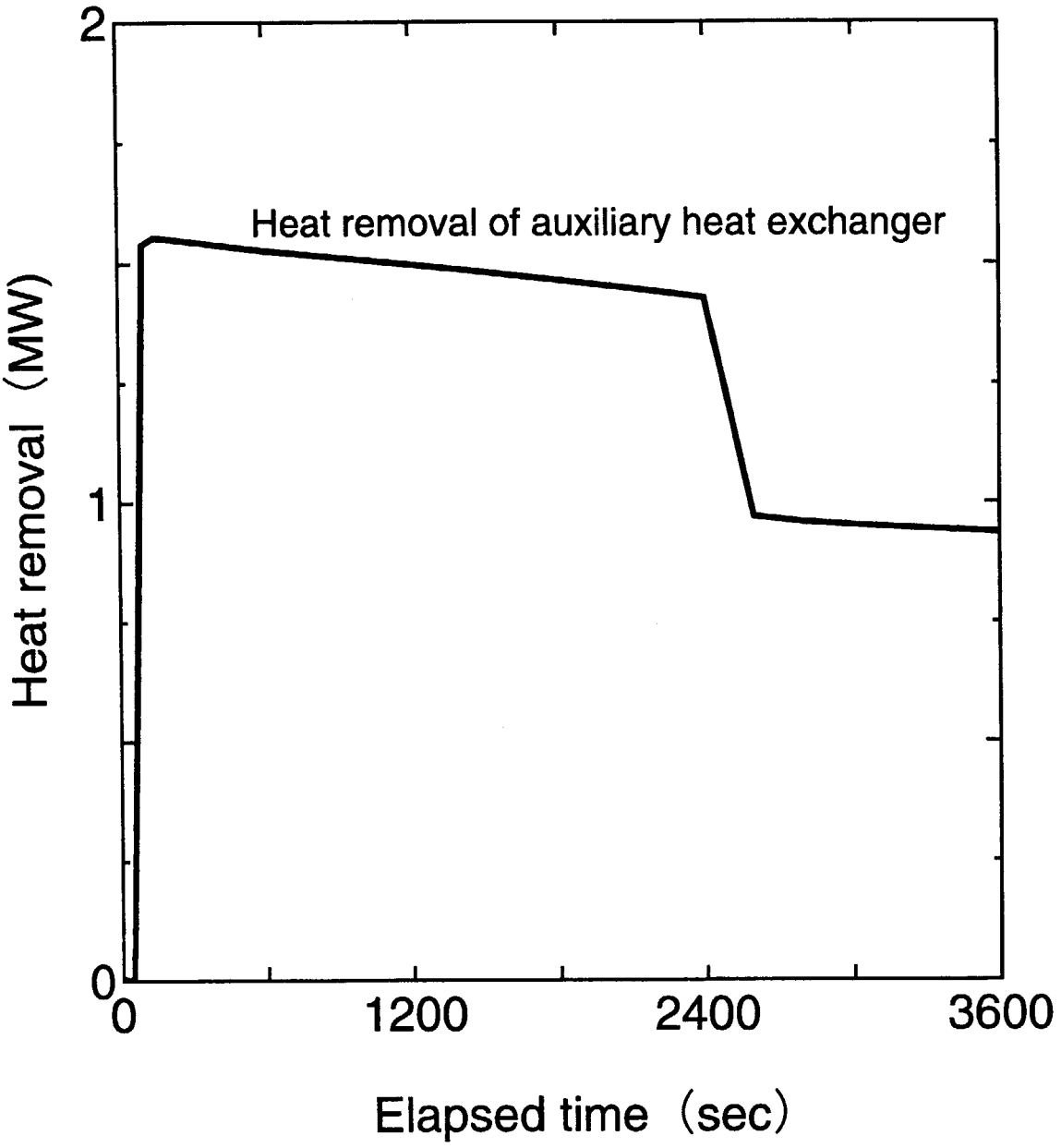

Fig. 10.3 Analytical results of transient behaviors of reactor and plant during loss of off-site electric power from normal operation under 15MW thermal power by 'ACCORD' code (3/3)

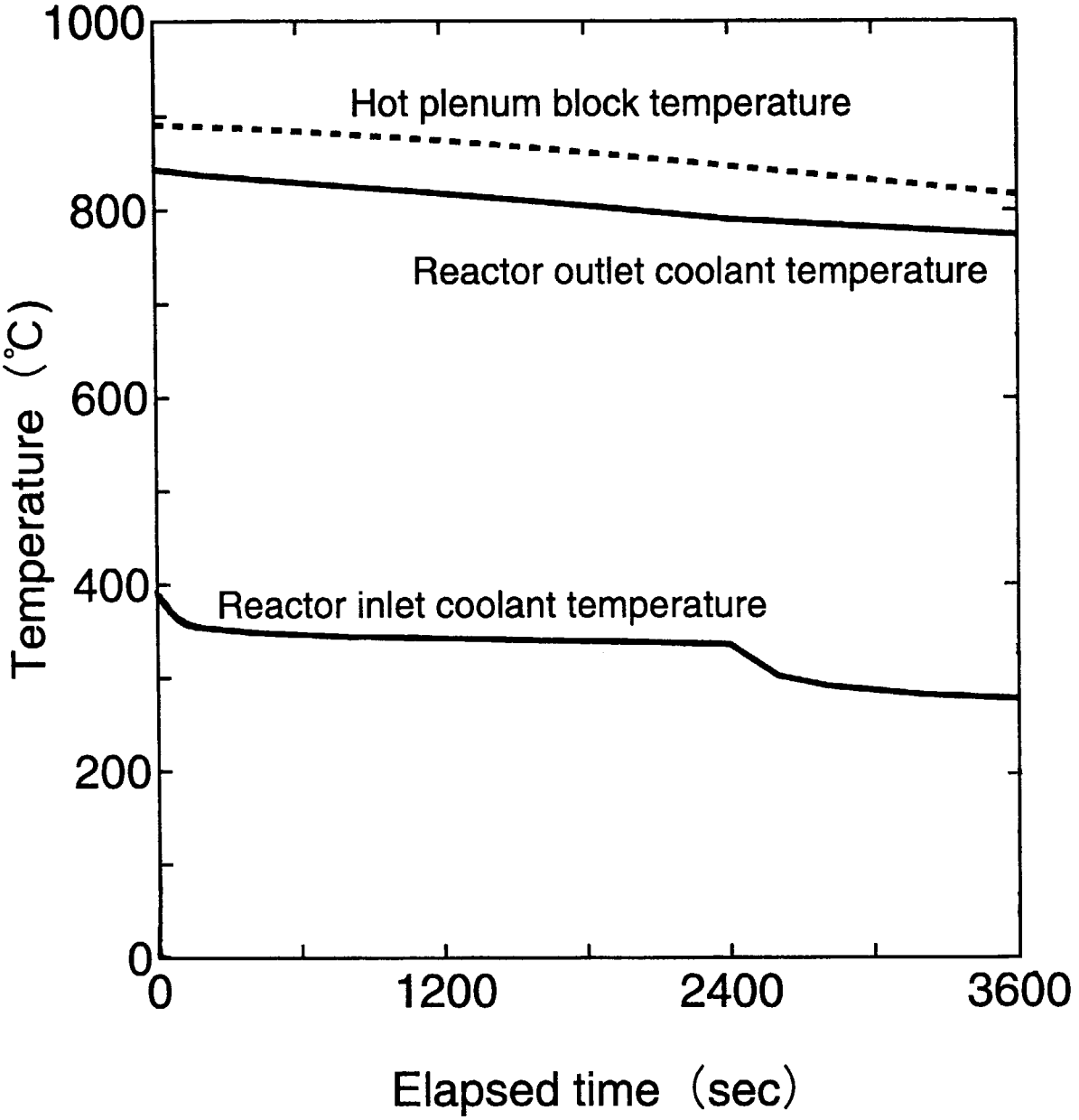

Fig. 10.4 Analytical results of transient behaviors of reactor and plant during loss of off-site electric power from normal operation under 30MW thermal power by 'ACCORD' code (1/3)

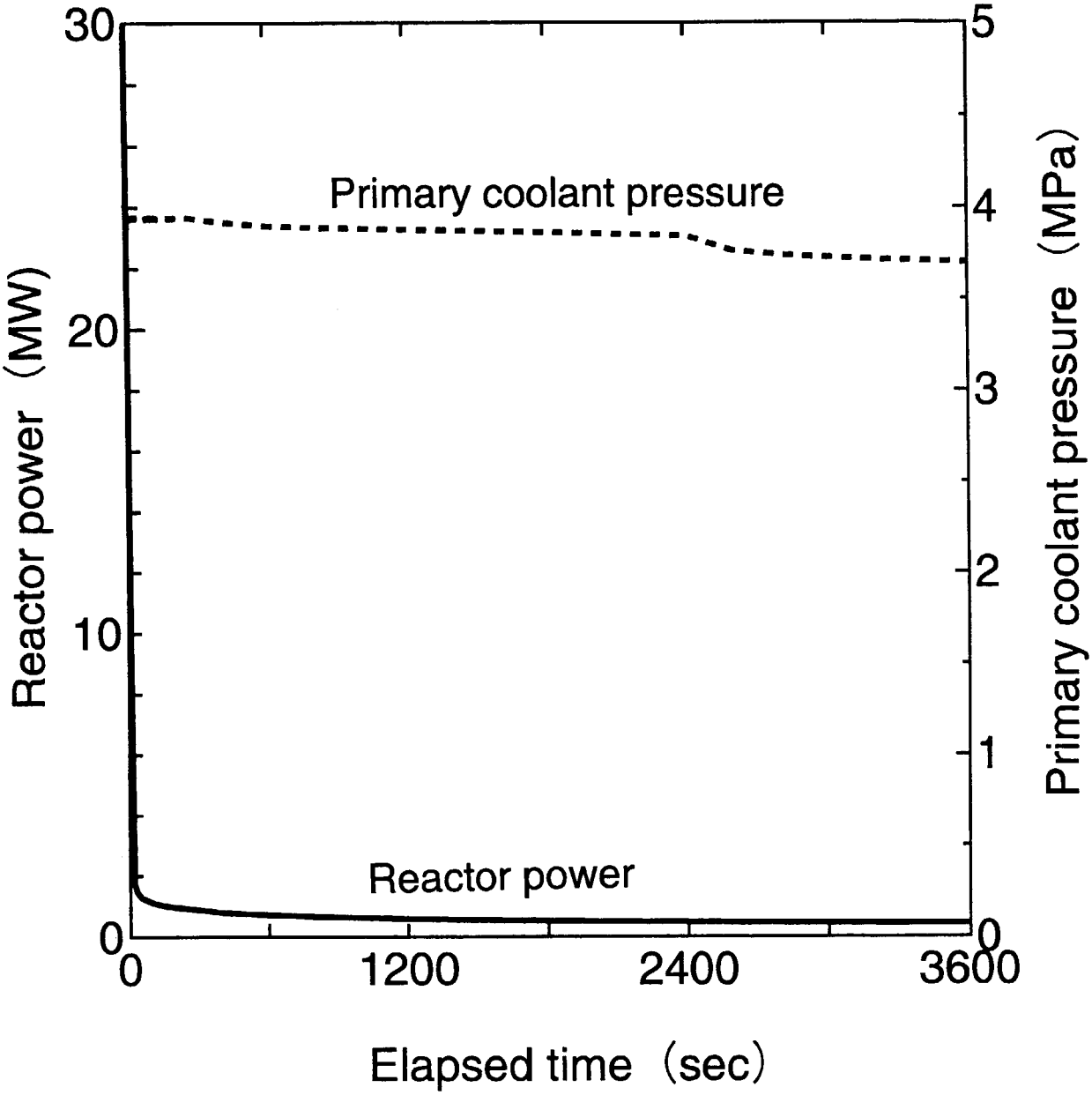

Fig. 10.5 Analytical results of transient behaviors of reactor and plant during loss of off-site electric power from normal operation under 30MW thermal power by 'ACCORD' code (2/3)

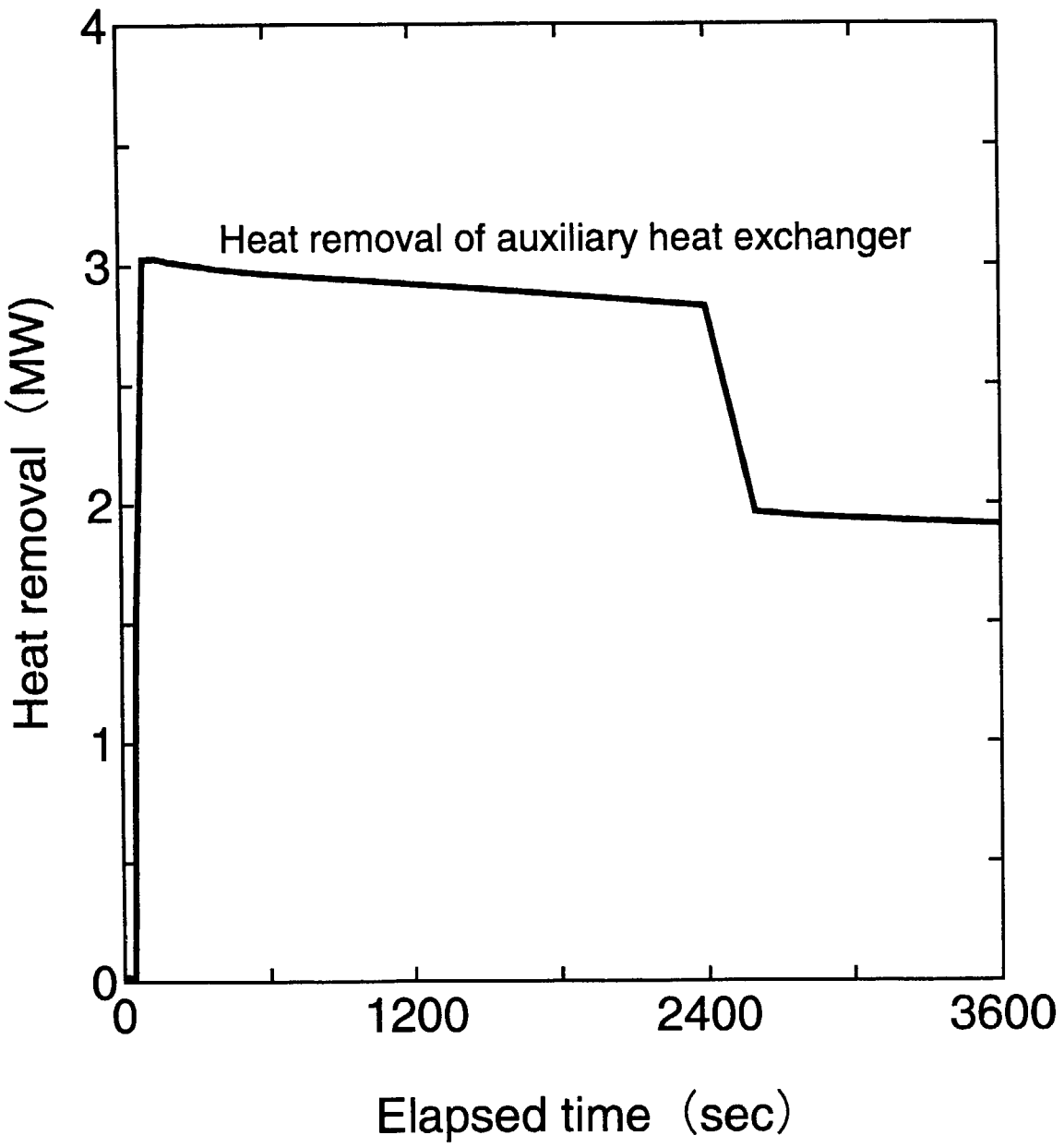

Fig. 10.6 Analytical results of transient behaviors of reactor and plant during loss of off-site electric power from normal operation under 30MW thermal power by 'ACCORD' code (3/3)

11. Conclusion

Analytical simulations on transient behaviors of the reactor and plant during the loss of off-site electric power from the normal operation under 15 and 30MW thermal power of the HTTR are proposed as benchmark problems for the IAEA coordinated research program on "Evaluation of HTGR Performance". The detailed thermal and nuclear data set (geometry, material, parameter for core dynamics, decay heat, performance of helium circulators, thermophysical properties, correlation of heat transfer coefficient, etc.) are prepared for solving the benchmark problems as precisely as possible. We expect that the benchmark problems described here are useful for the validation of analytical codes of participating countries and performance models to the actual operating conditions and results of the HTTR.

Acknowledgement

The authors would like to thank Dr K. Yamashita of Japan Atomic Energy Research Institute for his useful comments during this study and detailed presentation on the benchmark problems in the research coordination meeting (October 18-22, 1999, Beijing, China).

References

(1.1) Saito, S., et al., Design of High Temperature Engineering Test Reactor, Report JAERI 1332, Japan Atomic Energy Research Institute, 1994.

(1.2) Nojiri, N., et al., Benchmark Problem's Data for the HTTR's Start-up Core Physics Experiments (Prepared for IAEA Coordinated Research Program), private communication, Japan Atomic Energy Research Institute, 1998.

(1.3) Yamashita, K., Fujimoto, N., Nakano, M. and Ohlig, U., IAEA Benchmark Calculation Results of the HTTR's Start-up Core Physics Tests (Submitted by CRP-5's Members in Research Coordination Meeting (RCM)) (August 24-28, 1998, Vienna, Austria), private communication, Japan Atomic Energy Research Institute, 1999.

(1.4) Kunitomi, K., Tachibana, Y., Takeda, T., Saikusa, A. and Sawa, K., Research Program of the High Temperature Engineering Test Reactor for Upgrading the HTGR Technology, Report JAERI-Tech 97-030, Japan Atomic Energy Research Institute, 1997 (in Japanese).

(1.5) Takeda, T., Tachibana, Y., Kunitomi, K. and Itakura, H., Development of Analytical Code 'ACCORD' for Incore and Plant Dynamics of High Temperature Gas-cooled Reactor, Report JAERI-Data/Code 96-032, Japan Atomic Energy Research Institute, 1996 (in Japanese).

(6.1) Yamashita, K., Shindo, R., Murata, I., Nakagawa, S. and Nakata, T., Evaluation of Effective Delayed Neutron Fraction and Prompt Neutron Lifetime for High Temperature Engineering Test Reactor (HTTR), Report JAERI-M 89-198, Japan Atomic Energy Research Institute, 1989 (in Japanese).

(6.2) Yamashita, K., Shindo, R., Murata, I., Nakagawa, S., Nakata, T. and Tokuhara, K., Evaluation of Reactivity Coefficients for High Temperature Engineering Test Reactor (HTTR), Report JAERI-M 90-008, Japan Atomic Energy Research Institute, 1990 (in Japanese).

(6.3) Maruyama, S., Fujimoto, N., Yamashita, K., Murata, I., Shindo, R. and Sudo, Y., Core Thermal and Hydraulic Design of High Temperature Engineering Test Reactor (HTTR), Report JAERI-M 88-255, Japan Atomic Energy Research Institute, 1988 (in Japanese).

(6.4) Proposed ANS Standard for Decay Energy Release Rates Following Shutdown of Uranium-Fueled Thermal Reactors, ANS-5.1, 1971.

(6.5) Schrock, V. E., Revised ANS Standard for Decay Heat from Fission Products, Nucl. Technol., 46(2), 323-331, 1979.

(7.1) GEC ALSTHOM (RATEAU), private communication.

(8.1) Shindo, M. and Kondo, T., Studies on Improving Compatibility of Nickel-base Alloys with High Temperature Helium-Cooled Reactor (VHTR) Environment, BNES Conf., Gas-Cooled Reactors Today, Bristol, 1982.

(8.2) Kunitomi, K., Shinozaki, M., Fukaya, Y., Okubo, M., Baba, O., Maruyama, S. and Otani, A., Stress and Strain Evaluation of the Heat Transfer Tubes in the Intermediate Heat Exchanger for the HTTR, Report JAERI-M 92-147, Japan Atomic Energy Research Institute, 1992 (in Japanese).

(9.1) Dwyer, O. E., Nucl. Sci. Eng., 17, 336-344, 1963.

(9.2) Dalle Donne, M. and Merwald, E., Int. J. Heat Mass Transfer, 16, 787, 1973.

(9.3) Shenoy, A. S. and McEachern, D. W., HTGR Core Thermal Design Methods and Analysis, GA-A12985, 1974.

(9.4) Mori, Y. and Watanabe, K., Trans. Jpn Soc. Mech. Eng. B, 45, 397, 1979 (in Japanese).

(9.5) Fishenden, M. and Saunders, O. A., Introduction to Heat Transfer, Oxford Clarenden Press, 132, 1950.

(9.6) Mori, Y., Watanabe, K. and Taira, T., Trans. Jpn Soc. Mech. Eng. B, 46, 408, 1980 (in Japanese).

(9.7) Donohue, D. A., Heat Transfer and Pressure Drop in Heat Exchangers, Ind. Eng. Chem, 41(11), 1949.

(9.8) Dittus, F. W. and Boelter, L. M. K., Heat Transfer in Automobile Radiators of Tubular Tube, 2, 13, 1930.

(9.9) *"13th Nippon Dennetsu Shinpojium Koen Ronbunshu"*, B308, 1976 (in Japanese).

(9.10) ABB LUMMUS HEAT TRANSFER, private communication.

Appendix A Outline of 'ACCORD' code for incore and plant dynamics of HTGR

Steady state and transient behaviors of the reactor and plant of the HTGR can be evaluated through 'ACCORD' code developed by the JAERI. The following are the major characteristics of this code.

1. Plant system can be analyzed for over 1hr after an event occurrence by modeling the heat capacity of the reactor core.
2. Thermal hydraulics for each component can be analyzed by separating heat transfer calculation for component from fluid flow calculation for helium and water.

The 'ACCORD' code consists of modules for nuclear calculation, heat transfer calculation of reactor, heat exchangers and piping, fluid flow calculation of helium and water, control system and safety protection system of the HTTR. Figure A.1 shows a calculation system of the 'ACCORD' code. Each module of this code is reviewed briefly.

(1) Nuclear calculation module

Nuclear characteristic is evaluated by conventional point kinetics model with six delayed neutron groups. Thermal power is calculated by a balance of feedback reactivity due to fuel and moderator temperatures of the reactor core with additional reactivity caused by inserting and withdrawing the control rods. Decay heat of fission products after the reactor scram is estimated by Shure's formula and decay heat of actinide.

(2) Heat transfer calculation module

The reactor core is simulated by one channel model with one fuel rod taking into consideration thermal conduction through components and heat transfer of helium. Each heat exchanger is simulated by one channel model with one heat transfer tube.

(3) Fluid flow calculation module

Helium and water flow is approximated by one-dimensional flow network model including flow line and pressure point for calculating the flow rate and pressure.

(4) Control system module

This module is incorporated with the proportional and integral control applied to the HTTR control system for reactor power, inlet and outlet temperatures of the reactor, primary and secondary helium flow rate, etc.

(5) Safety protection system module

This module is incorporated with the HTTR scram signal system including time until the occurrence of the scram signal and time until the startup of the auxiliary cooling system after the achievement of the established scram value.

The validity of the 'ACCORD' code for the nuclear calculation, heat transfer and fluid flow calculation, control system and safety protection system, was confirmed through cross checks with other available codes used in safety analyses of the HTTR [A.1][A.2].

References

(A.1) Shimakawa, Y., Tanji, M., Nakagawa, S. and Fujimoto, N., The Plant Dynamics Analysis Code ASURA for the High Temperature Engineering Test Reactor (HTTR), Proc. of a Specialist's Meeting on Uncertainties in Physics Calculations for Gas Cooled Reactor Cores, 59-66, 1991.

(A.2) Hirano, M. and Hada, K., Development of THYDE-HTGR : Computer Code for Transient Thermal-hydraulics of High-Temperature Gas-cooled Reactor, Report JAERI-M 90-071, Japan Atomic Energy Research Institute, 1990.

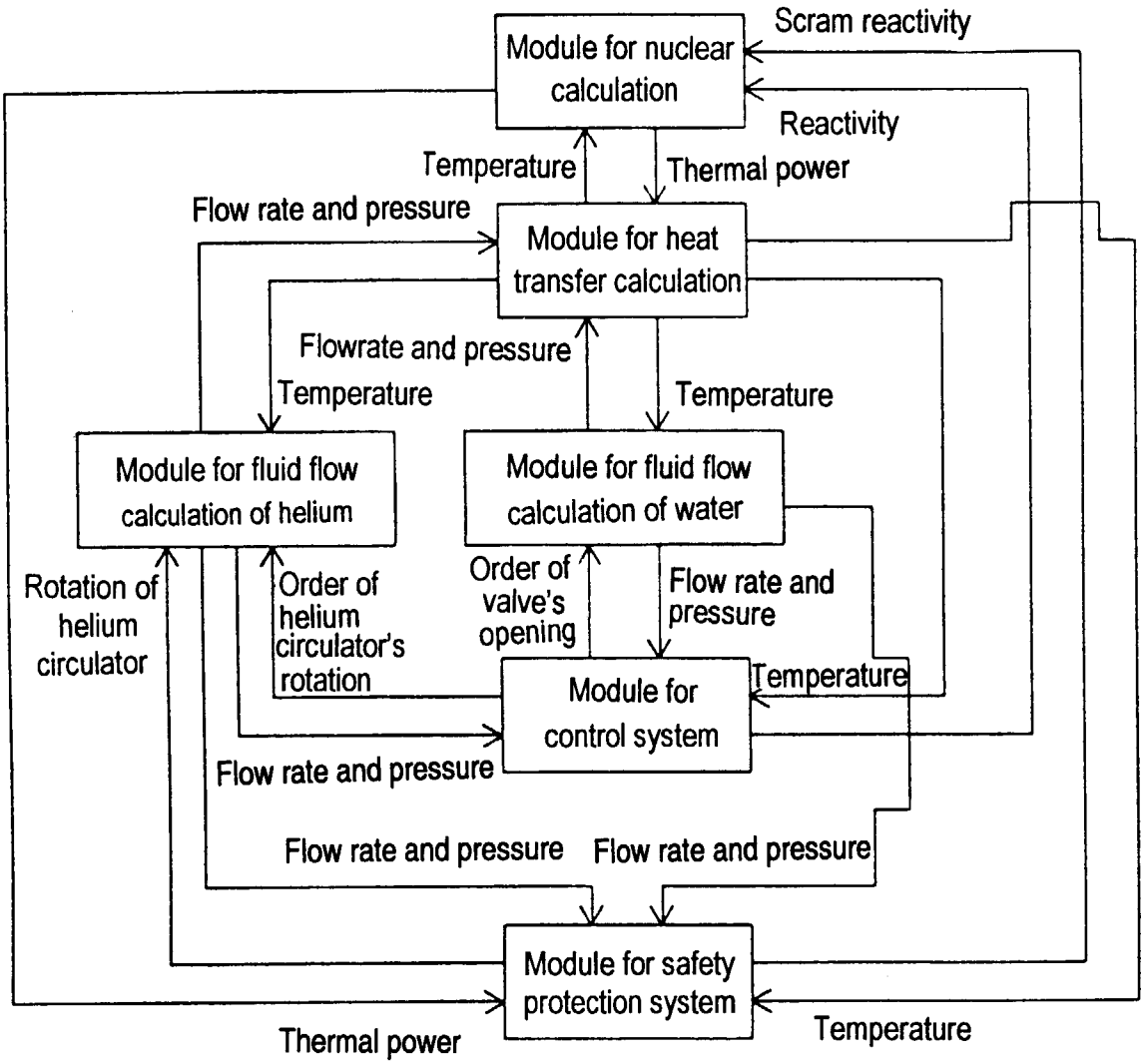

Fig. A.1 Calculation system of 'ACCORD' code

国際単位系（SI）と換算表

表1　SI基本単位および補助単位

量	名称	記号
長さ	メートル	m
質量	キログラム	kg
時間	秒	s
電流	アンペア	A
熱力学温度	ケルビン	K
物質量	モル	mol
光度	カンデラ	cd
平面角	ラジアン	rad
立体角	ステラジアン	sr

表2　SIと併用される単位

名称	記号
分，時，日	min, h, d
度，分，秒	°, ′, ″
リットル	l, L
トン	t
電子ボルト	eV
原子質量単位	u

1 eV=1.60218×10^{-19}J

1 u=1.66054×10^{-27}kg

表3　固有の名称をもつSI組立単位

量	名称	記号	他のSI単位による表現
周波数	ヘルツ	Hz	s^{-1}
力	ニュートン	N	m·kg/s^2
圧力，応力	パスカル	Pa	N/m^2
エネルギー,仕事,熱量	ジュール	J	N·m
工率，放射束	ワット	W	J/s
電気量，電荷	クーロン	C	A·s
電位，電圧，起電力	ボルト	V	W/A
静電容量	ファラド	F	C/V
電気抵抗	オーム	Ω	V/A
コンダクタンス	ジーメンス	S	A/V
磁束	ウェーバ	Wb	V·s
磁束密度	テスラ	T	Wb/m^2
インダクタンス	ヘンリー	H	Wb/A
セルシウス温度	セルシウス度	C	
光束	ルーメン	lm	cd·sr
照度	ルクス	lx	lm/m^2
放射能	ベクレル	Bq	s^{-1}
吸収線量	グレイ	Gy	J/kg
線量等量	シーベルト	Sv	J/kg

表4　SIと共に暫定的に維持される単位

名称	記号
オングストローム	Å
バーン	b
バール	bar
ガル	Gal
キュリー	Ci
レントゲン	R
ラド	rad
レム	rem

1 Å=0.1nm=10^{-10}m

1 b=100fm^2=10^{-28}m^2

1 bar=0.1MPa=10^{5}Pa

1 Gal=1cm/s^2=10^{-2}m/s^2

1 Ci=3.7×10^{10}Bq

1 R=2.58×10^{-4}C/kg

1 rad=1cGy=10^{-2}Gy

1 rem=1cSv=10^{-2}Sv

表5　SI接頭語

倍数	接頭語	記号
10^{18}	エクサ	E
10^{15}	ペタ	P
10^{12}	テラ	T
10^{9}	ギガ	G
10^{6}	メガ	M
10^{3}	キロ	k
10^{2}	ヘクト	h
10^{1}	デカ	da
10^{-1}	デシ	d
10^{-2}	センチ	c
10^{-3}	ミリ	m
10^{-6}	マイクロ	μ
10^{-9}	ナノ	n
10^{-12}	ピコ	p
10^{-15}	フェムト	f
10^{-18}	アト	a

（注）

1．表1　5は「国際単位系」第5版，国際度量衡局1985年刊行による。ただし，1eVおよび1 uの値はCODATAの1986年推奨値によった。

2．表4には海里，ノット，アール，ヘクタールも含まれているが日常の単位なのでここでは省略した。

3．barは，JISでは流体の圧力を表わす場合に限り表2のカテゴリーに分類されている。

4．EC閣僚理事会指令ではbar，barnおよび「血圧の単位」mmHgを表2のカテゴリーに入れている。

換　算　表

力	N(=10^{5}dyn)	kgf	lbf
	1	0.101972	0.224809
	9.80665	1	2.20462
	4.44822	0.453592	1

粘度　1Pa·s(N·s/m^2)=10P(ポアズ)(g/(cm·s))

動粘度　1m^2/s=10^{4}St(ストークス)(cm^2/s)

圧力	MPa(=10bar)	kgf/cm^2	atm	mmHg(Torr)	lbf/in^2(psi)
	1	10.1972	9.86923	7.50062×10^3	145.038
	0.0980665	1	0.967841	735.559	14.2233
	0.101325	1.03323	1	760	14.6959
	1.33322×10^{-4}	1.35951×10^{-3}	1.31579×10^{-3}	1	1.93368×10^{-2}
	6.89476×10^{-3}	7.03070×10^{-2}	6.80460×10^{-2}	51.7149	1

エネルギー・仕事・熱量	J(=10^7 erg)	kgf·m	kW·h	cal(計量法)	Btu	ft·lbf	eV
	1	0.101972	2.77778×10^{-7}	0.238889	9.47813×10^{-4}	0.737562	6.24150×10^{18}
	9.80665	1	2.72407×10^{-6}	2.34270	9.29487×10^{-3}	7.23301	6.12082×10^{19}
	3.6×10^6	3.67098×10^5	1	8.59999×10^5	3412.13	2.65522×10^6	2.24694×10^{25}
	4.18605	0.426858	1.16279×10^{-6}	1	3.96759×10^{-3}	3.08747	2.61272×10^{19}
	1055.06	107.586	2.93072×10^{-4}	252.042	1	778.172	6.58515×10^{21}
	1.35582	0.138255	3.76616×10^{-7}	0.323890	1.28506×10^{-3}	1	8.46233×10^{18}
	1.60218×10^{-19}	1.63377×10^{-20}	4.45050×10^{-26}	3.82743×10^{-20}	1.51857×10^{-22}	1.18171×10^{-19}	1

1 cal= 4.18605J（計量法）

= 4.184J（熱化学）

= 4.1855J（15 C）

= 4.1868J（国際蒸気表）

仕事率　1 PS(仏馬力)

= 75 kgf·m/s

= 735.499W

放射能	Bq	Ci
	1	2.70270×10^{-11}
	3.7×10^{10}	1

吸収線量	Gy	rad
	1	100
	0.01	1

照射線量	C/kg	R
	1	3876
	2.58×10^{-4}	1

線量当量	Sv	rem
	1	100
	0.01	1

（86年12月26日現在）